

Liquid Xe Detectors

田内利明、平成18年7月12日
測定器開発室勉強会、素核研、KEK

General Property of Liquid Xenon

<http://www.pd.infn.it/~conti/LXe.html>

Rich detection media : Scintillation and Ionization

Scintillation

energy

photomultipliers

GEM/photocathod

Avalanche Photodiodes

Ionization

position

ionization chamber with low noise amp. 300e

GEM in 2 phase Xe

22,000 VUV photons/511KeV with 3ns, 27ns and 45ns

30,000 electron-ion pairs/511KeV

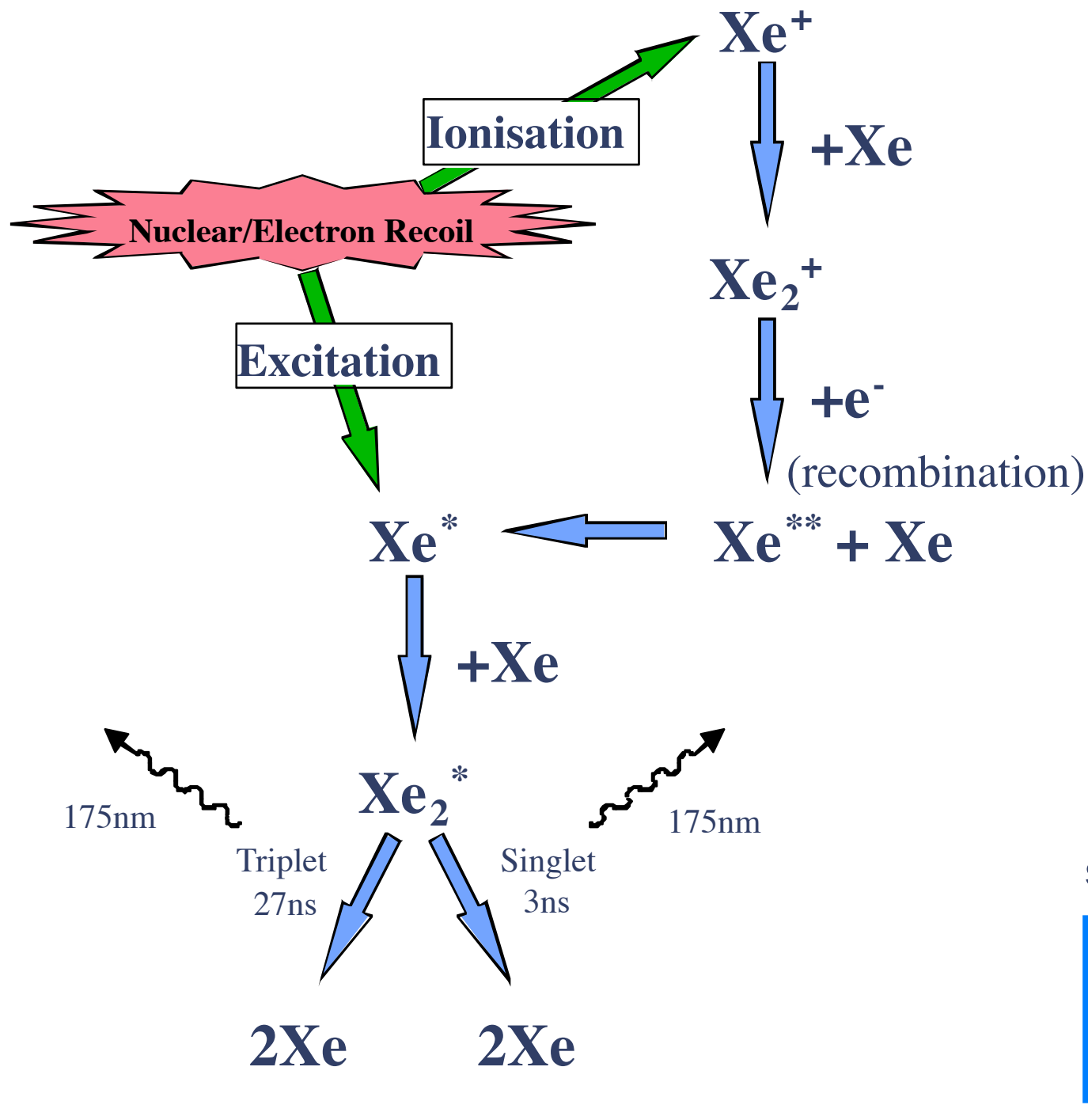
electron drift at 2.3mm/us with 2kV/cm

At 511 keV, 22% photoelectric, 78% Compton with xenon
half a mm for 511 keV photoelectron

Primary ionization signal is weak: of the order of 1, 10, 100 and 500 keV
for coherent neutrino, dark matter, solar neutrino and PET respectively.



XENON (PSD and Scint/Ion)

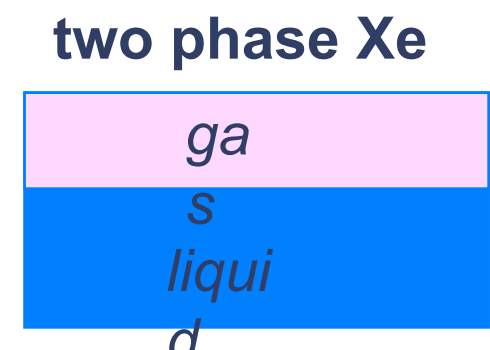


three discrimination techniques

(1) scintillation pulse shape

(2) ionisation-scintillation
- low field-

(3) ionisation-scintillation
- high field, low threshold -



World expertise

- ICARUS-UCLA
- Doke group (Japan)
- DAMA
- Columbia
- UKDMC
- ITEP

Table 1.5: Physical properties of noble liquids (adapted from Ref. (98)).

	LAr	LKr	LXe
Atomic Number Z	18	36	54
Atomic Weight A	39.95	83.8	131.3
Density (g/cc)	1.39	2.45	3.06
Melting Point T_m (K)	83.8	115.8	161.4
Boiling Point T_b (K)	87.3	119.8	165.1
Critical Temperature T_c (K)	150.7	209.5	289.7
Critical Pressure P_c (atm)	48.3	54.3	57.64
Critical Density (g/cc)	0.54	0.91	1.10
Volume Ratio (ρ_l/ρ_g)	784	641	519
Fano Factor	0.107	0.057	0.041
Drift Velocity (mm/ μ sec) @ 1(5) kV/cm	1.8(3.0)	2.4(4.0)	2.2(2.7)
Mobility (cm $V^{-1}s^{-1}$)	525	1800	2000
Radiation Length (cm)	14.3	4.76	2.77
(dE/dx) (MeV/cm)	2.11	3.45	3.89
Liquid Heat Capacity (cal/g-mole/K)	10.05	10.7	10.65
W-value (eV) (ionization)	23.3	18.6	15.6
W-value (eV) (scintillation)	19.5	15.5	14.7
Wavelength of Scintillation Light (nm)	130	150	175
Decay const.			
fast (ns)	6.5	2	2
slow (ns)	1100	85	30
Refractive index @ 170 nm	–	1.41	1.60
Dielectric constant	1.51	1.66	1.95

1 Phase

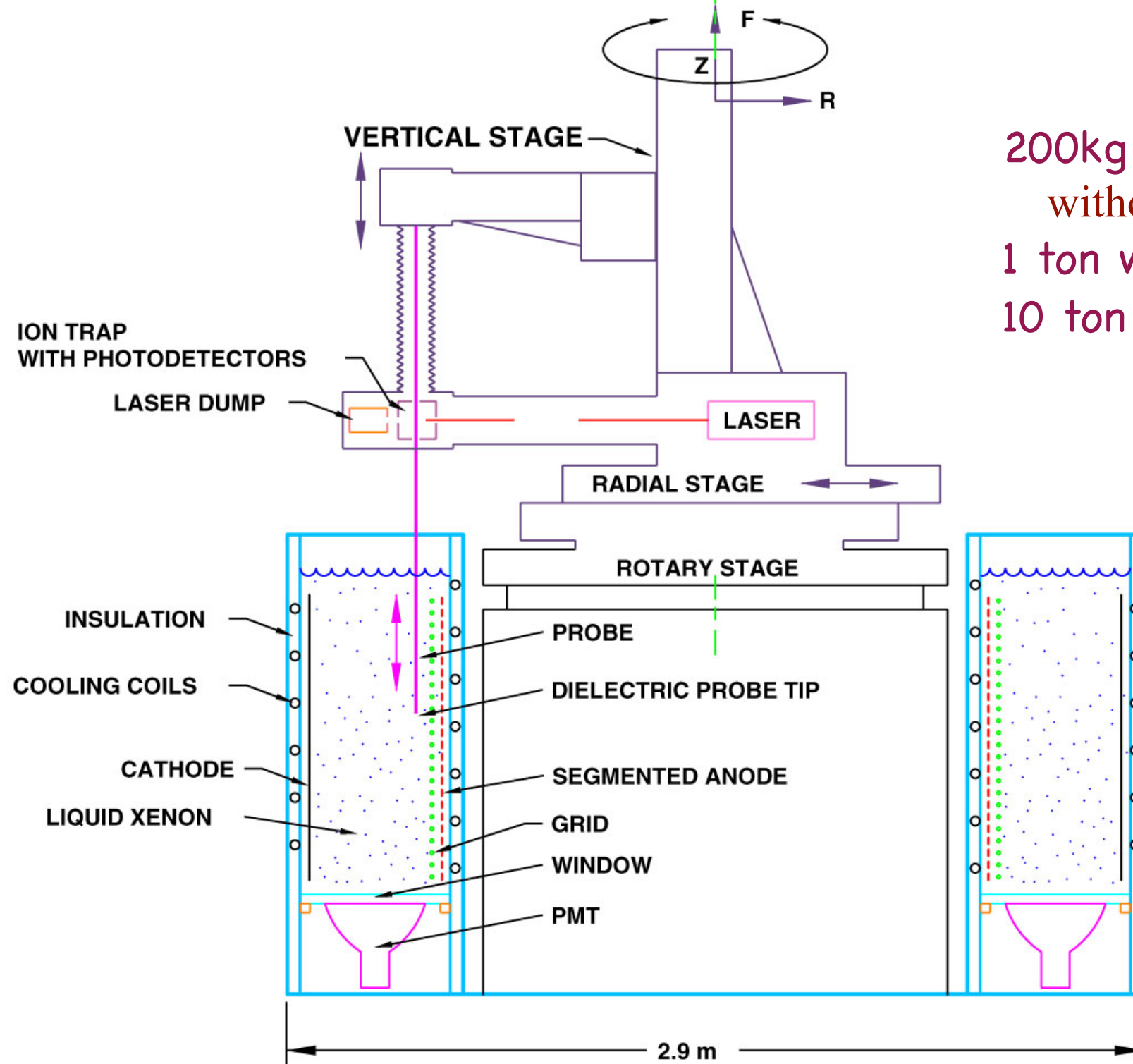
EXO TPC ; 1 phase

2006

<http://www-project.slac.stanford.edu/exo/> ; Double β Decay

liqXe-TPC, grid and segmented anode and PMT, 10ton (3m^3)

WIPP : Waste Isolation Pilot Plant Carlsbad NM, Excavated in underground salt – lower U/Th activity. $\sim 2,000$ m.w.e. depth



200kg (63l), enriched ^{136}Xe (80%) 2006
without Ba tagging for 2 years
1 ton with Ba tagging for 5 years
10 ton with Ba tagging for 10 years



- Extract the Barium ion from the event location (electrostatic probe)
- Deliver the Barium to a laser system for Ba^{136} identification.

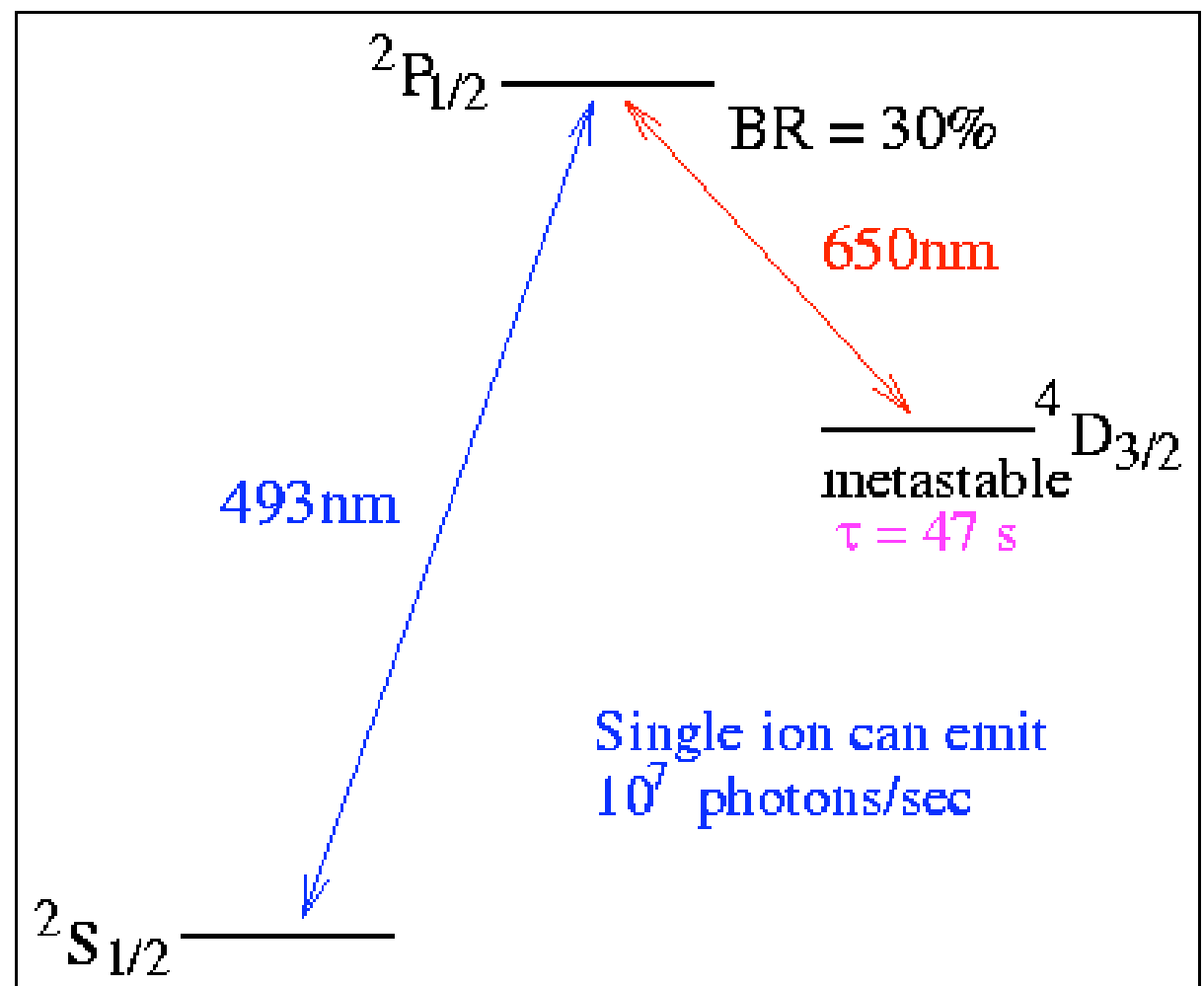
Xe offers a new tool to reduce background:

$^{136}\text{Xe} \rightarrow ^{136}\text{Ba}^{++}$ final state can be identified
using optical spectroscopy (M.Moe PRC44 (1991) 931)

Ba⁺ system best studied
(Neuhauser, Hohenstatt,
Toshek, Dehmelt 1980)
Very specific signature
“shelving”

Single ions can be detected
from a photon rate of $10^7/\text{s}$

Barium tagging would
eliminate all radioactive
backgrounds, leaving
only $2\nu\beta\beta$.



Level structure for Ba⁺

It's just crazy enough to work

Assuming that the Xe chamber + Ba tagging reduce to 0 all radioactive background...

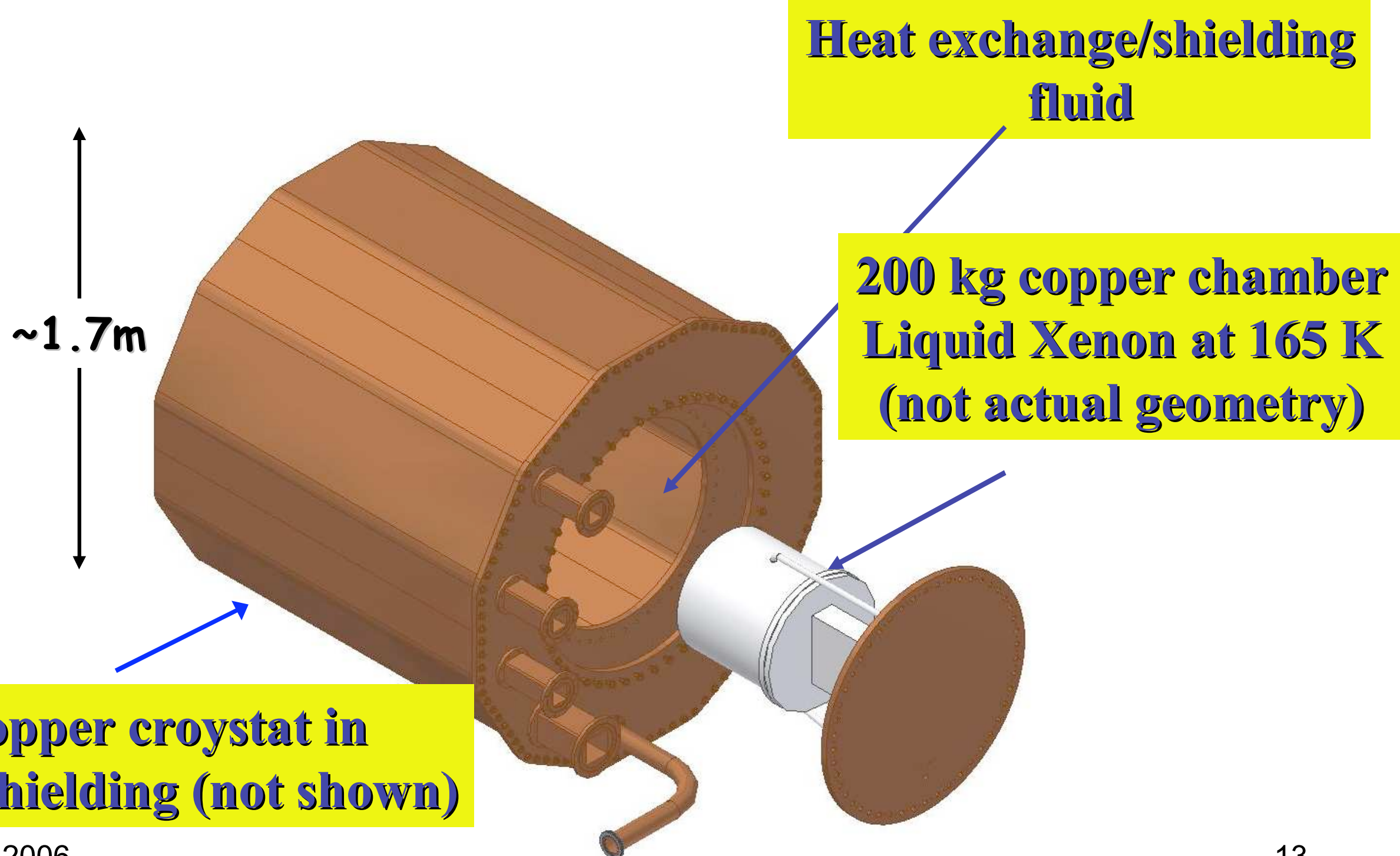
Isotope	Det mass (kg)	Enrich. (%)	Eff. (%)	Measur. time (yr)	Background	$T_{1/2}^{0\nu\beta\beta}$ (yr)	$\langle m_n \rangle$ QRPA	$\langle m_n \rangle$ NSM	(eV)
$^{136}\text{Xe}^*$	1000	80	70	5	0 + 1.8 events	8.3×10^{26}	0.051	0.14	
$^{136}\text{Xe}^{**}$	10000	80	70	10	0 + 5.5 events	1.3×10^{28}	0.013	0.037	

* $\sigma(E)/E = 2.8\%$ R.Luescher et al. Phys. Lett. B434 (1998) 407

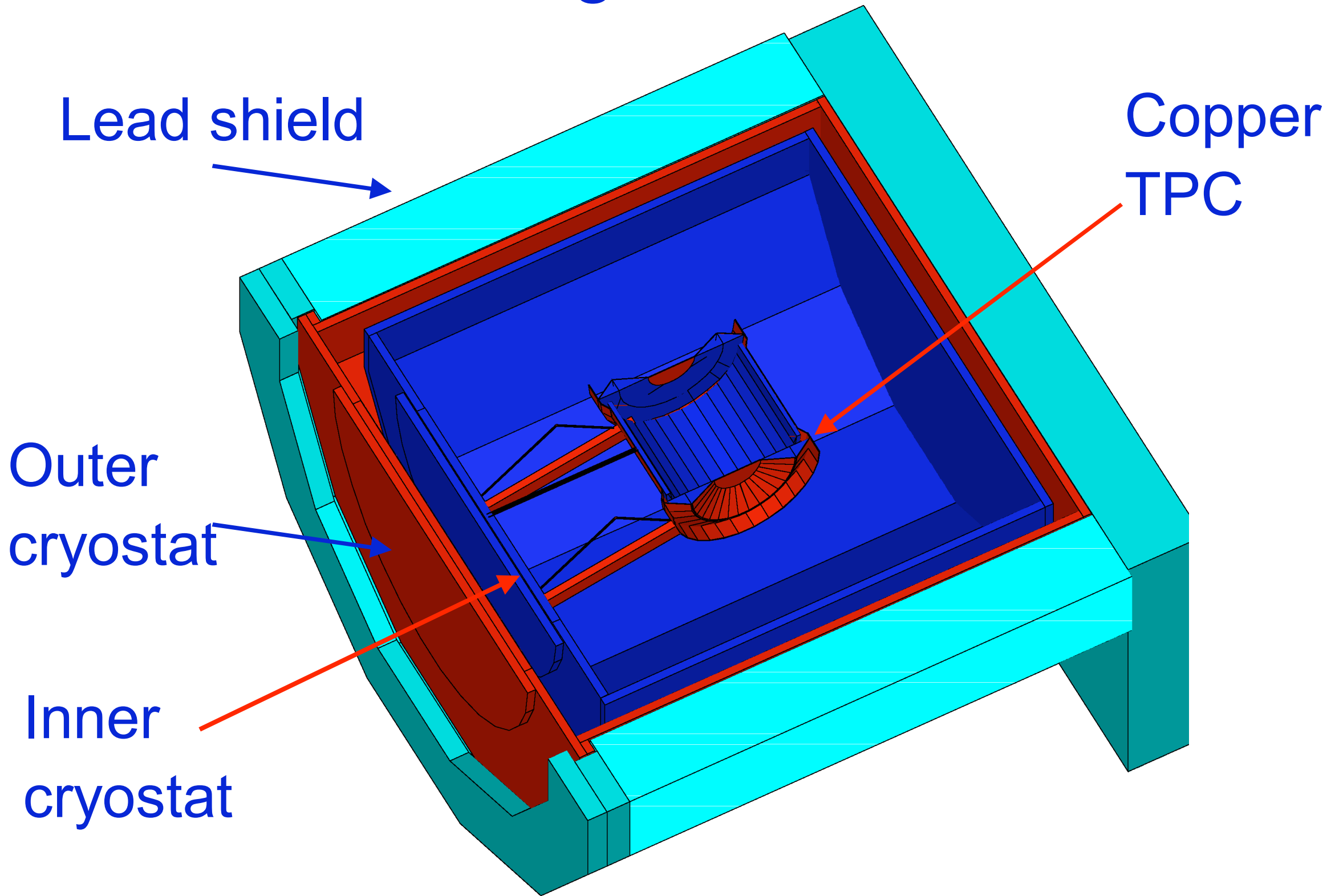
** $\sigma(E)/E = 2.0\%$ Modest improvement on the above.

The meV region is within reach.

The EXO-200 is an ultra-low background cryogenic apparatus

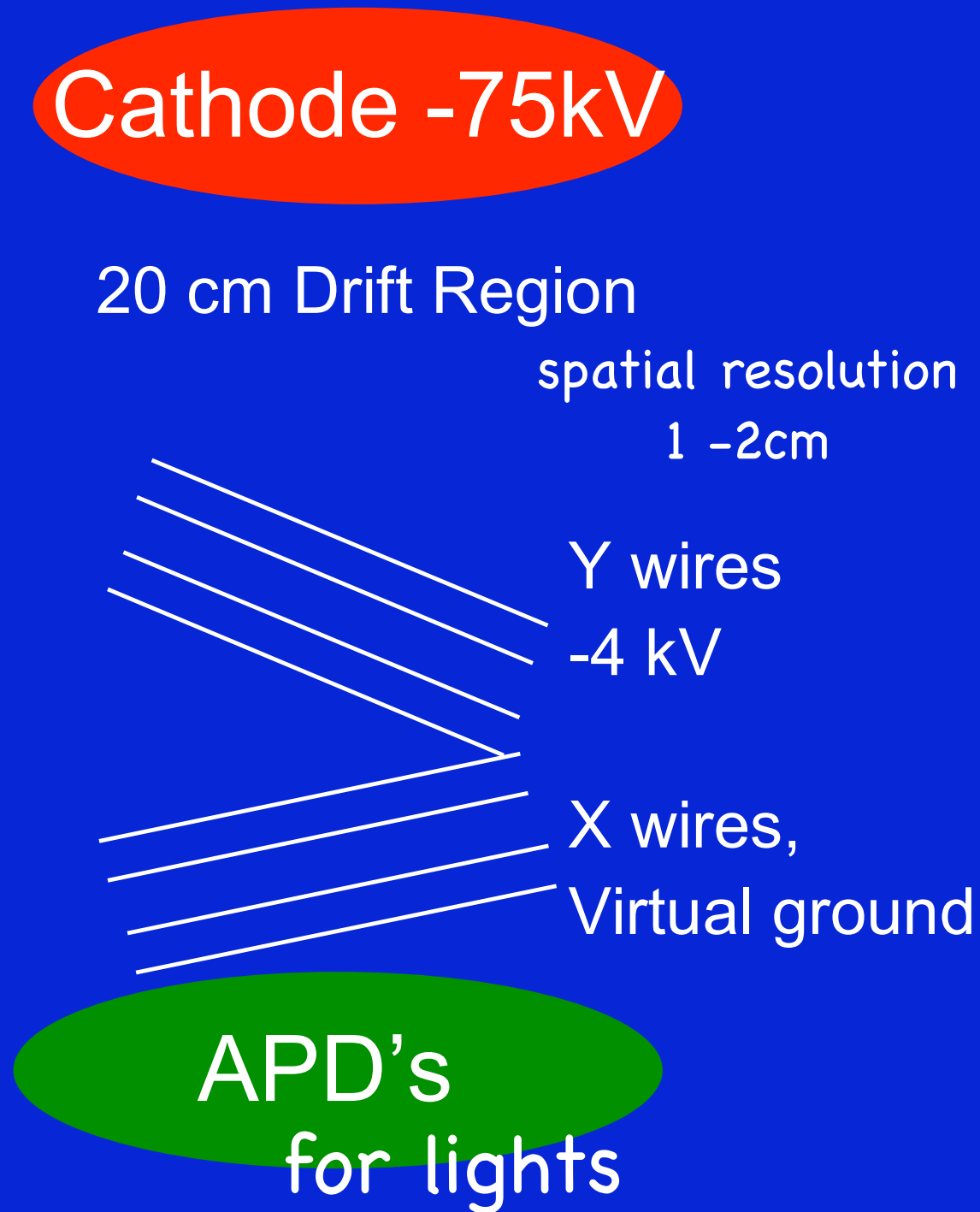


Realistic Monte Carlo Geometry for Background Studies.



Charge Detection

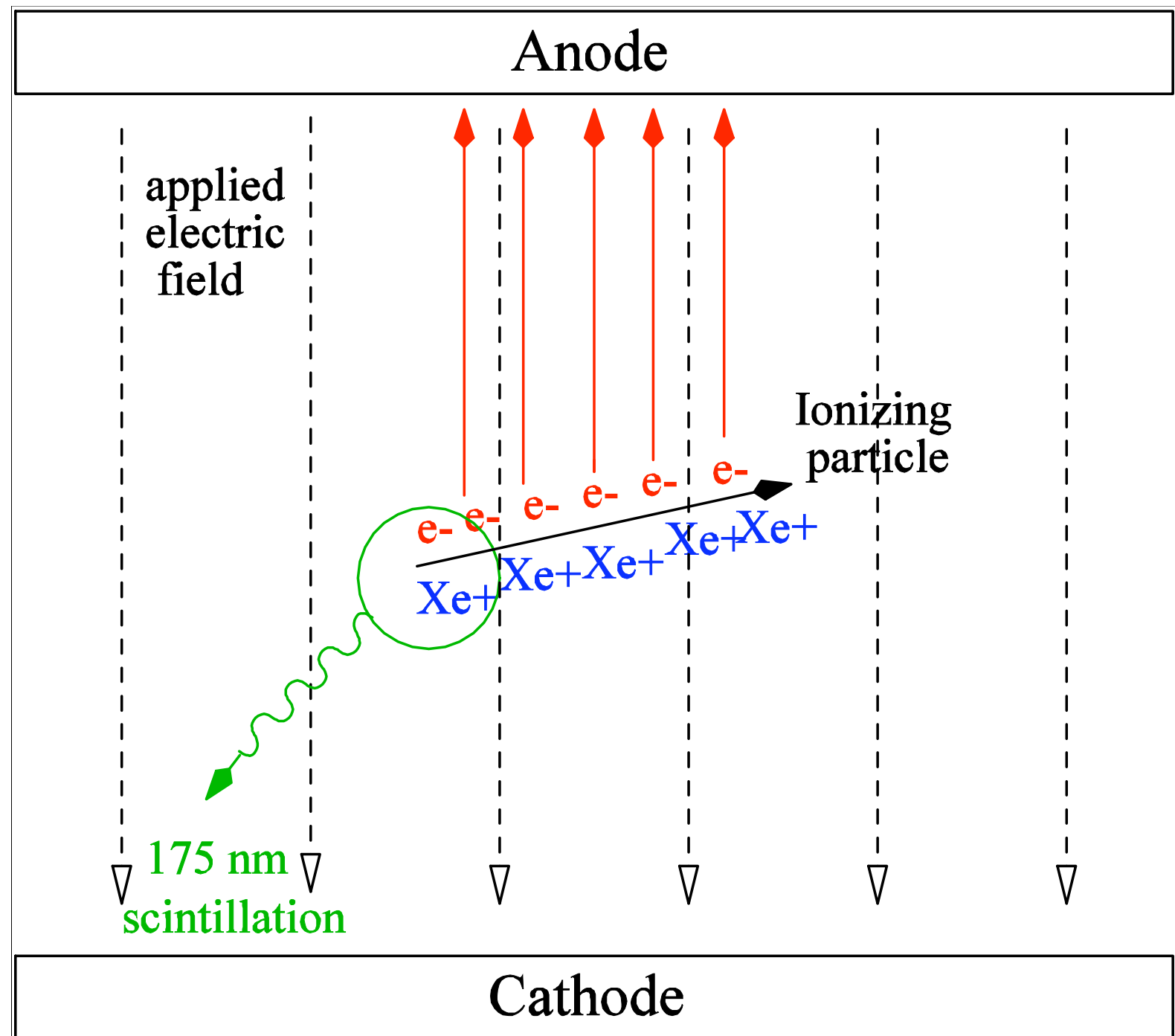
- Double-ended TPC chamber with ~20 cm drift regions
- Mid-plane cathode biased at -75 kV
- 38 Inductive “Y” wires per side at -4 kV, 100% charge transparent.
- 38 “X” wires at virtual ground to collect the charge.
- LXe electron mobility ~ 2000 $\text{cm}^2/(\text{Vs})$
- Saturation velocity $\sim 0.28 * \text{cm}/\mu\text{s}$
- Electron lifetime goal of 3ms
 $\Rightarrow 2.4\%$ loss at 20 cm.



Xenon calorimetry

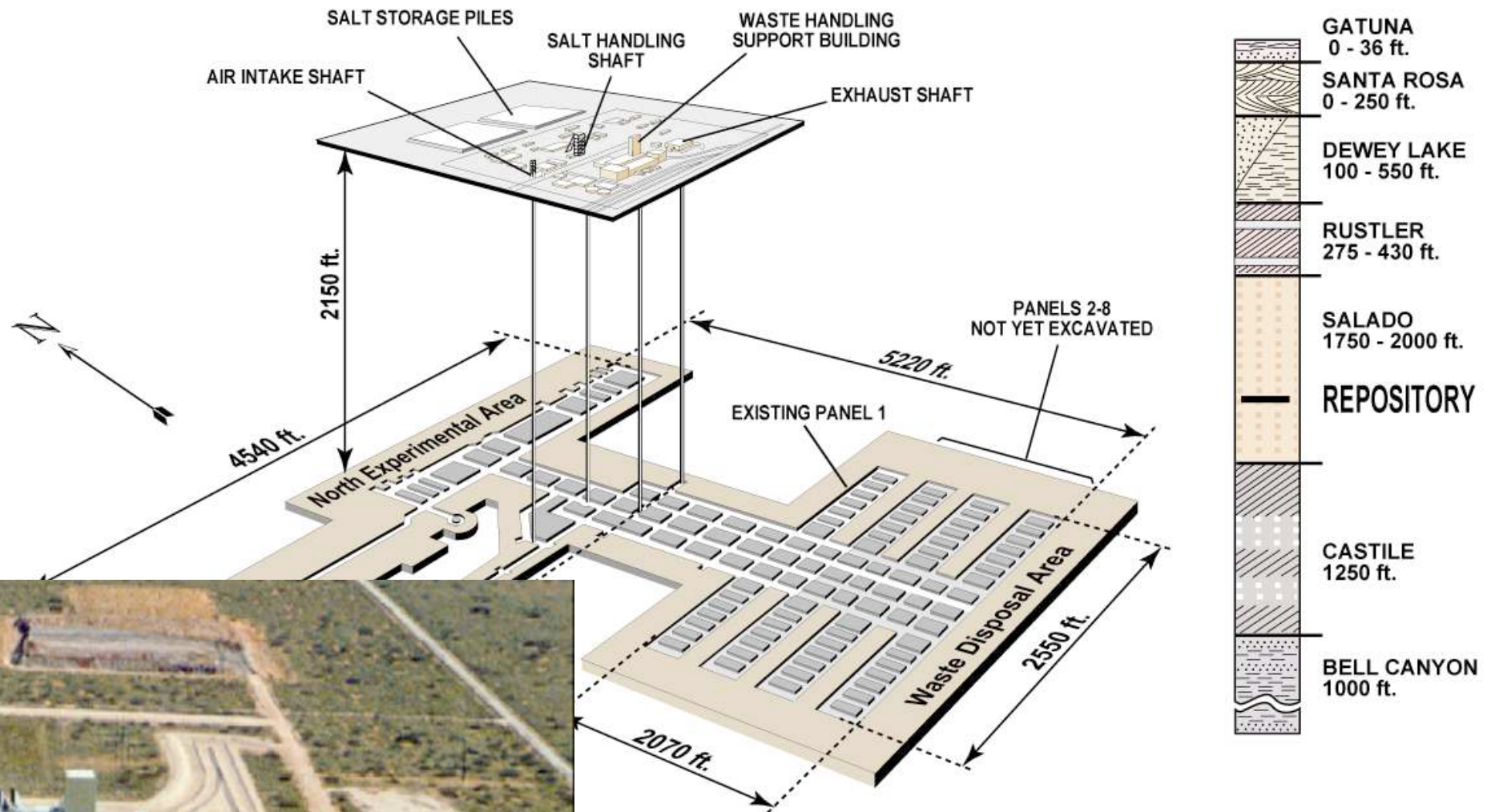
We measure the event energy by collecting the ionization on the anode and/or observing the scintillation.

As the electric field is increased, the collected ionization increases and the scintillation decreases.



200 kg prototype to be installed at DoE's WIPP, NM

shielding depth
~2.5 km w.e.



A salt mine to store
the military radioactive
waste...
...and perform low
background
physics experiments

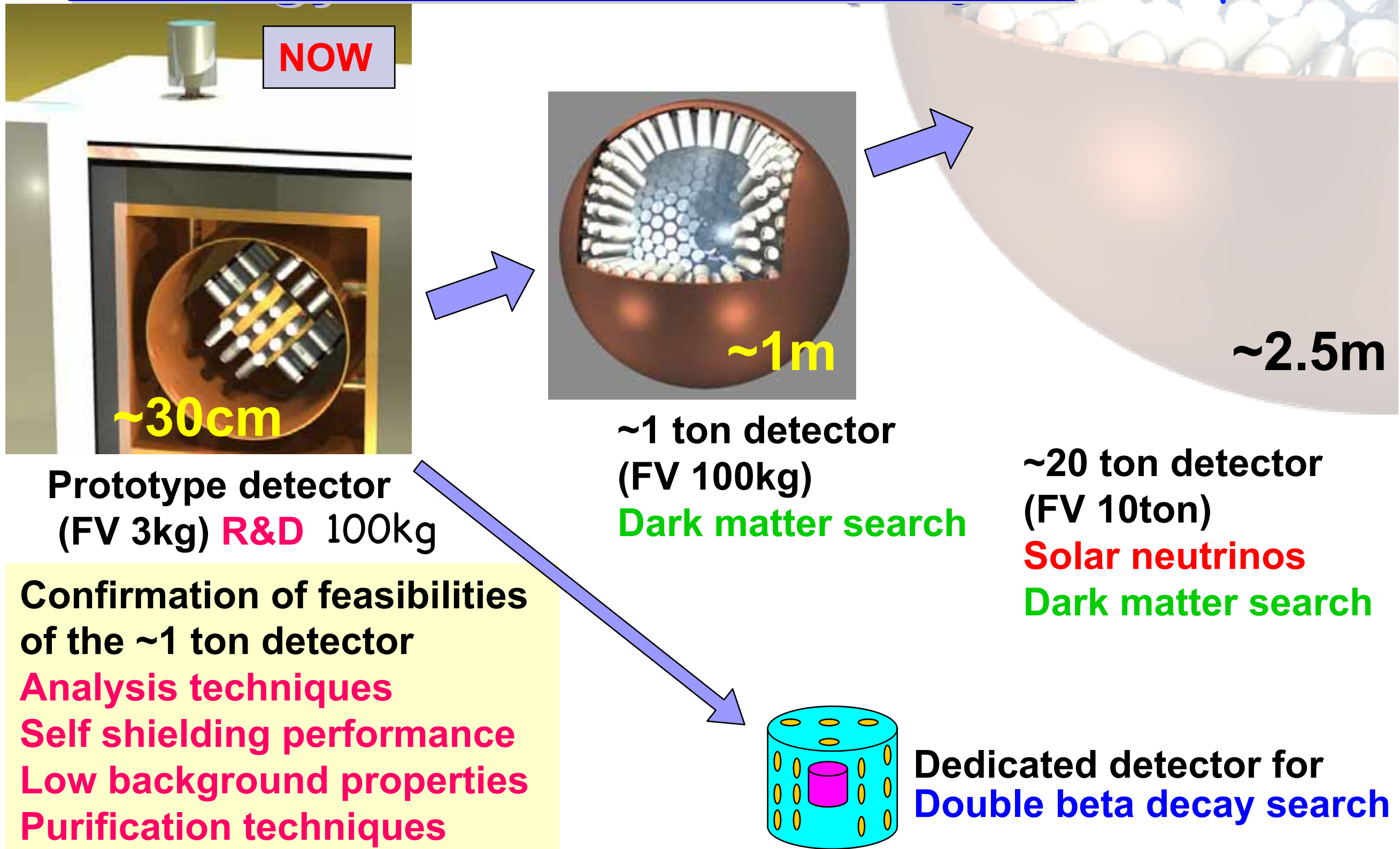
An experimental facility for EXO



Excavated in underground
salt – lower U/Th activity.
~2,000 m.w.e. depth



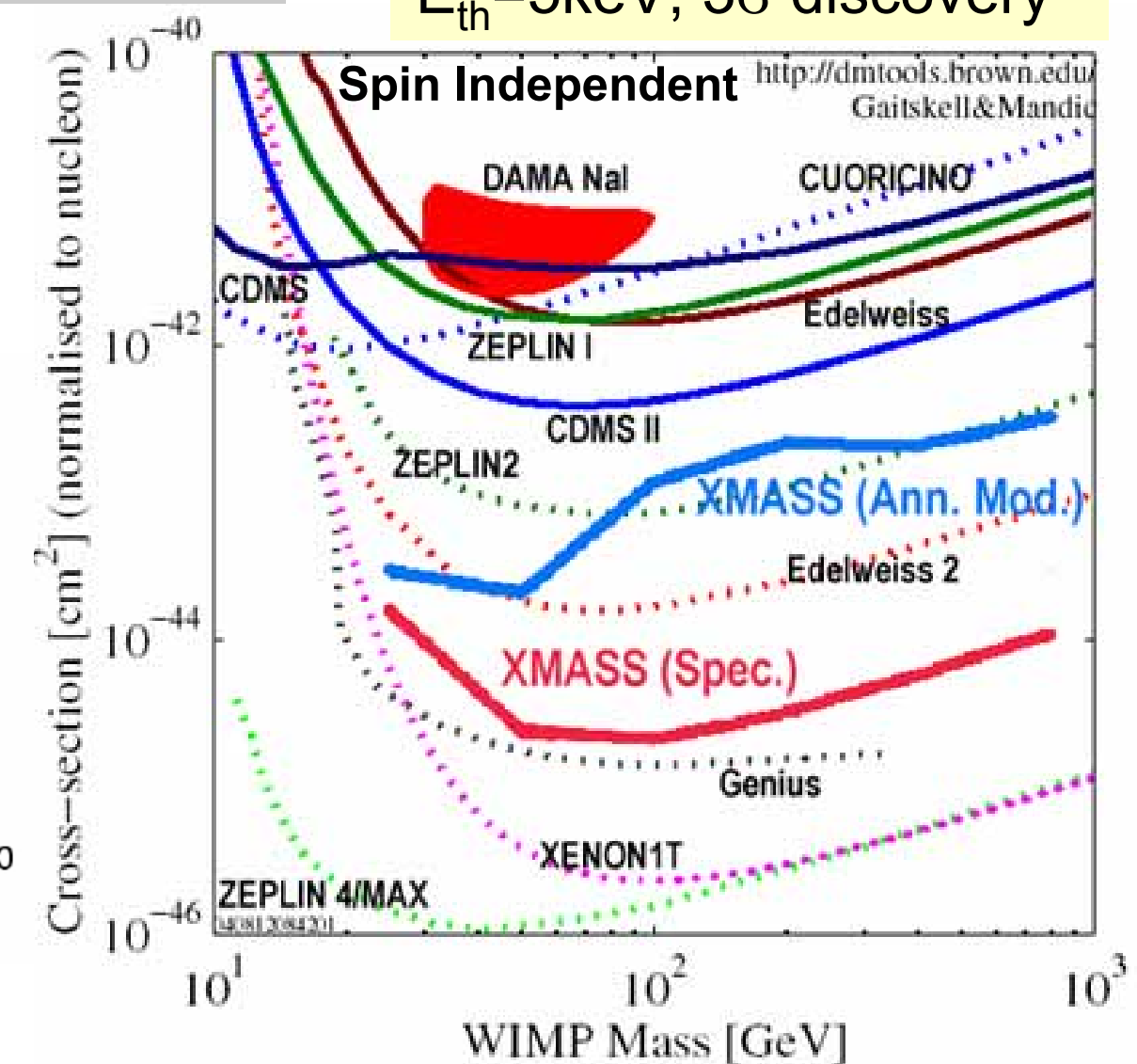
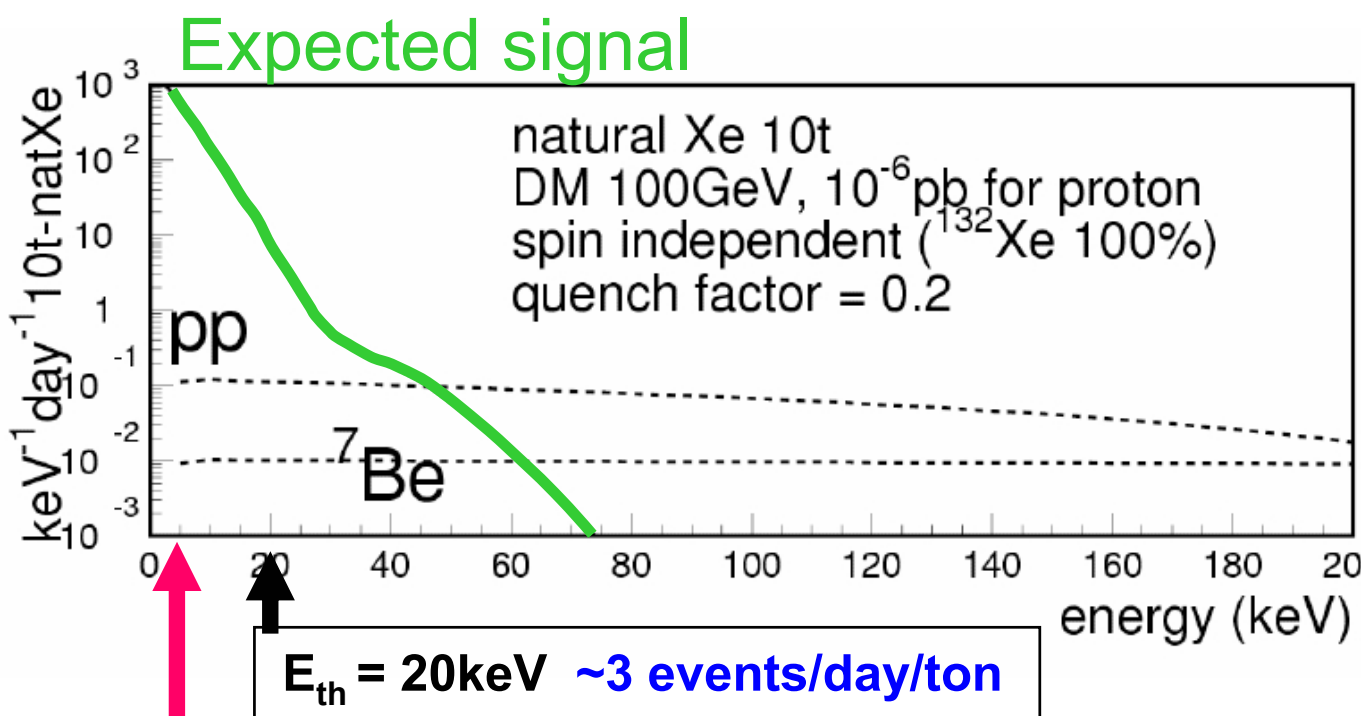
Strategy of the XMASS project ; 1 phase



Physics goals at XMASS

XMASS FV 0.5ton year
 $E_{th}=5\text{keV}$, 3σ discovery

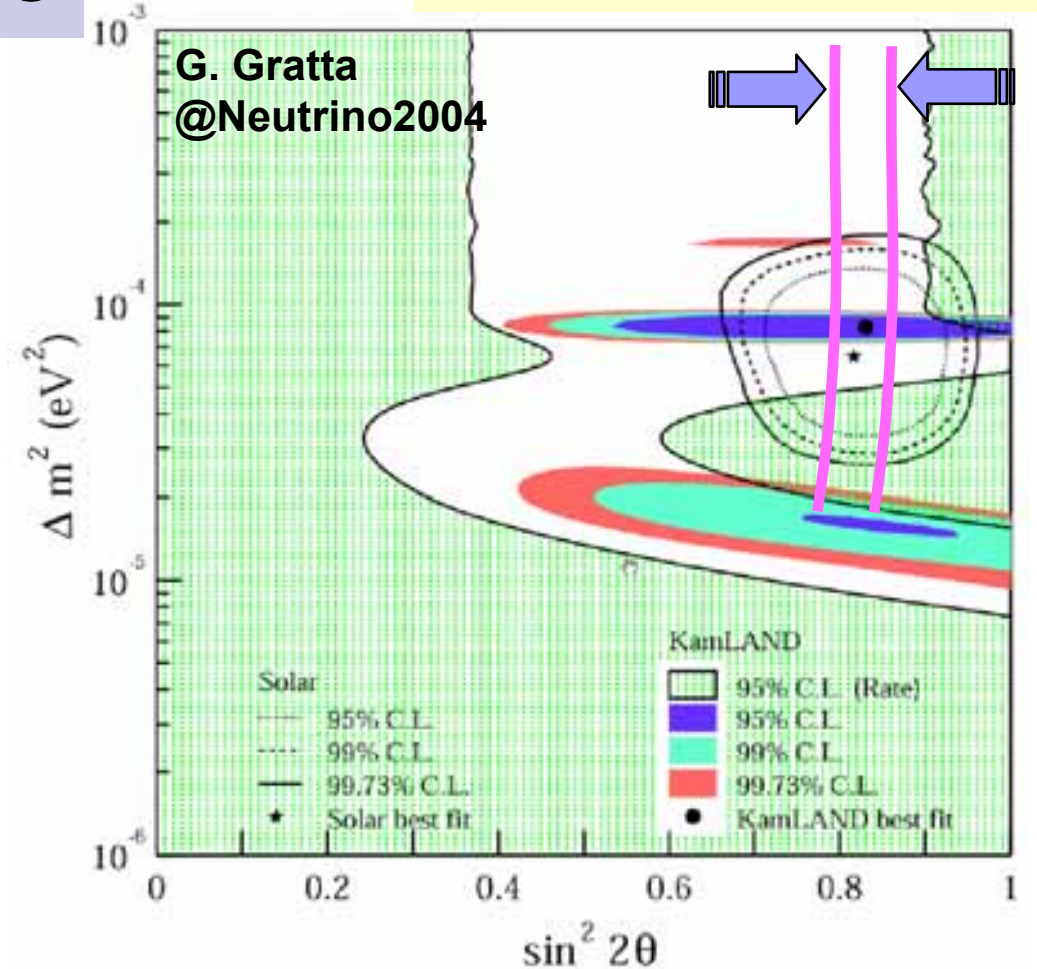
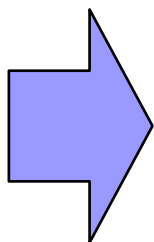
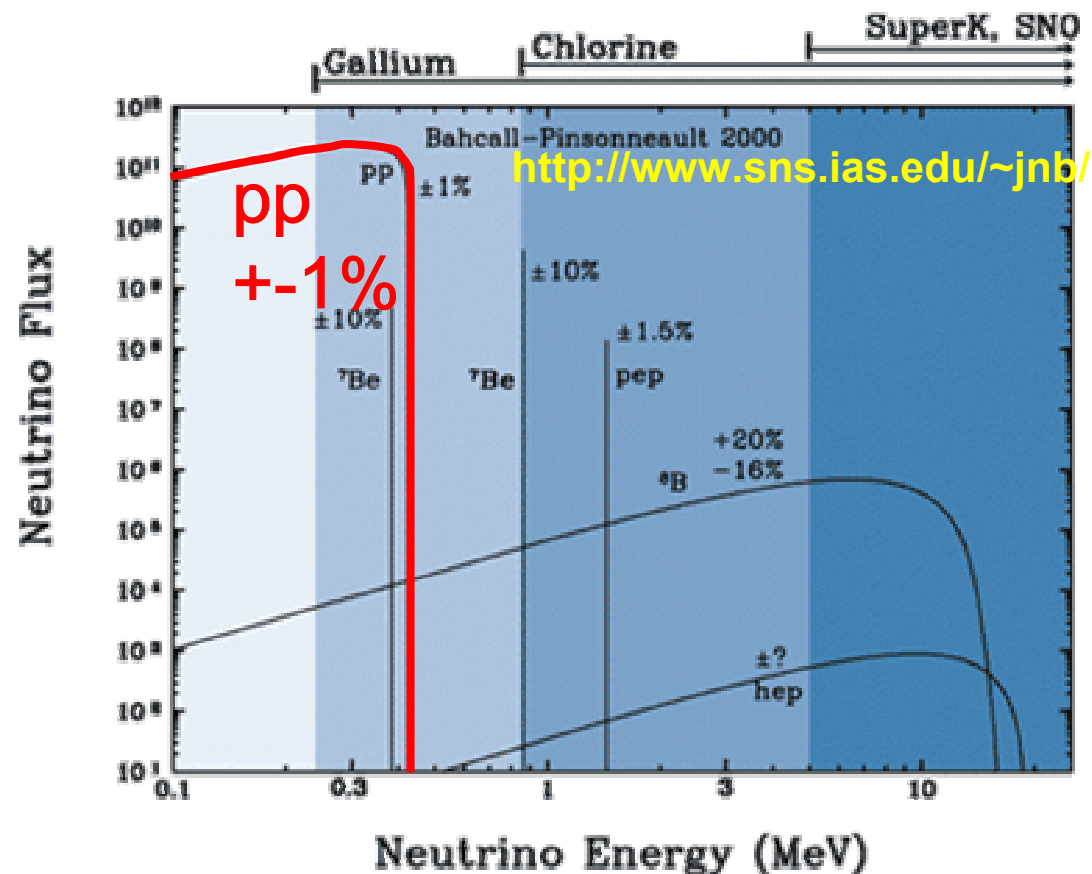
Direct search via nuclear elastic scattering



- Xenon MASSive Detector for Solar Neutrinos (pp/ ^7Be)
- Xenon Detector for Weakly Interacting MASSive Particles (Dark Matter Search)
- Xenon Neutrino MASS Detector (Double Beta Decay)

Physics goals at XMASS

Measure pp ν via $\nu + e \rightarrow \nu + e$

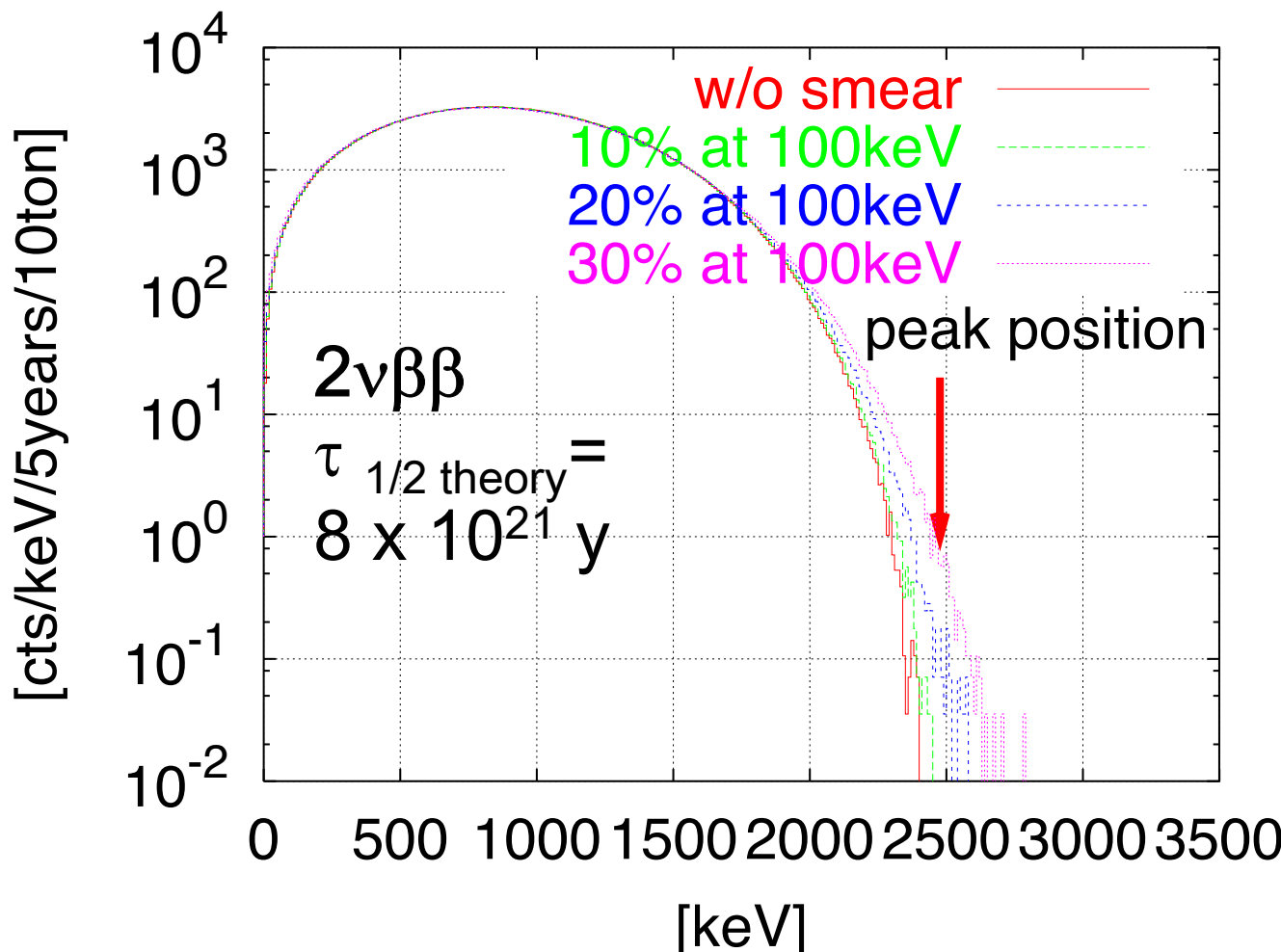


- Xenon MASSive Detector for Solar Neutrinos (pp/⁷Be)
- Xenon Detector for Weakly Interacting MASSive Particles (Dark Matter Search)
 - 2νββ life time should be measured
 - Isotope separation would be needed
- Xenon Neutrino MASS Detector (Double Beta Decay)

Physics goals at XMASS



Q-Value: 2.48 MeV



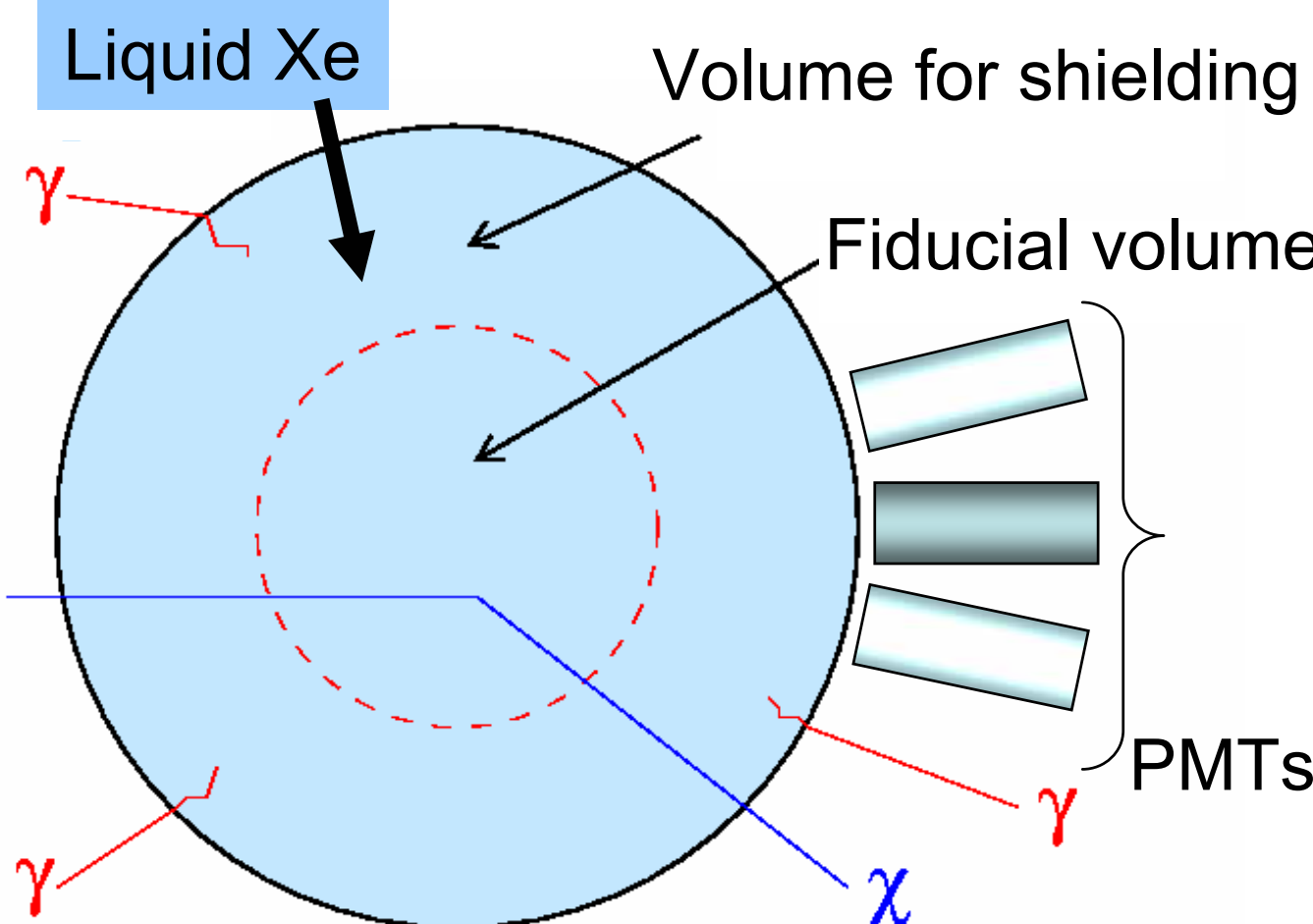
- Search for 0 $\nu\beta\beta$ (2 $\nu\beta\beta$) decay of ^{136}Xe (na 8.87%)
- High purity and enriched Xe can be used.
- Energy region is different from solar ν / DM.
- PMTs should not be placed near the detector.

→ Need another design
of the detector!
(low priority, at moment...)

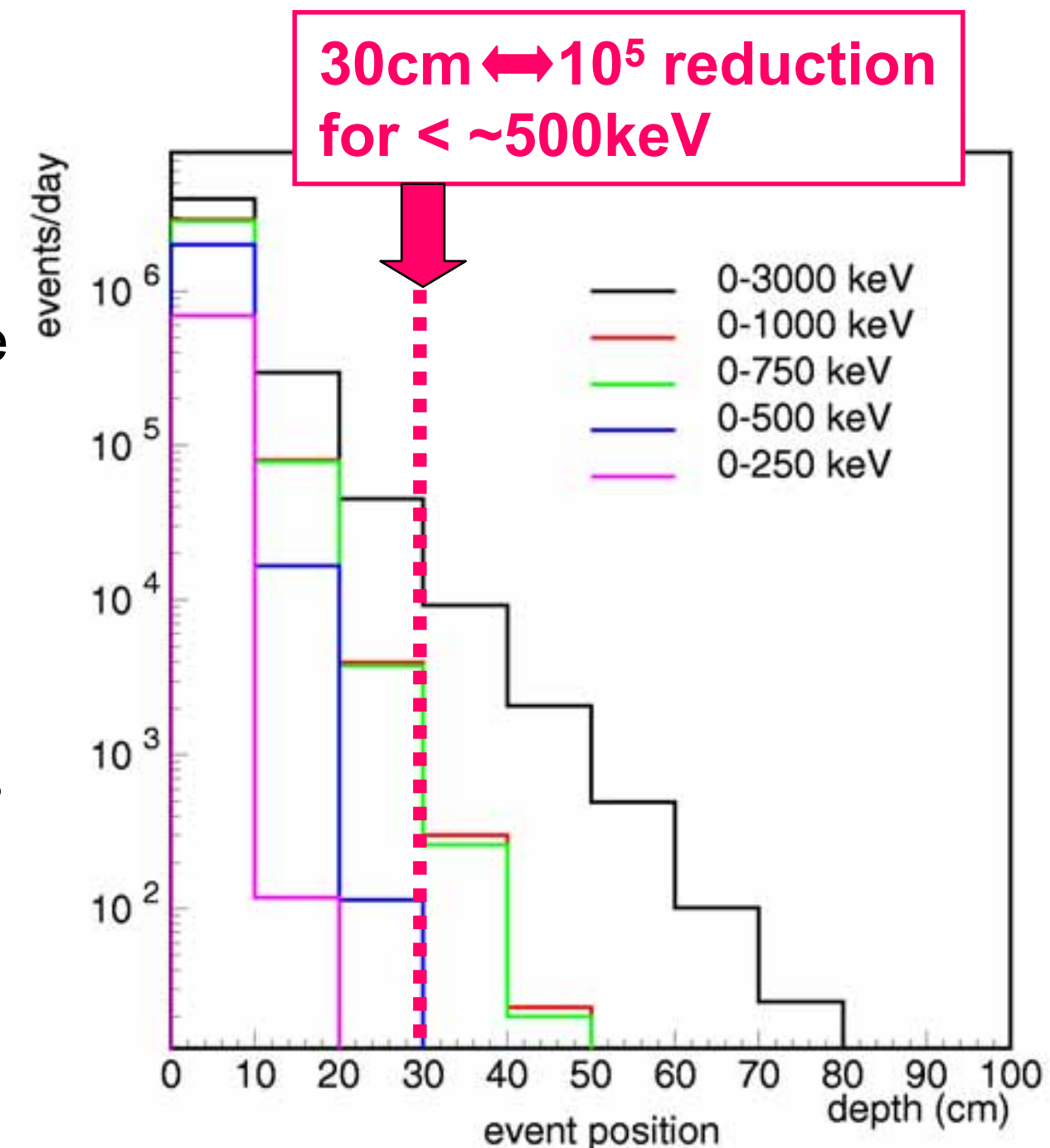
or Solar Neutrinos (pp/ ^7Be)

- Xenon Detector for weakly Interacting MASSive Particles (Dark Matter Search)
- Xenon Neutrino MASS Detector (Double Beta Decay)

Self shielding

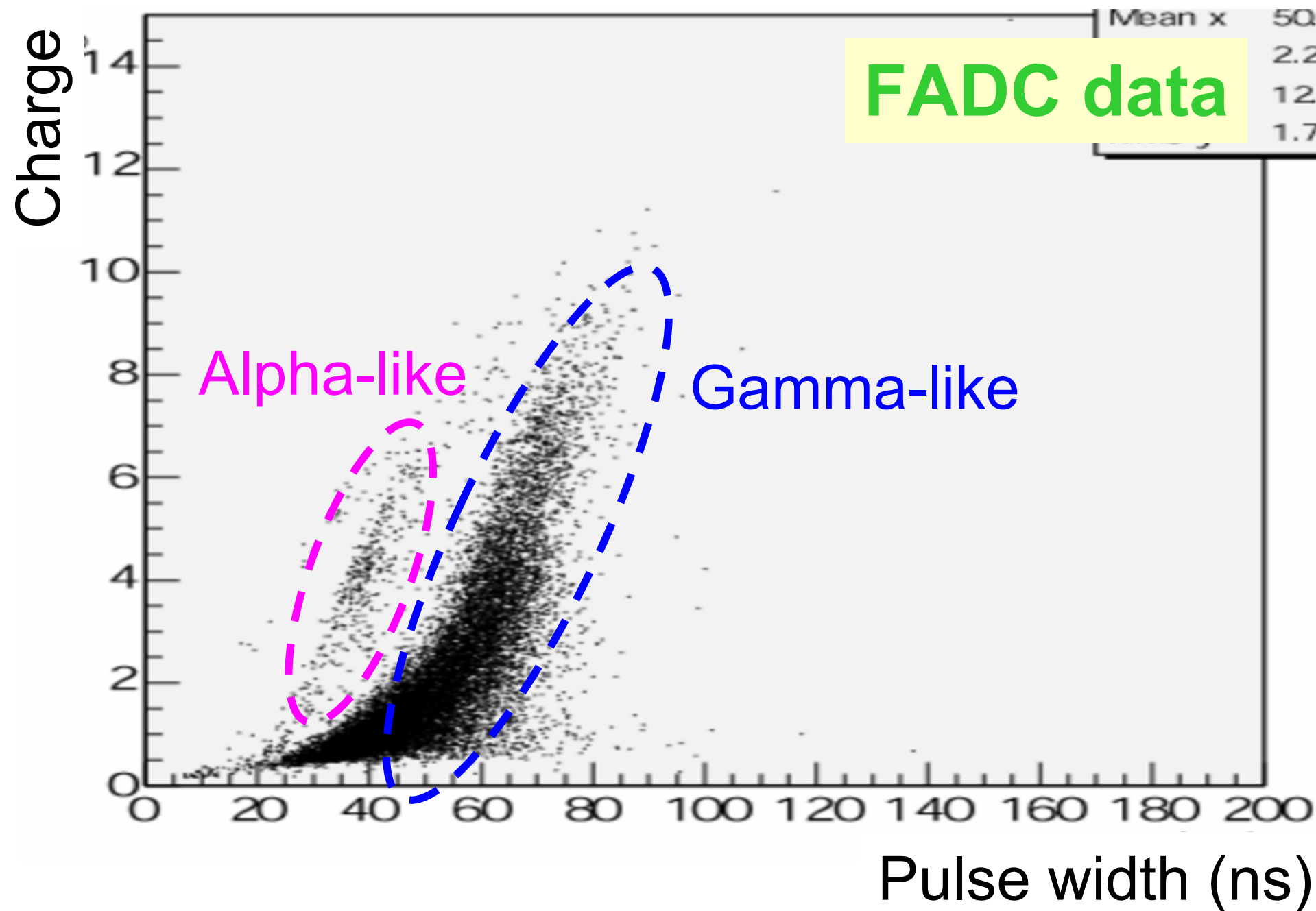


Reconstruct the vertex and energy based on PMTs information (light pattern)



- Quite effective for the events below \sim 500 keV (pp ν & DM)
- Not effective for double beta decay experiment

Alpha vs Gamma separation

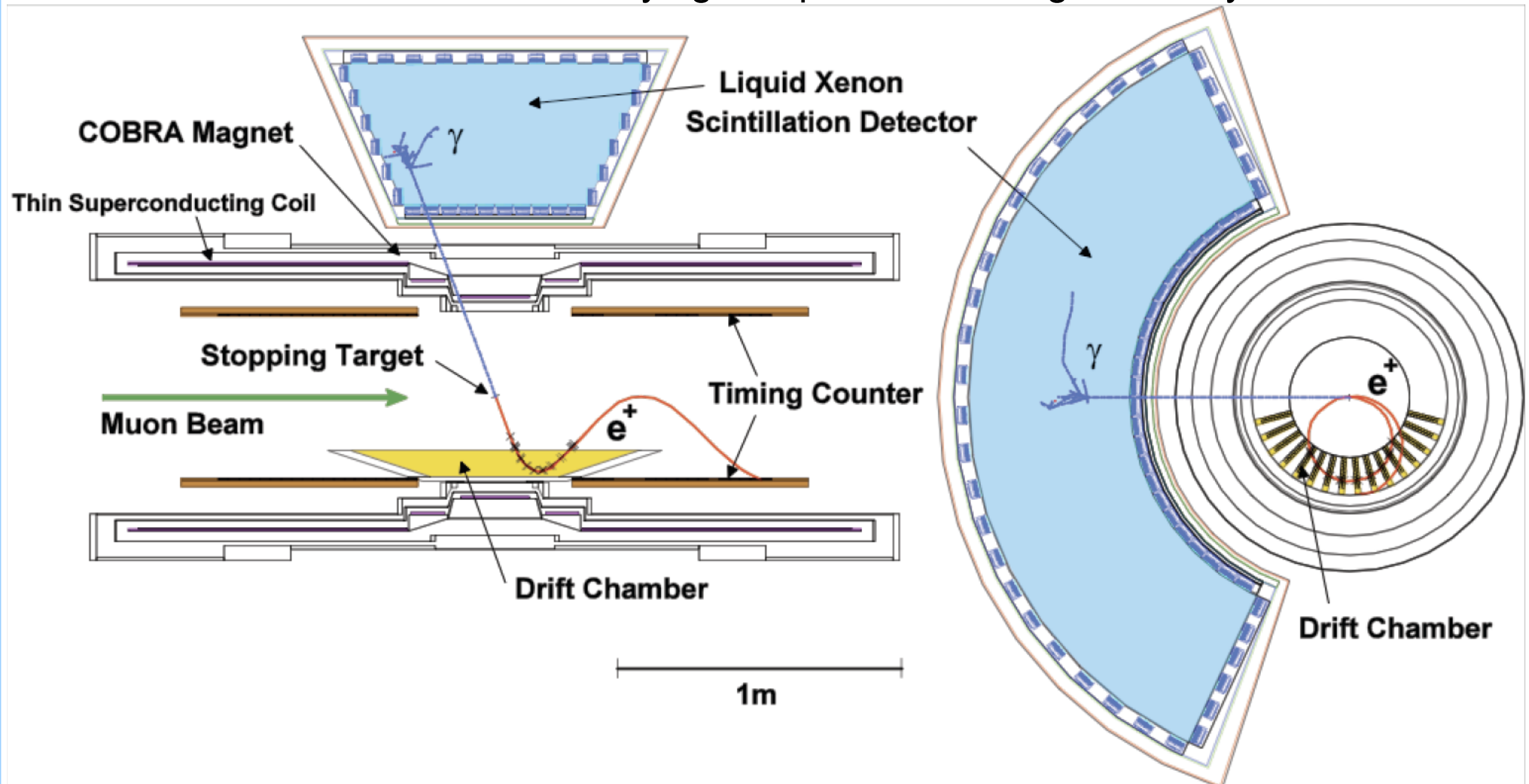


Alpha-gamma separation by using FADC wave form
would be possible (under further investigation)

MEG Detector ; 1 phase

<http://meg.web.psi.ch/>

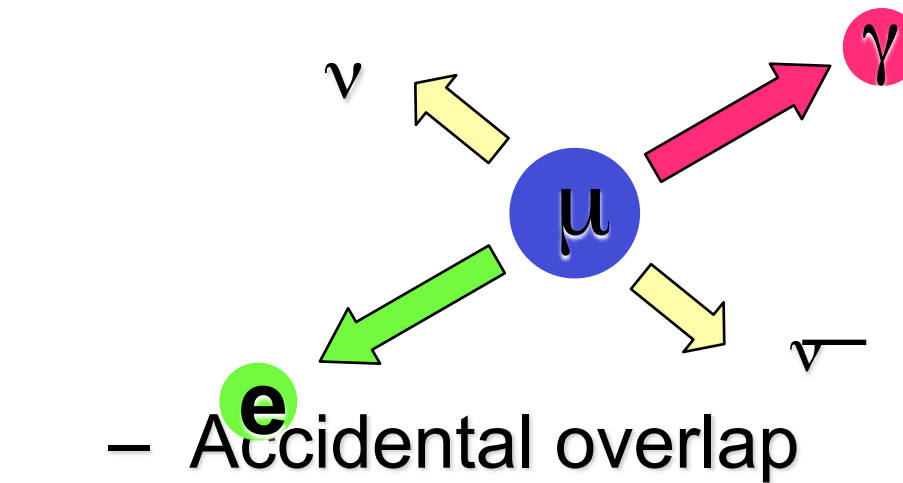
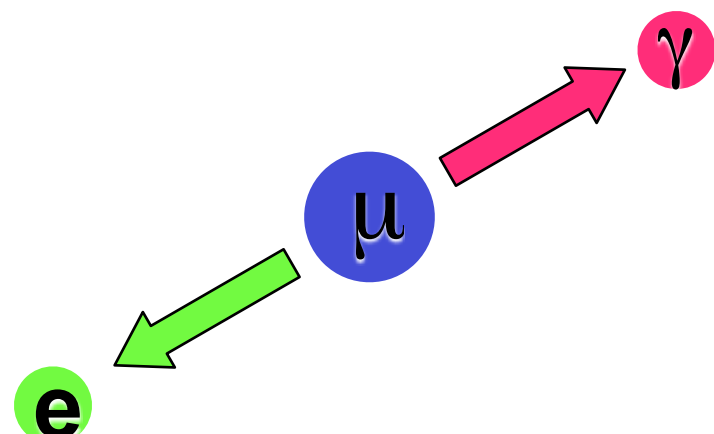
search for muons decaying into positrons and gamma rays



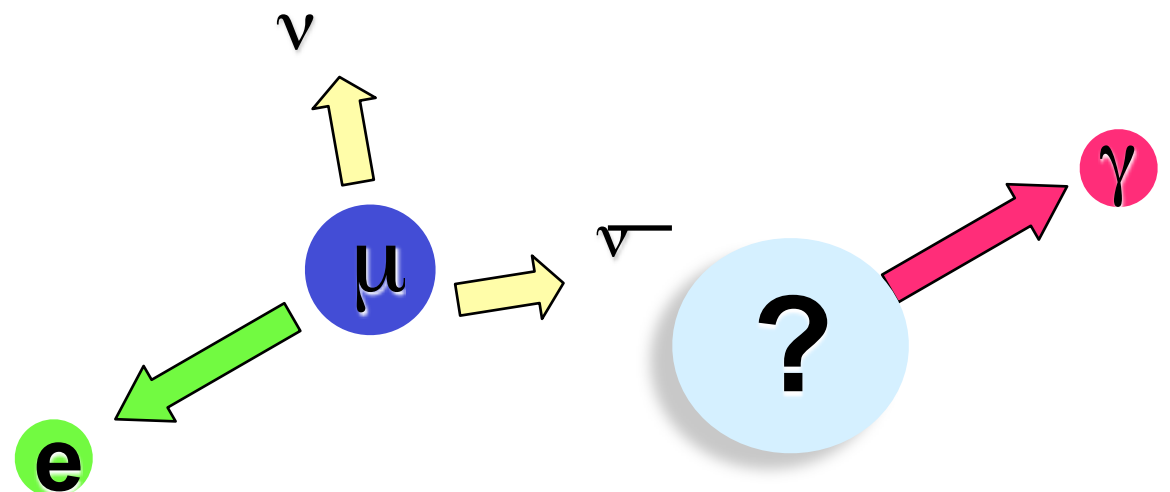
- 800~900 l liquid xenon
- 846 PMTs immersed in the liquid
- No segmentation

Signal and Background

- Signal
 - Radiative μ decay
- Background
 - Accidental overlap

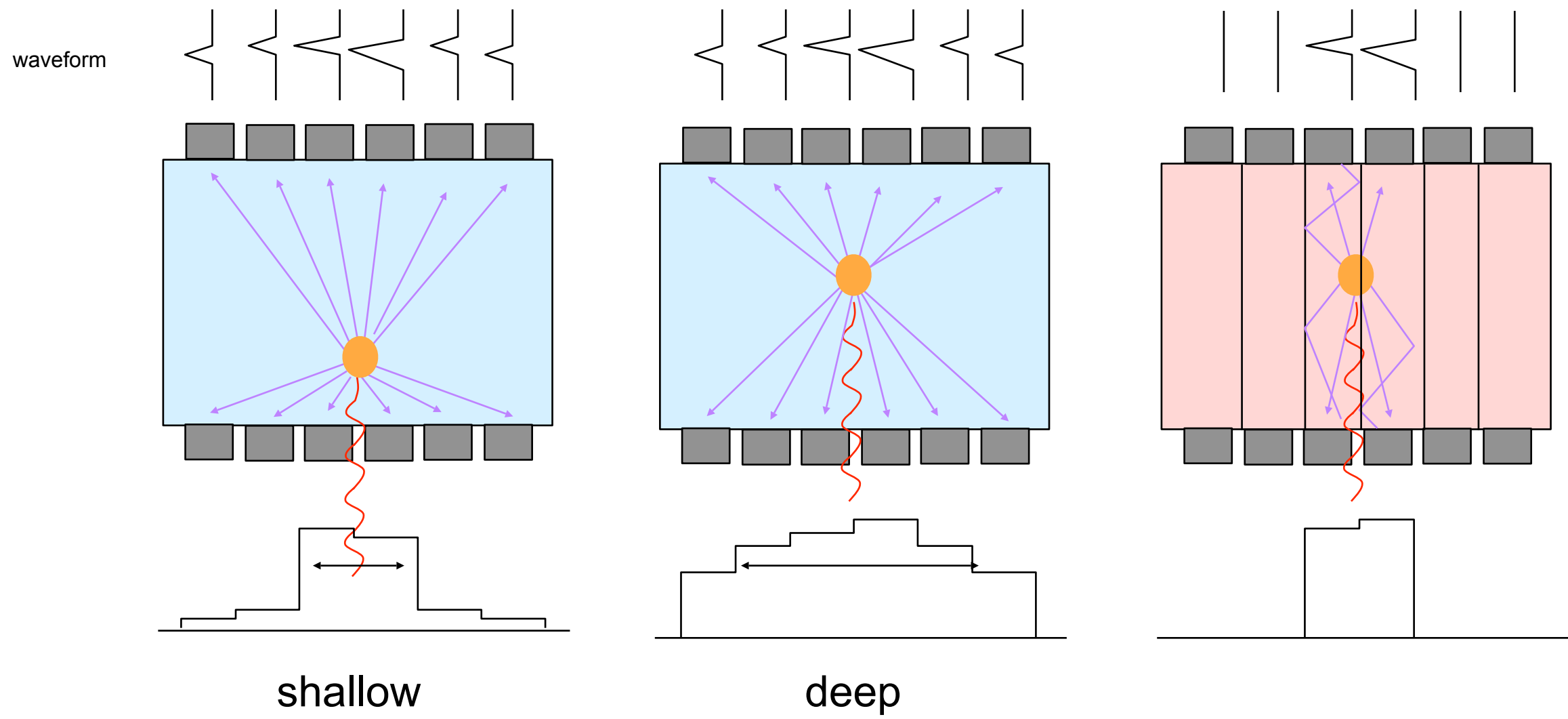


- $E_\gamma = m_\mu/2 = 52.8\text{MeV}$
- $E_e = m_\mu/2 = 52.8\text{MeV}$
- $\theta = 180^\circ$
- Time coincidence



Depth Reconstruction

- Broadness of light distribution at the entrance side



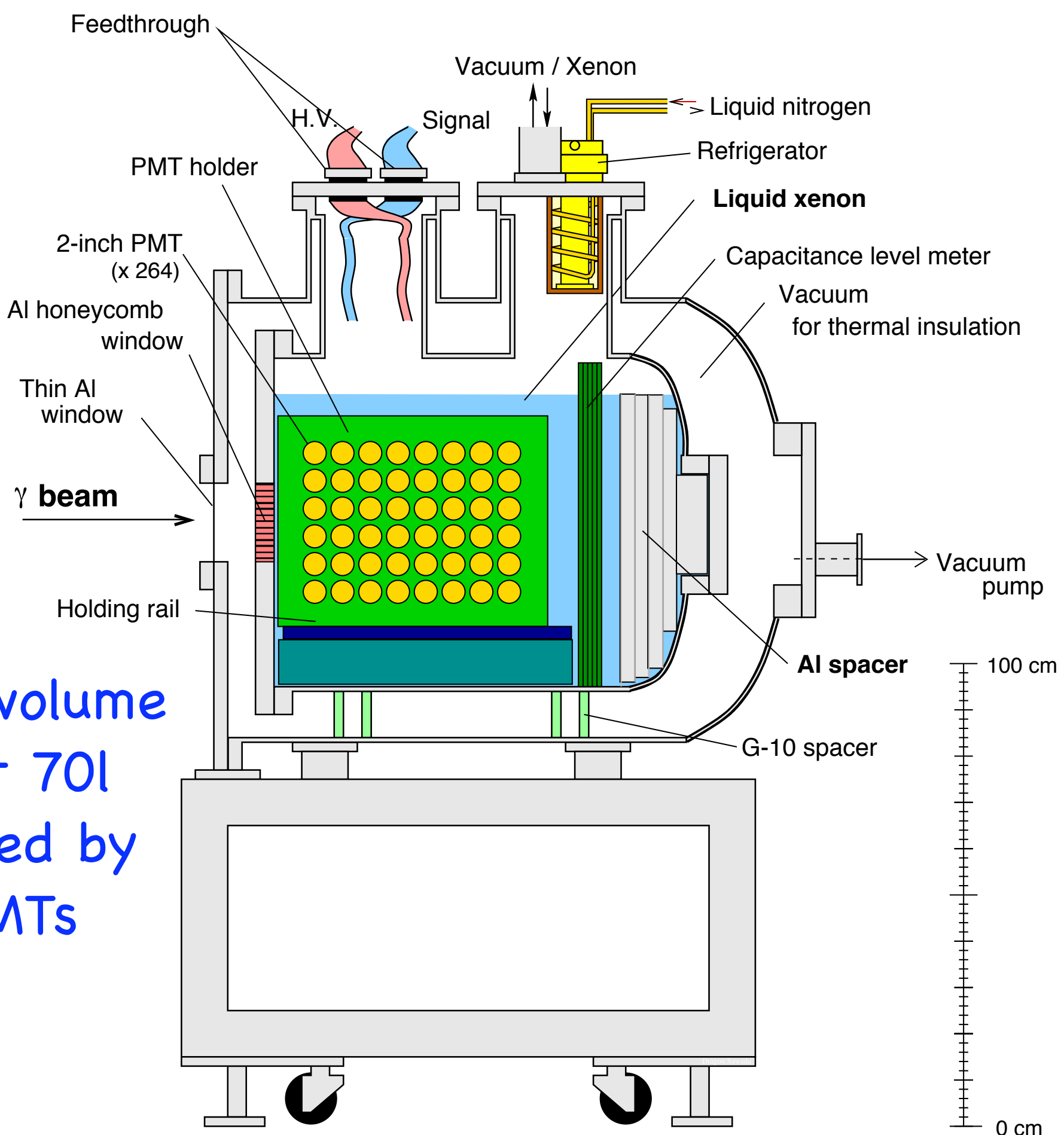


Fig. 1. Schematic view of the large prototype.

LXe-GRIT ; 1 phase

2004

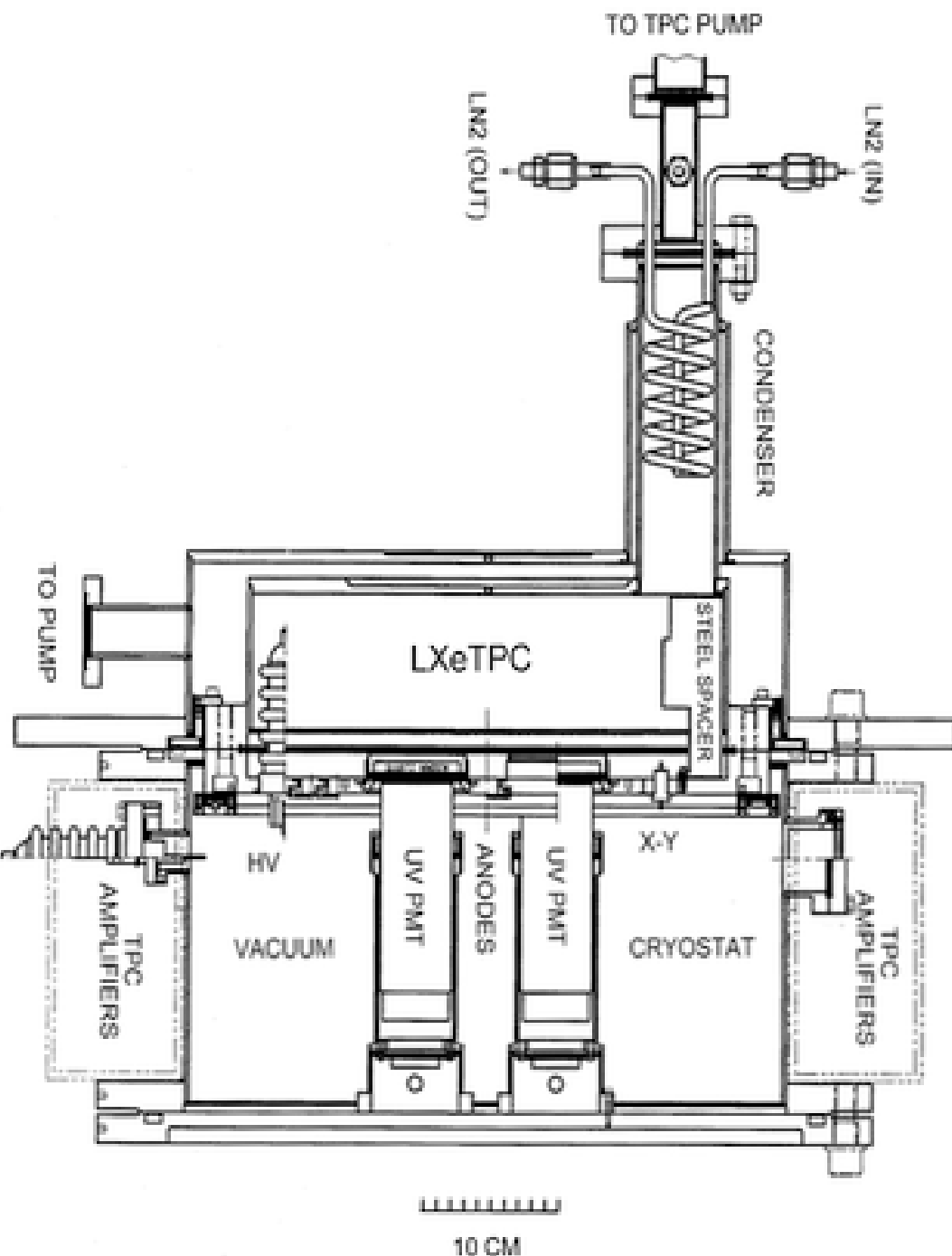
Columbia university - XENON collaboration

balloon flights(1997-2000) of the Liquid Xenon Gamma-Ray Imaging Telescope

γ energy range = 0.511 - 70MeV (e^+ - π^0)

LXeTPC (prototype of Compton telescope) with 7cm long drift

-direction of incident γ can be estimated by sequence of Compton scattering



LXeTPC : $18.6 \times 18.6 \times 7 \text{ cm}^3$ (2.4 l)

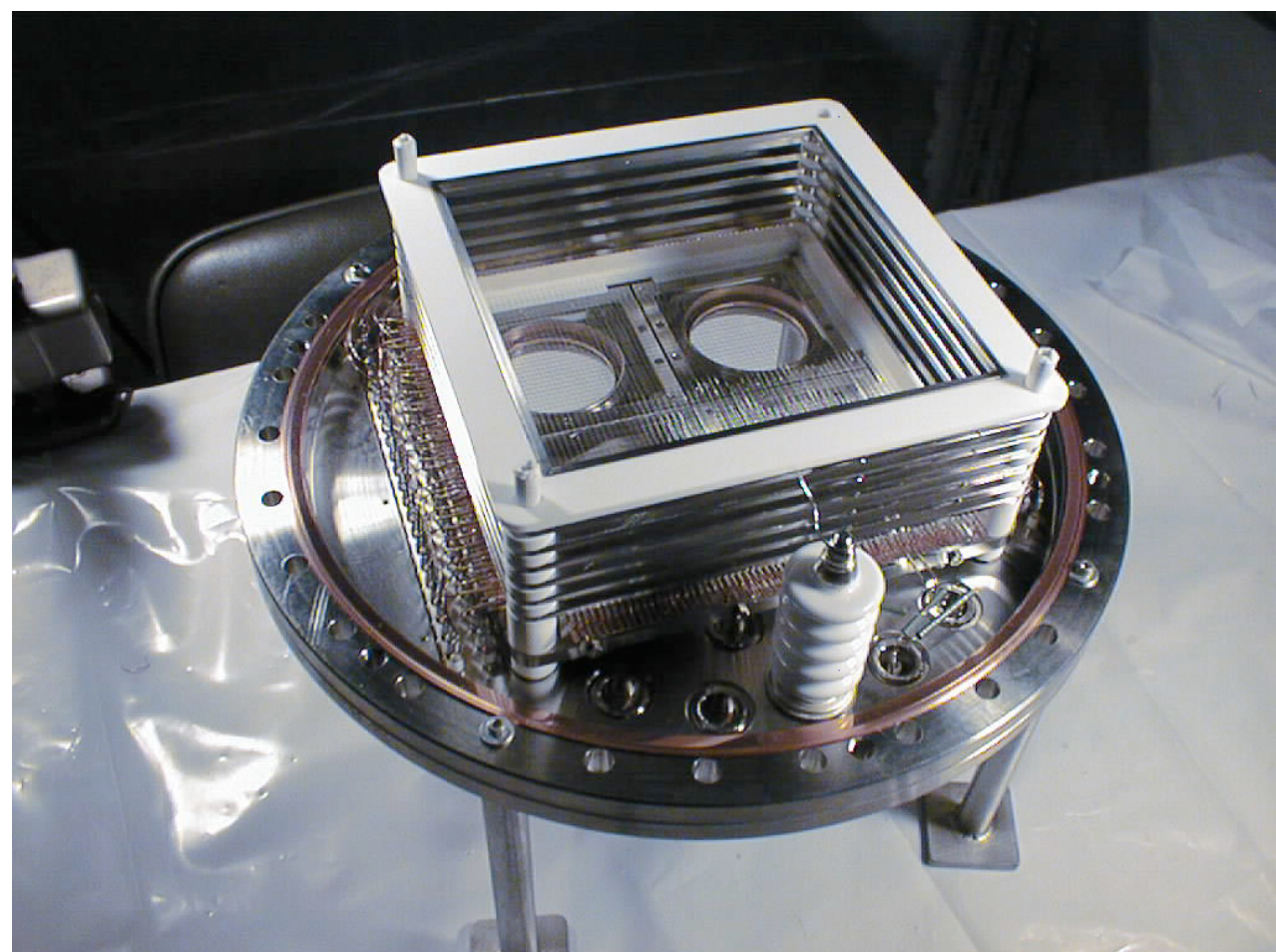


Figure 2.3: Top view of the LXeTPC with the field-shaping rings. The ceramic HV feedthrough is visible in the lower part of the picture.

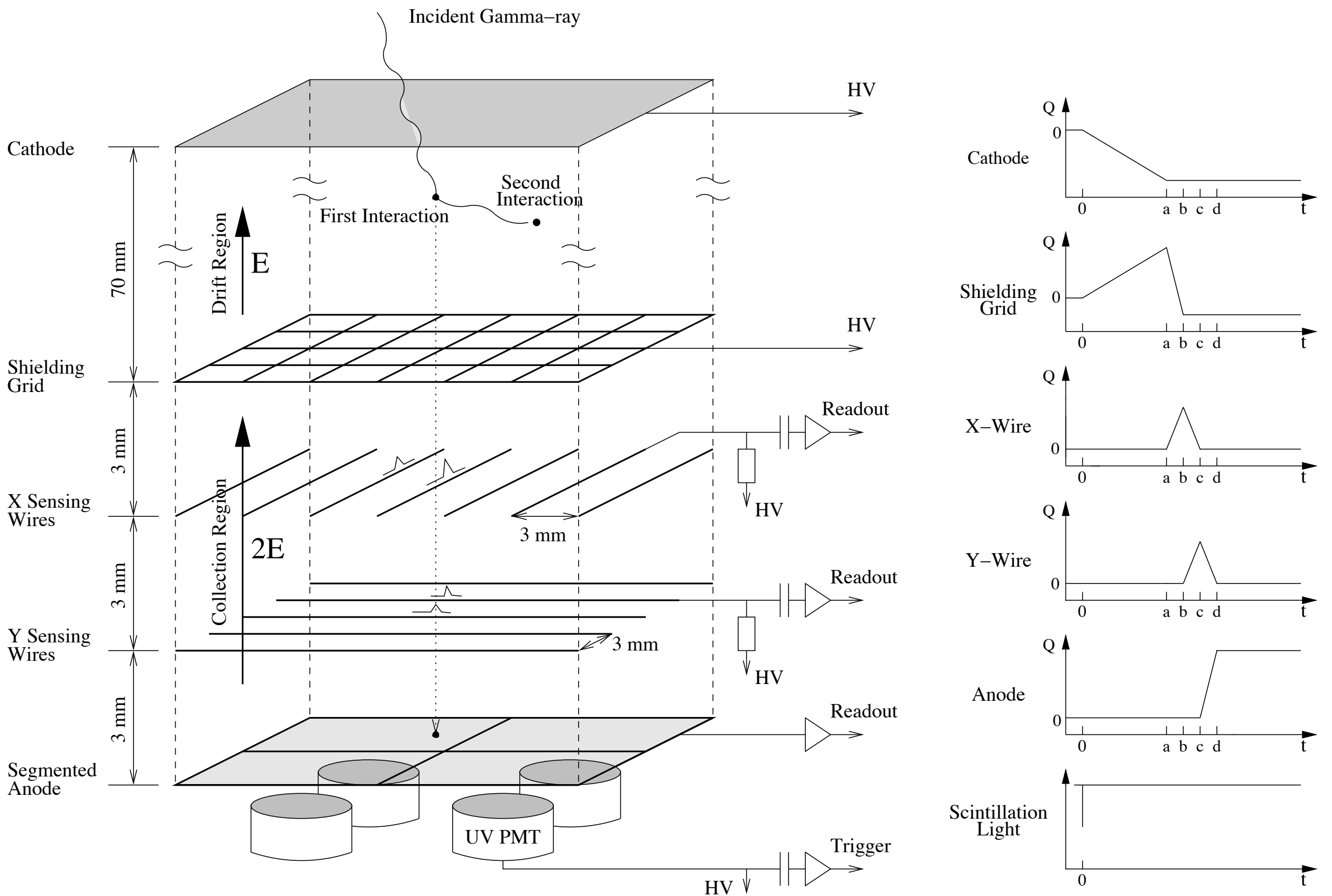


Figure 2.6: Schematic of the LXeTPC read-out structure with corresponding light trigger and charge signals (from (98) and (74)).

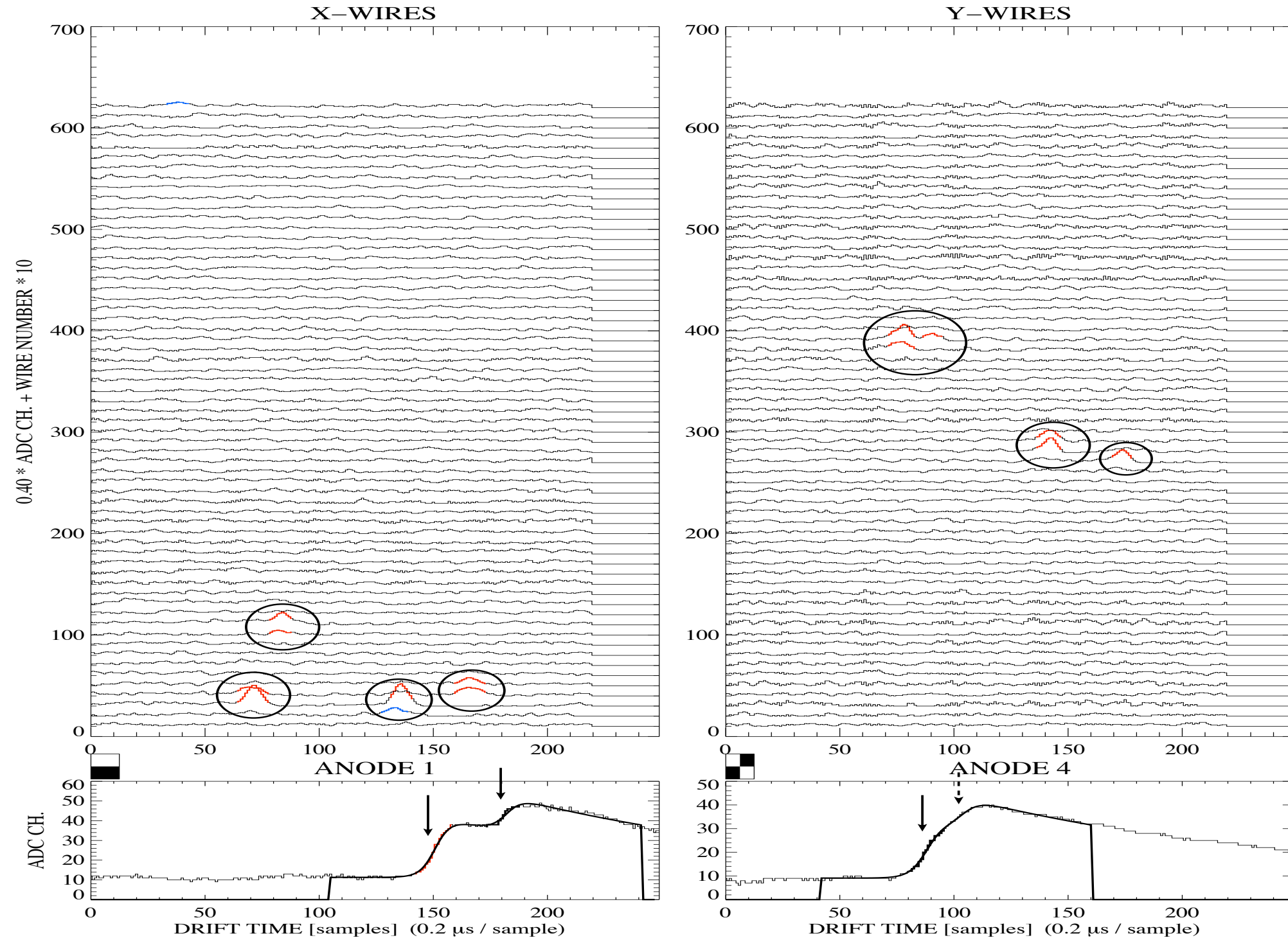


Figure 2.9: Digitized waveforms on wires and active anodes as a function of drift time in FADC samples, for an ^{88}Y 1836 keV γ -ray event with 4 interactions. The upper panels show all wire waveforms, in scaled units of ADC channels, each separated by an offset. Matched wire signals are indicated by circles, and only their corresponding anodes are shown. The wire-anode correspondence is indicated by the dark fields at the top left corner of each anode display. The solid arrows mark three steps found by the anode signal algorithm, and the dashed arrow marks an additional step, included in the fit (smooth solid line) after signal recognition on the wires (from Ref. (74)).

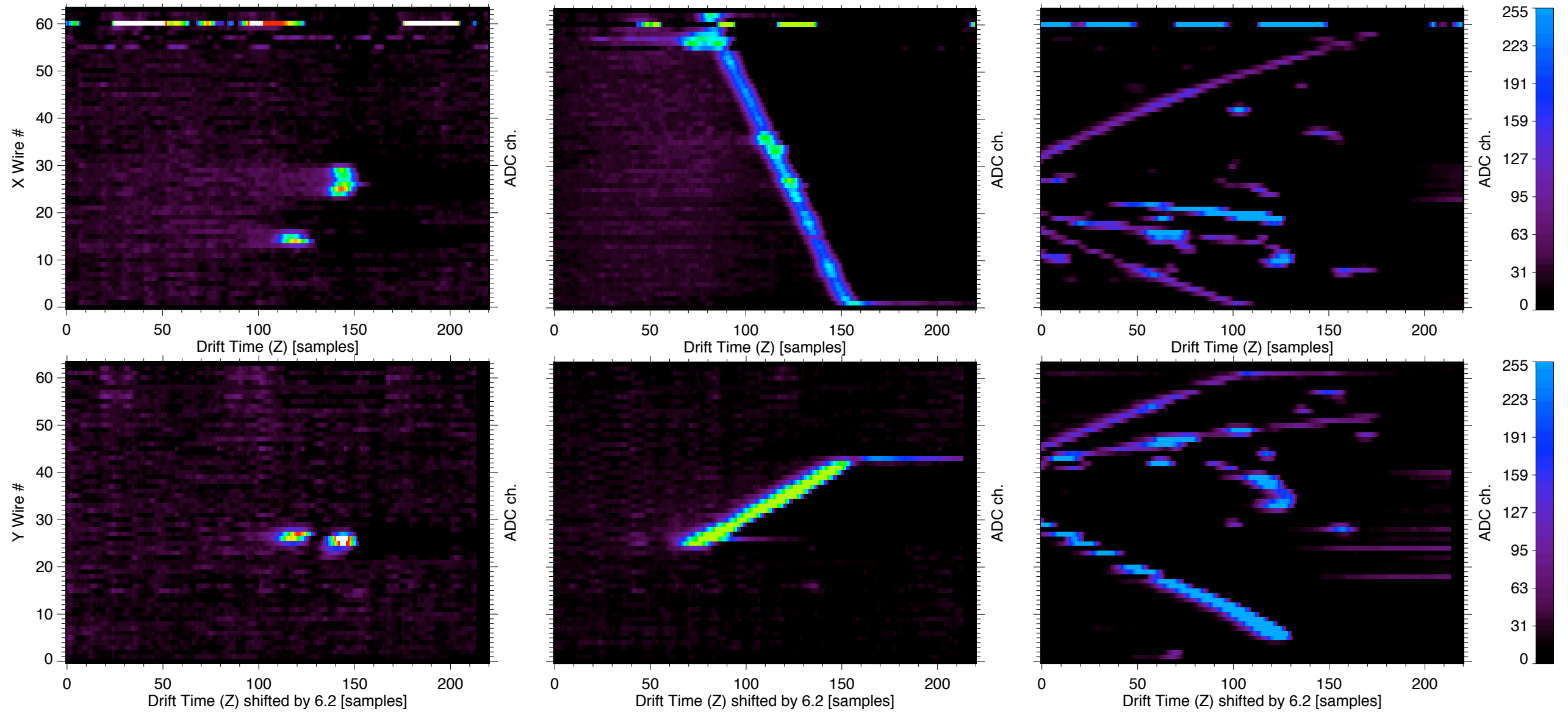


Figure 5.7: “Snapshots” of three different events in the LXeTPC recorded during the balloon flight in year 2000; for each of them the X-Z view and the Y-Z view are shown. *Left:* a 2-site γ -ray interaction. *Center:* a relativistic particle passing through the fiducial volume. Several δ -rays are visible in the X-Z view. *Right:* a more complex interaction with several particles detected in the fiducial volume. The vertex happens below the fiducial volume, i.e. at $Z < 0$.



Figure A.4: The LXeGRIT gondola on the launch pad at the National Scientific Balloon Facility (NSBF) in Ft. Sumner, NM, on May 7, 1999 at 7:26:54 local time (13:26:54 UT).

LXe TPC PET ; 1 phase

2005

Subatech, Ecole des Mines de Nantes, IN2P3- CNRS and Université de Nantes, France 1 Service de médecine nucléaire, Hôpital de Nantes, France

$1 \times 1 \times 9 \text{ cm}^3$ cell ; a module of $24 \times 60 \times 9 \text{ cm}^3$ 9cm drift
 $24 \times 60 \text{ cm}^3$ anode place segmented by $0.5 \times 0.5 \text{ mm}^2$ pads

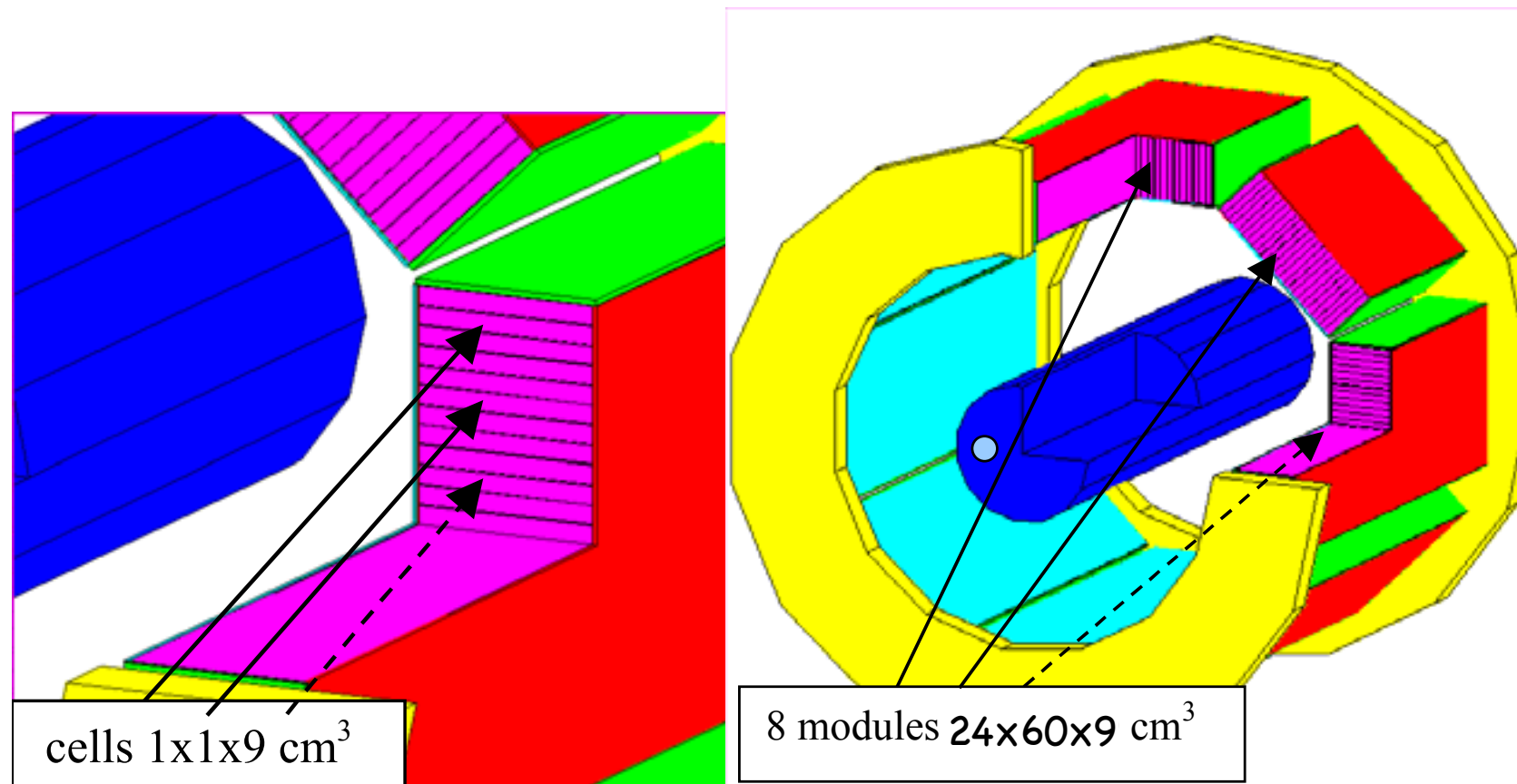


Fig. 1. GEANT3 simulation of a LXe PET camera with a NEMA NU 2-2001 phantom (right) and zoom on individual cells (left). The ^{18}F source is homogeneously distributed in a 3 mm diameter and 70 cm length cylinder positioned at ($x=4.5 \text{ cm}$, $y=0 \text{ cm}$) in the transverse field of view.

250, 250 and 140 μm (FWHM) for x, y and z coordinates
for γ -conversion point

PET camera	Activity (kBq/ml)	Sensitivity – Net Trues (cps/Bq/ml)	Spatial cut (spatial resolution FWHM) (mm)	Energy resolution (FWHM)
BGO	3	30	10 (~7)	26.7
LXe	0.4	190	3 (~1.7)	13.8

Table 1: Performances of the proposed LXe-TPC PET compared to a standard BGO PET camera.

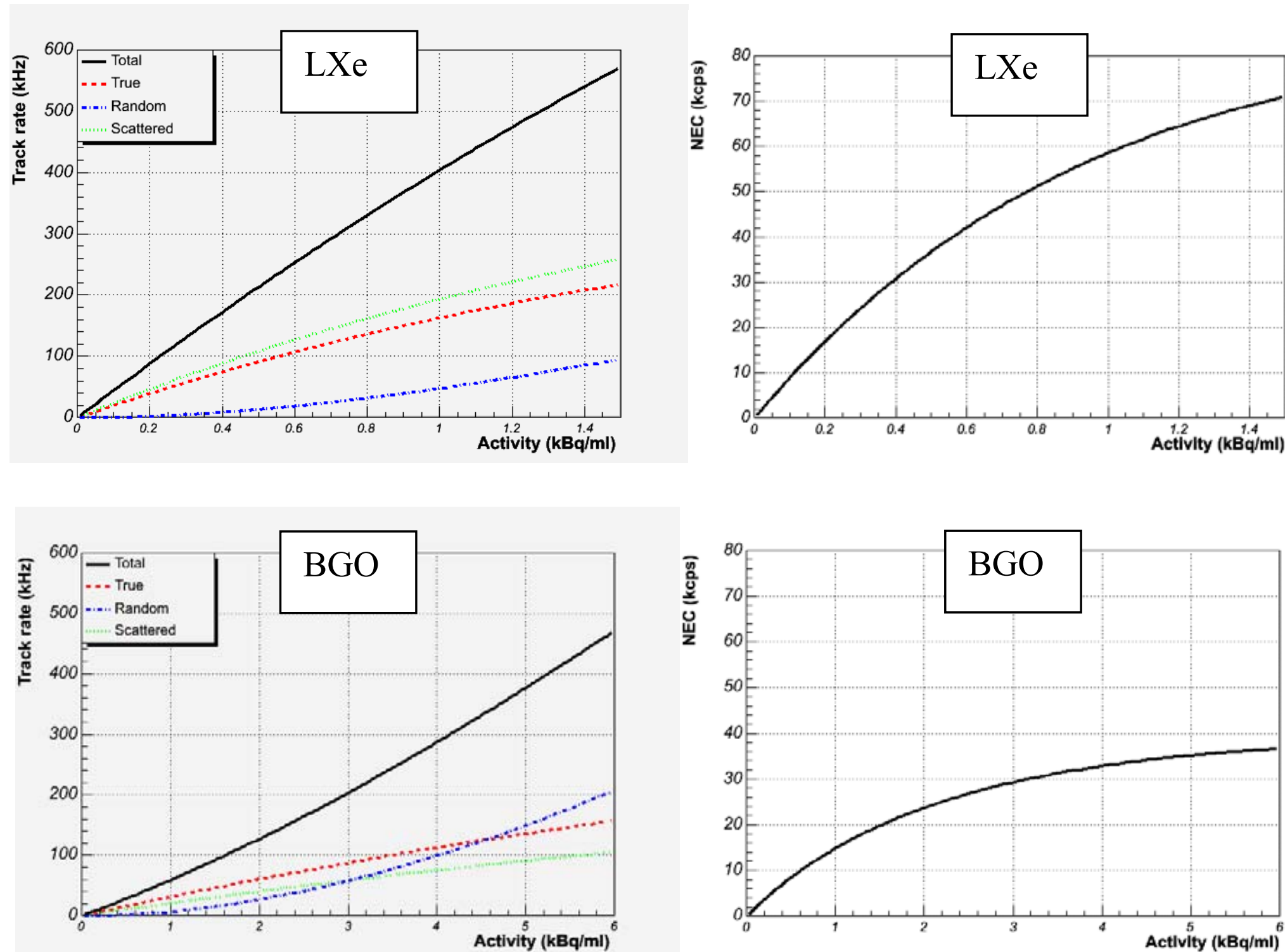


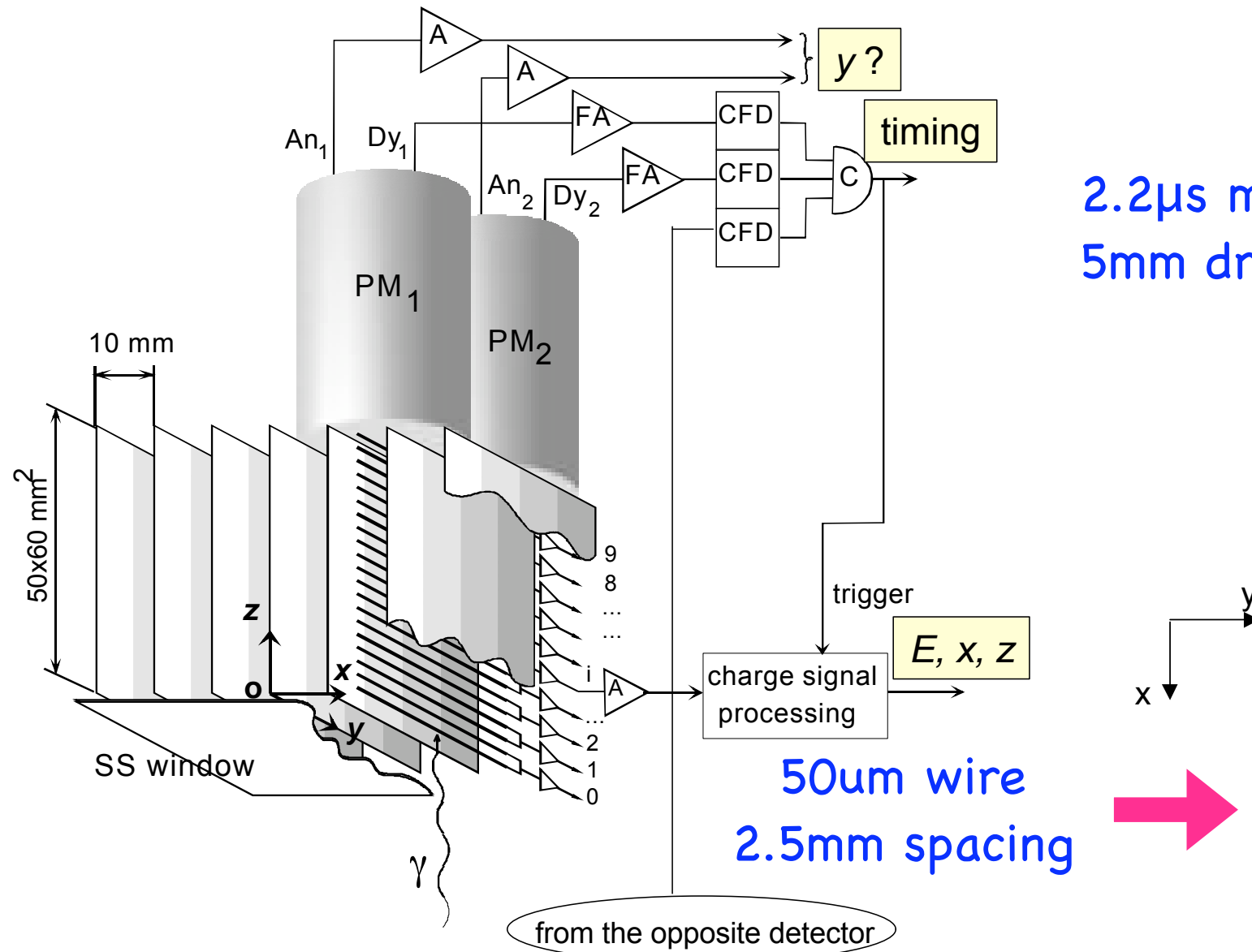
Fig. 5. Track rate for true, scattered and random events (left) and NEC (right) as a function of the activity concentration for the proposed LXe-TPC PET (top) and the standard BGO camera (bottom).

PETYA ; 1 phase

2002

LIP-Coimbra and Department of Physics of the University of Coimbra,
3004-516 Coimbra, Portugal

segmented drift chamber with PMT $1 \times 5 \times 6 \text{cm}^3$ cell (LXe 6cm long)



$2.2 \mu\text{s}$ max. collection time
5mm drift

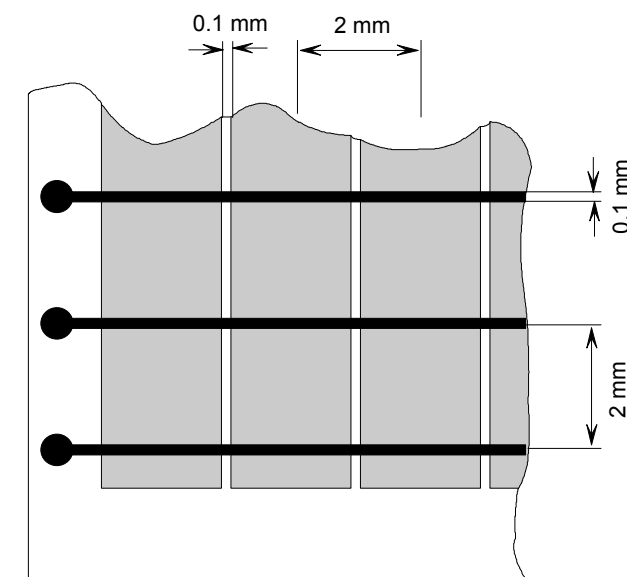


Figure 4. The mini-strip plate.

Figure 2. A schematic of the liquid xenon module for PET and its readout system.

$800 \mu\text{m}, 800 \mu\text{m}, 2 \text{mm}$ (FWHM) for x, y, z coordinates

Compare to the crystal, the reconstruction of the event topology is possible so that the first interaction in the detector can be found and its position used in the image reconstruction.

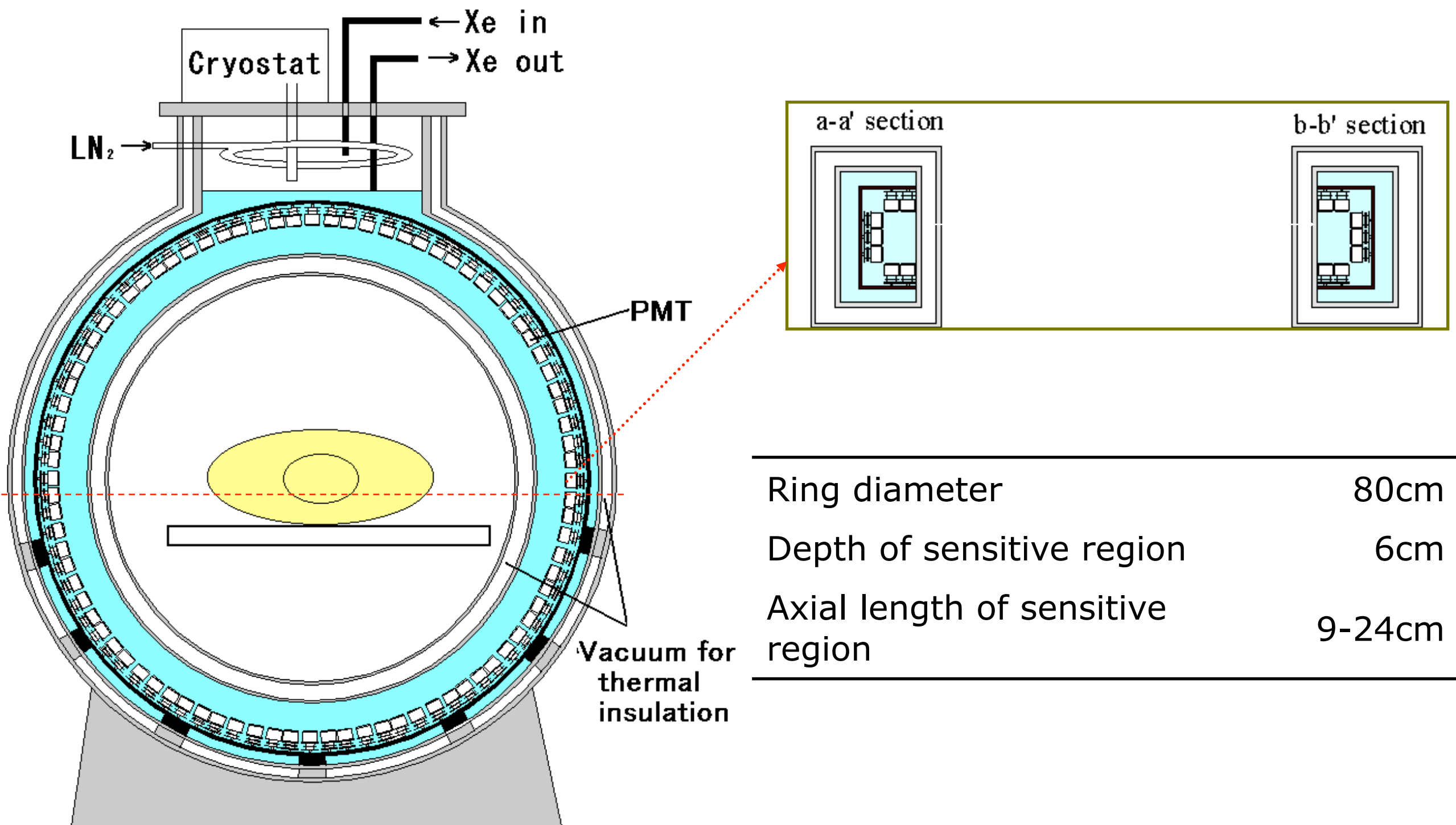
Table 1. Comparison of the liquid xenon detector with scintillation crystal systems

	PETYA	BGO block detector [20]	LSO block detector (CTI) [21]
Time resolution	1.3 ns	2 ns	1.5 ns
Position resolution	$0.8 \times 0.8 \text{ mm}^2$ (*)	$5 \times 5 \text{ mm}^2$	$2 \times 2 \text{ mm}^2$
Interaction depth resolution	2 to 5 mm	None	7.5 mm
Energy resolution	15% to 17%	20%	14% to 20% (**)
Efficiency	60%	80%	not quoted
Dead time	$50 \mu\text{s}\cdot\text{cm}^2$	$25 \mu\text{s}\cdot\text{cm}^2$	not quoted

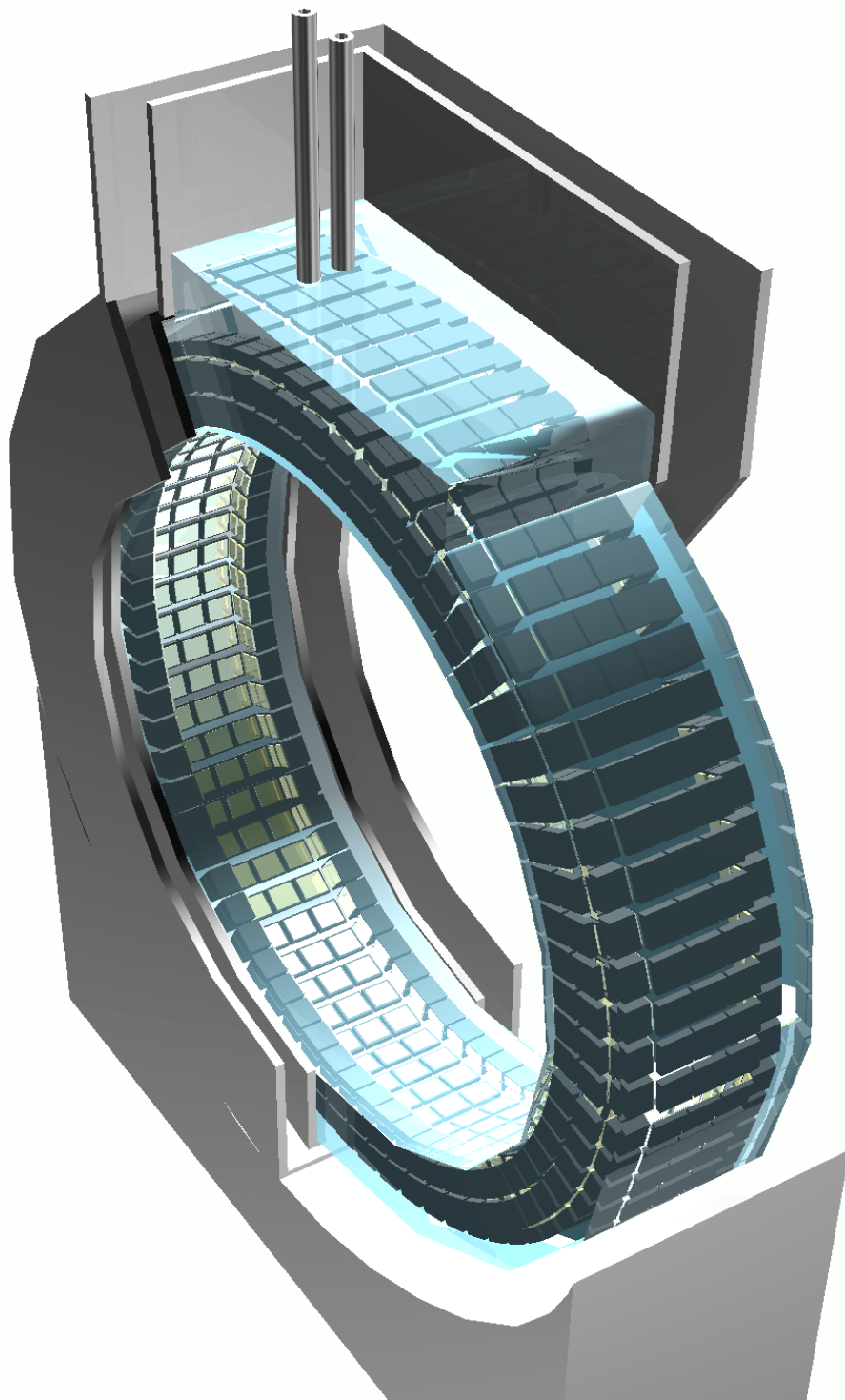
* $\Delta x \times \Delta y$; Δx - from the drift time measurement; Δy – obtained with the center of gravity method with the mini-strip plate (extrapolated from the measurements with α -source and convoluted with the photoelectron range)

** for a single crystal

液体キセノンTOF-PET装置



再構成画像による評価

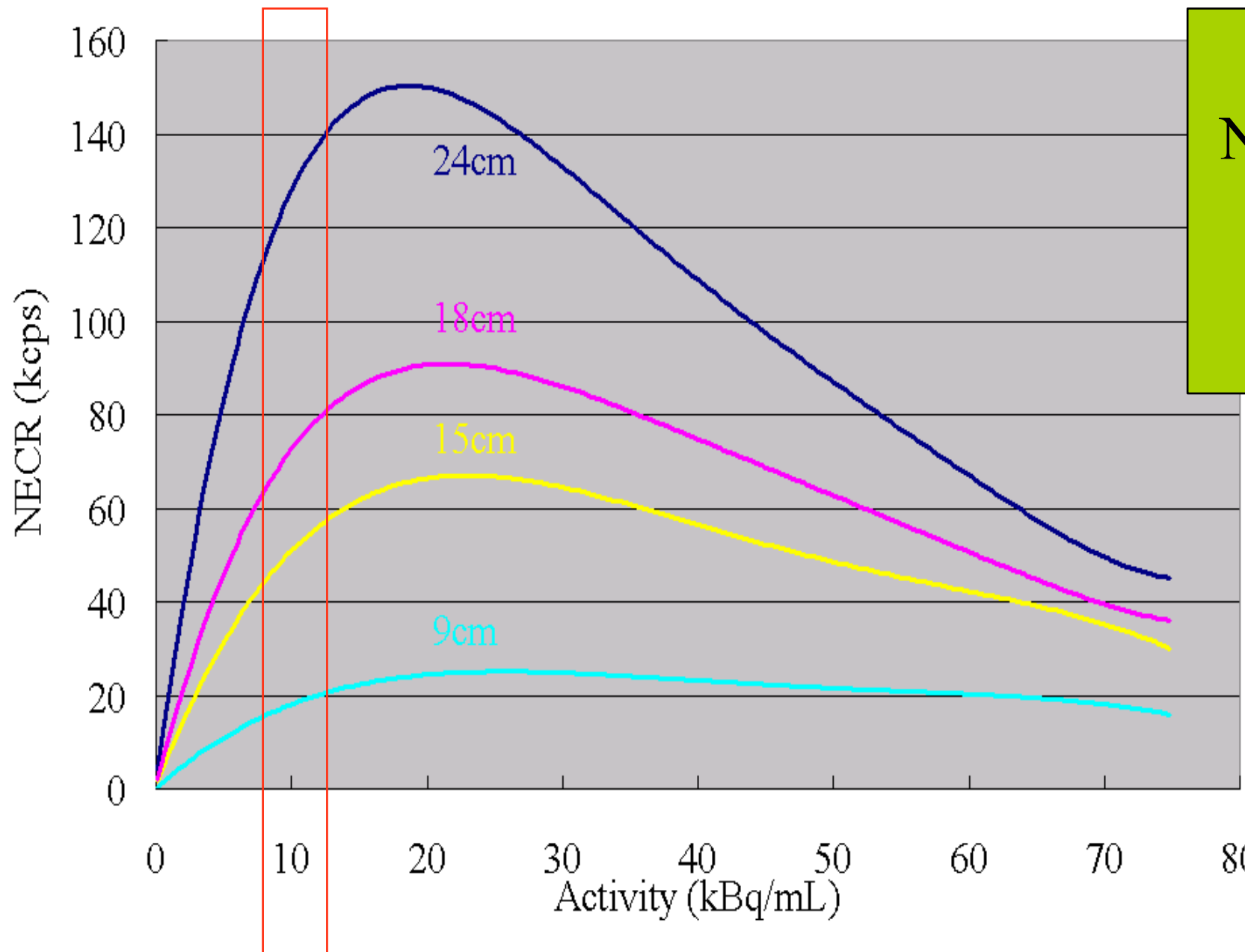


実機を想定したリング型の検出器を仮定してシミュレーションを行い、現段階のプロトタイプ実験で得られている基本特性で、画像を再構成した場合に液体**XePET**がどの程度の性能を発揮するのかを評価する。

- ポイントソースを使った分解能評価。
- **TOF**を使った再構成画像と通常の再構成を行った場合の比較評価。

全身用液体XePETイメージ図

NECR



$$\text{NECR} = \frac{T^2}{T+S+R}$$

T: 真の同時計数イベント
S: 散乱同時計数イベント
R: 偶発同時計数イベント

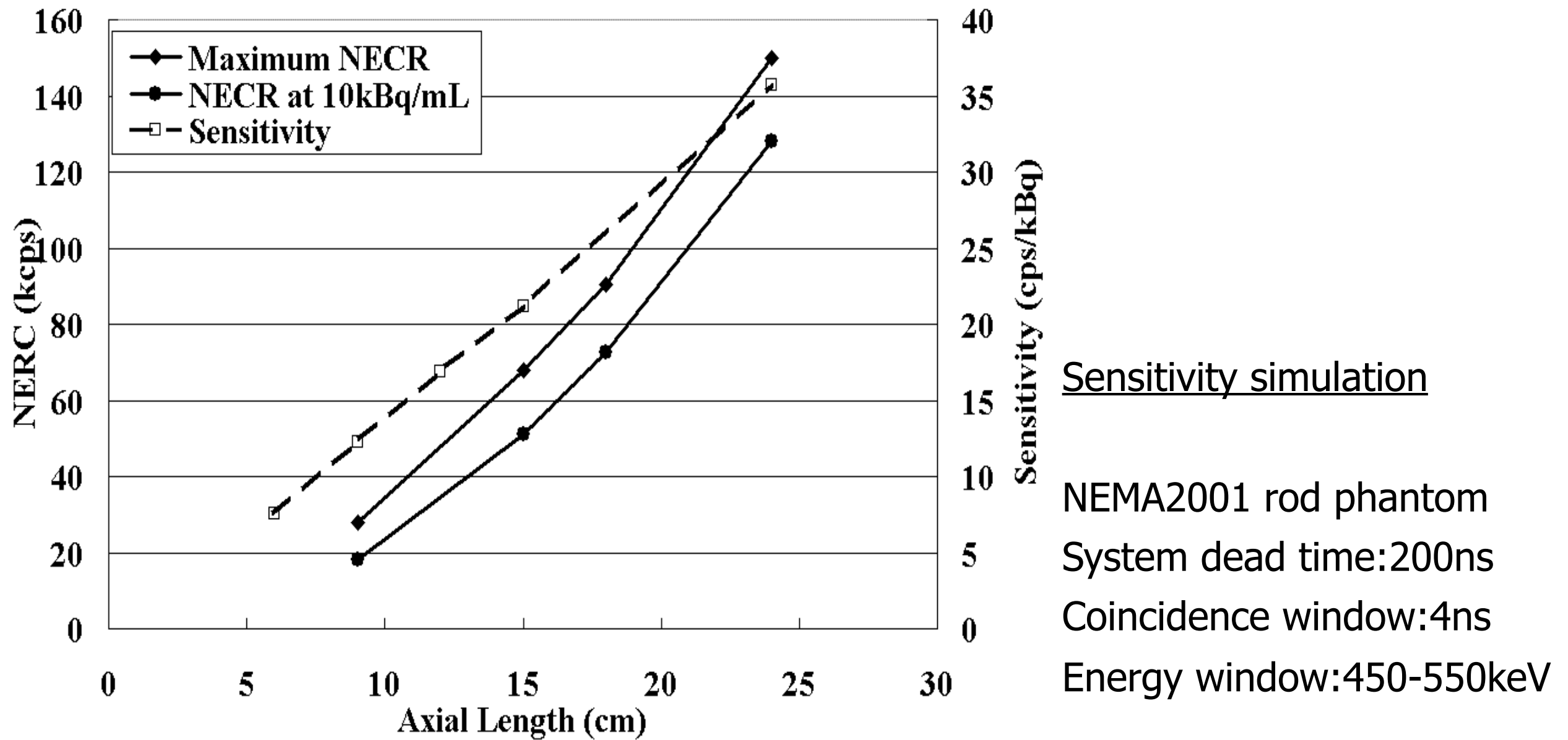
NEC simulation

System dead time: 200ns

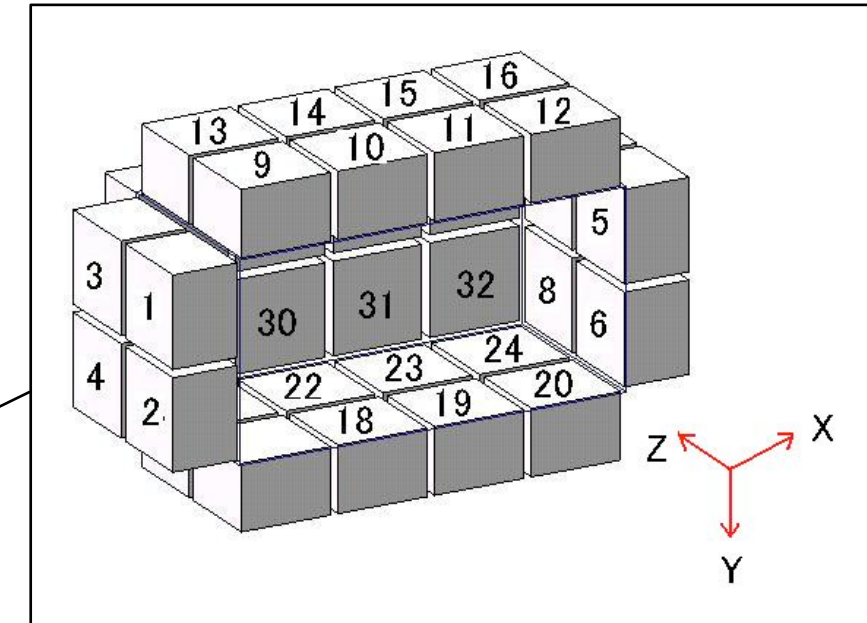
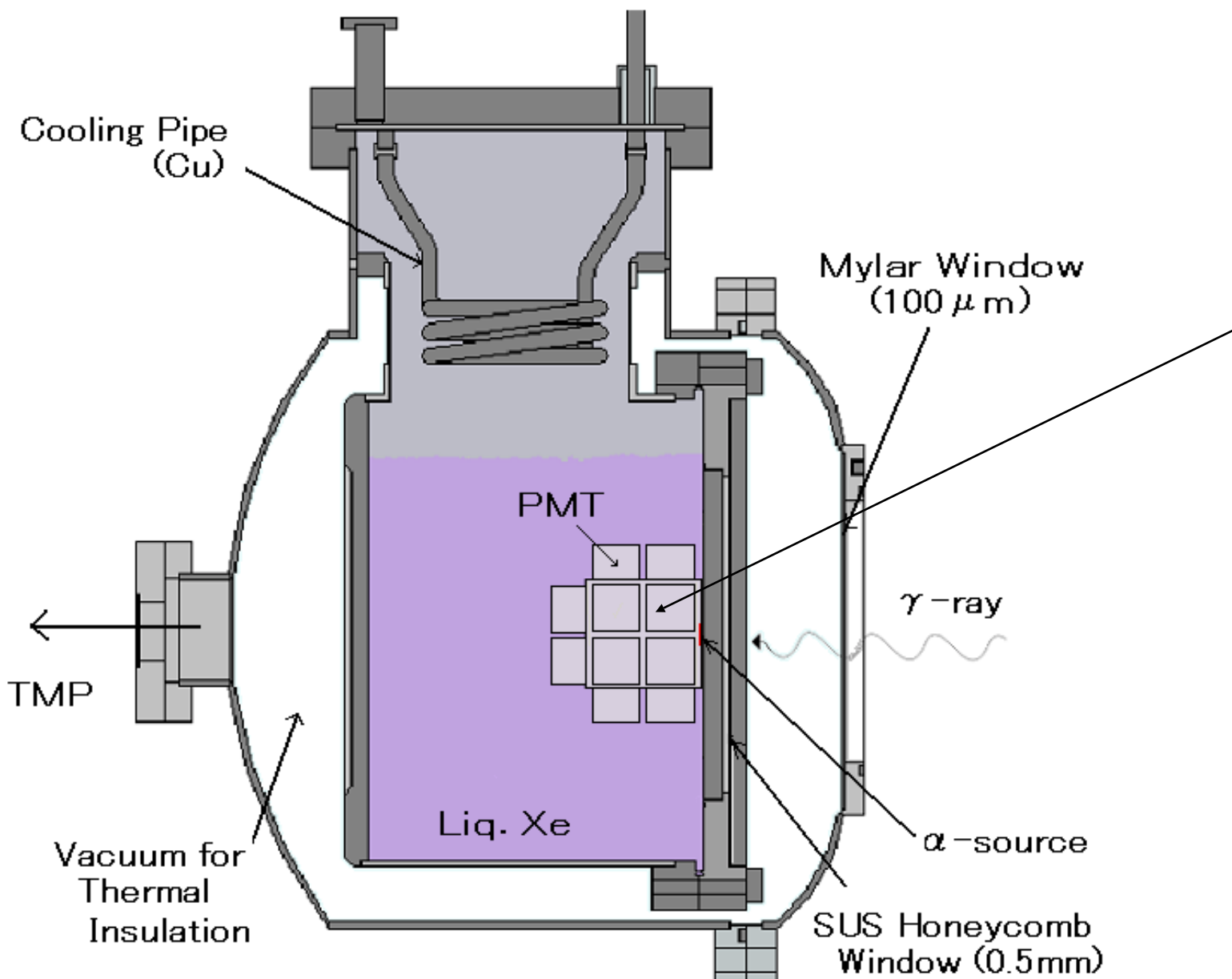
Coincidence window: 4ns

Energy window: 450-550keV

装置感度



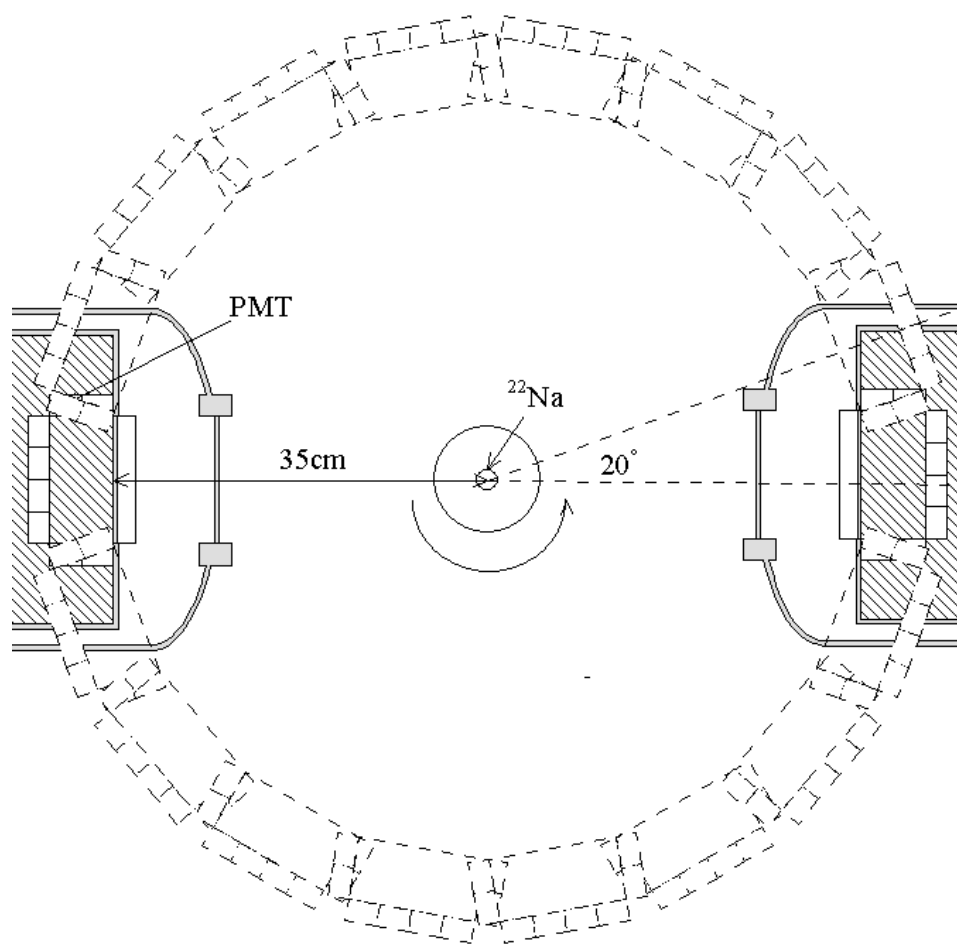
試作型液体キセノンPET検出器



温度 **-110°C**
圧力 **1~2atm**
有感領域 **12×6×6cm³**
到達真空度 **10⁻⁶Torr**
32PMT
R5900-06MOD×32
liquid Xe 12L

試作型液体キセノンPET検出器

画像再構成



再構成条件

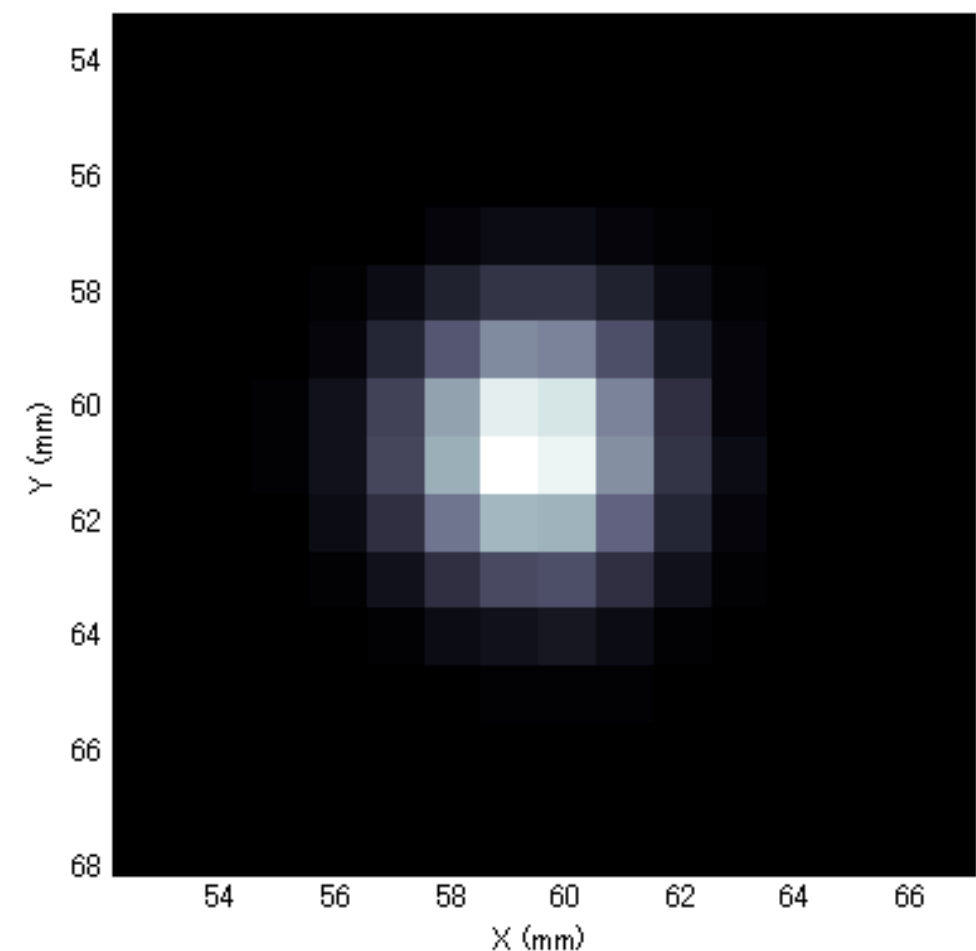
ML-EM法

反復回数100回

-5 < Y < 5 の範囲を用いる

→ 2Dモードを仮定

^{22}Na 点線源の再構成画像



空間分解能: 3.3mm(FWHM)

2 Phase

LXeComp (TPC) $\beta+\gamma$; 2 phase

2006

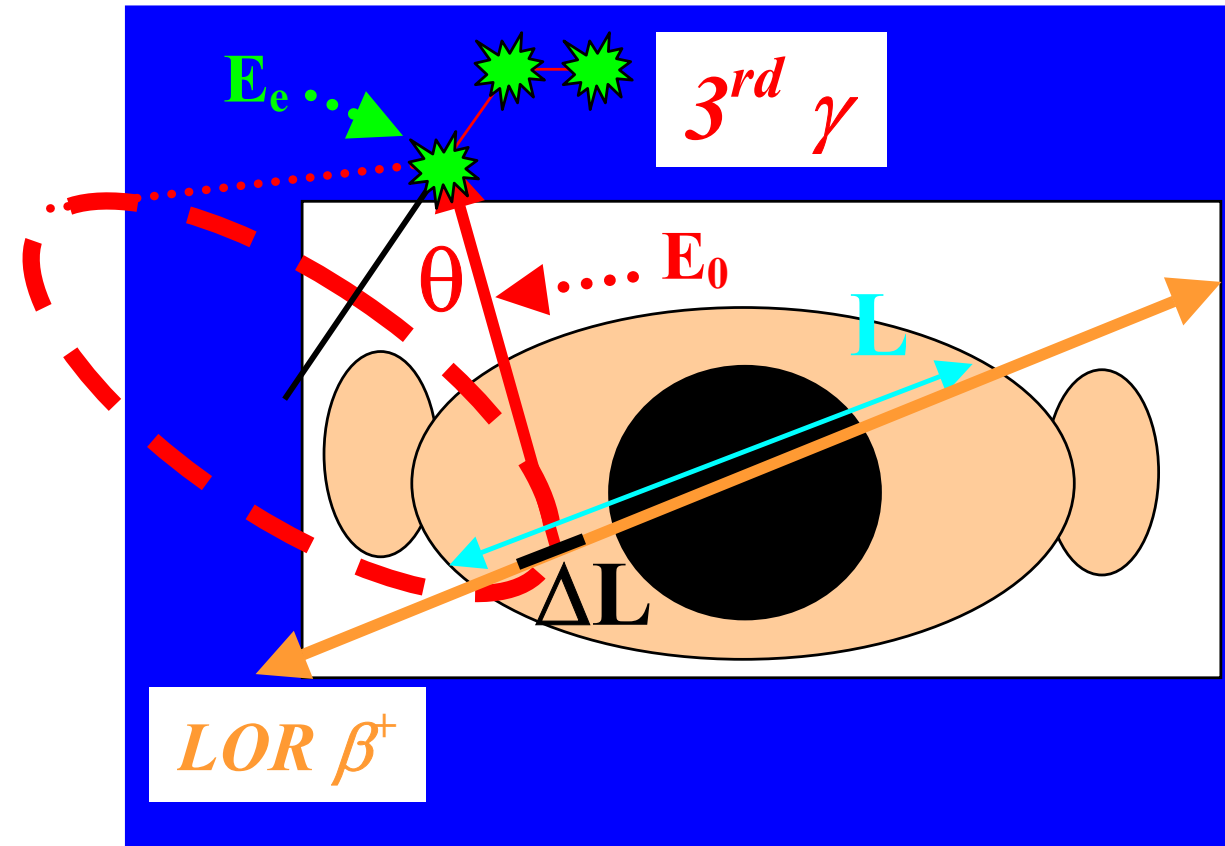
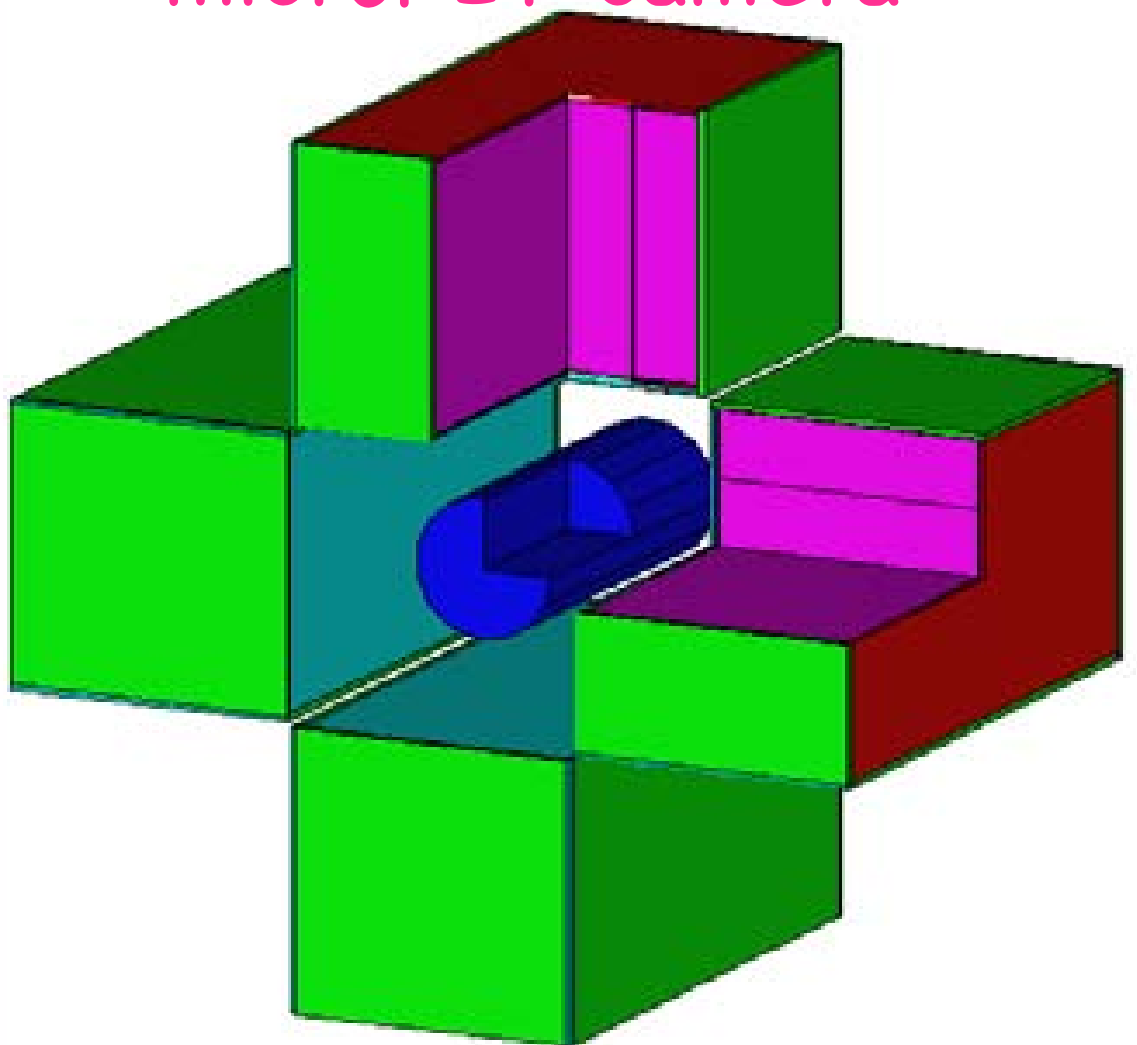
Subatech, Ecole des Mines de Nantes, IN2P3- CNRS and Université de Nantes,

Liquid Xenon (LXe) based detector coupled to large-area fast gas-avalanche imaging photomultipliers (GPM), the UV photons resulting from Xe scintillation are detected in the GPM (Gas Photon Multiplication)

^{44}Sc : a good $\beta+\gamma$ yield (94.3%) with only one γ -ray of 1.157 MeV

3x3x12cm³ cell in 24x12x12cm³ ; 12cm long liq.Xe for 1.156MeV gamma

microPET camera



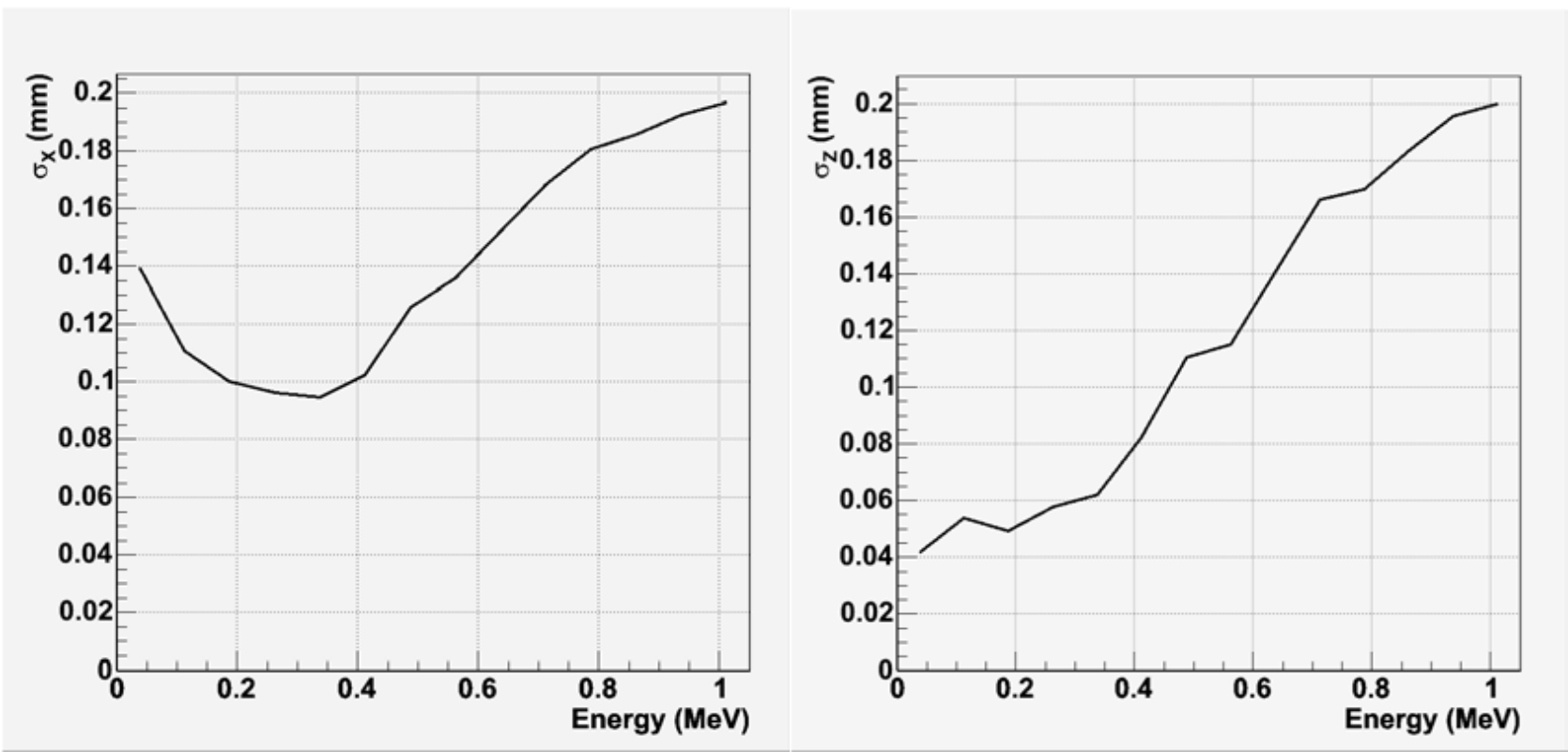


Figure 11: Spatial resolution as a function of the energy deposited by electrons in liquid xenon obtained from simulation, in the anode plane (left) and along the drift direction (right).

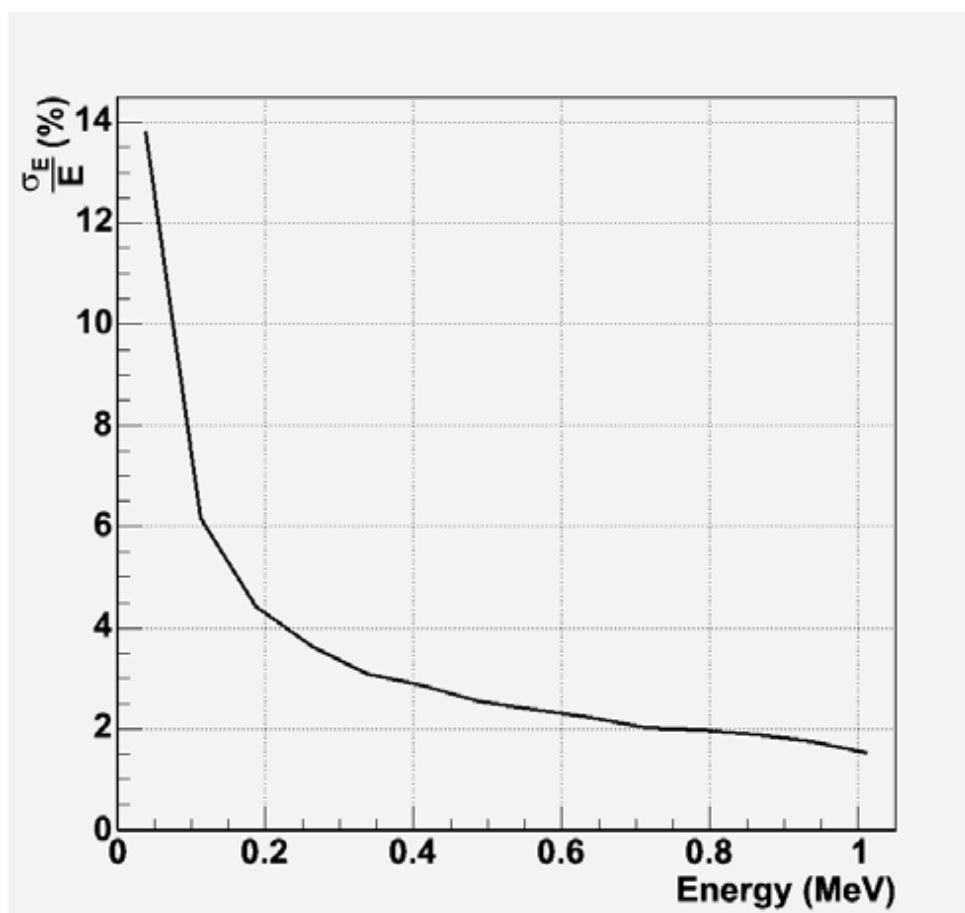


Figure 12: Energy resolution as a function of the energy deposited by electrons in liquid xenon obtained from simulation.

The position of each $\beta^+\gamma$ correlated events has been reconstructed according to the algorithm presented on paragraph 4.1. The obtained image is shown on figure 17. The spatial resolution deduced from the projection of the transverse image slice on a single coordinate is 2.3 mm.

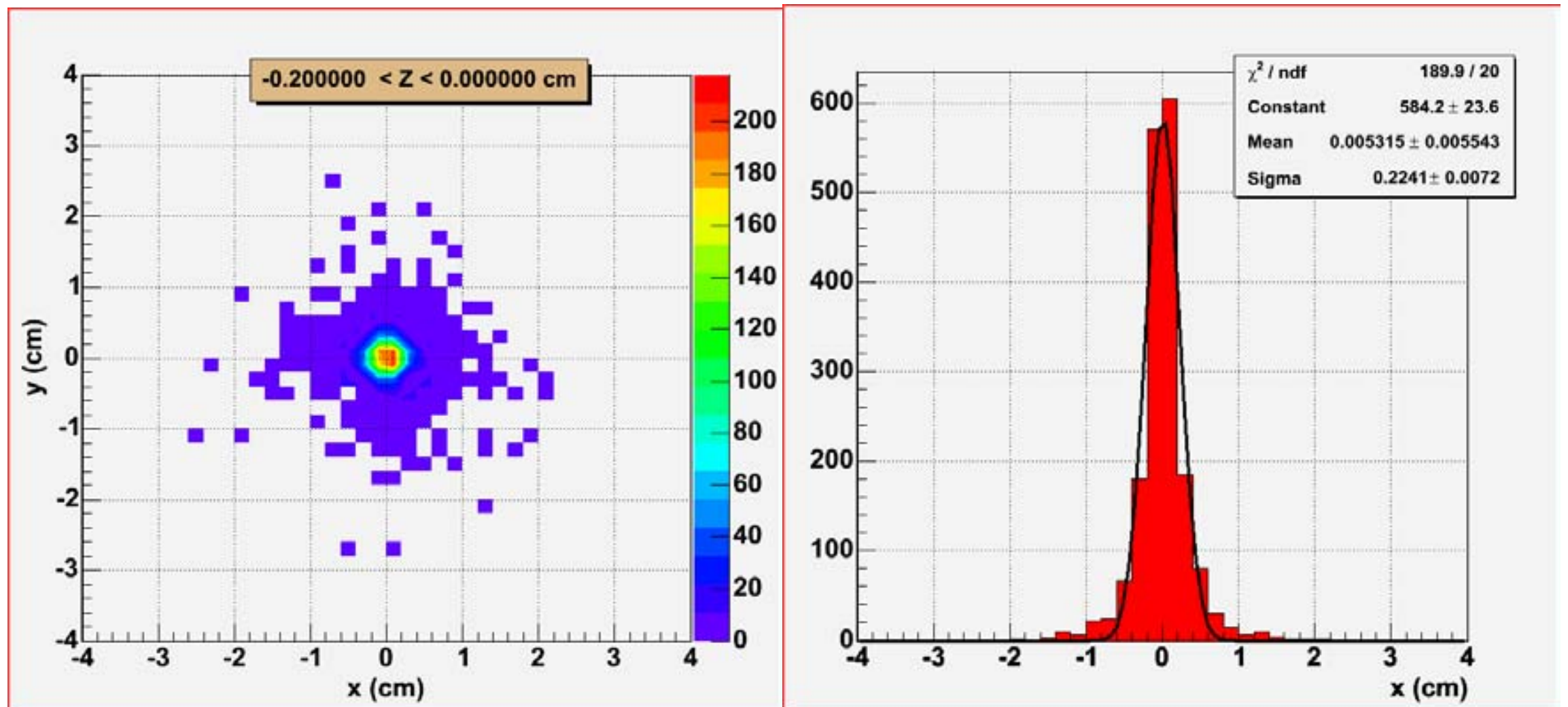


Figure 17: Transverse slice of the reconstructed image of a point source with a voxel size of $2 \times 2 \times 2$ mm 3 (left) and its projection on one x axis (right). Results have been obtained with 0.5 millions of generated ^{44}Sc decays.

The overall reconstruction efficiency for the events is 1.3%

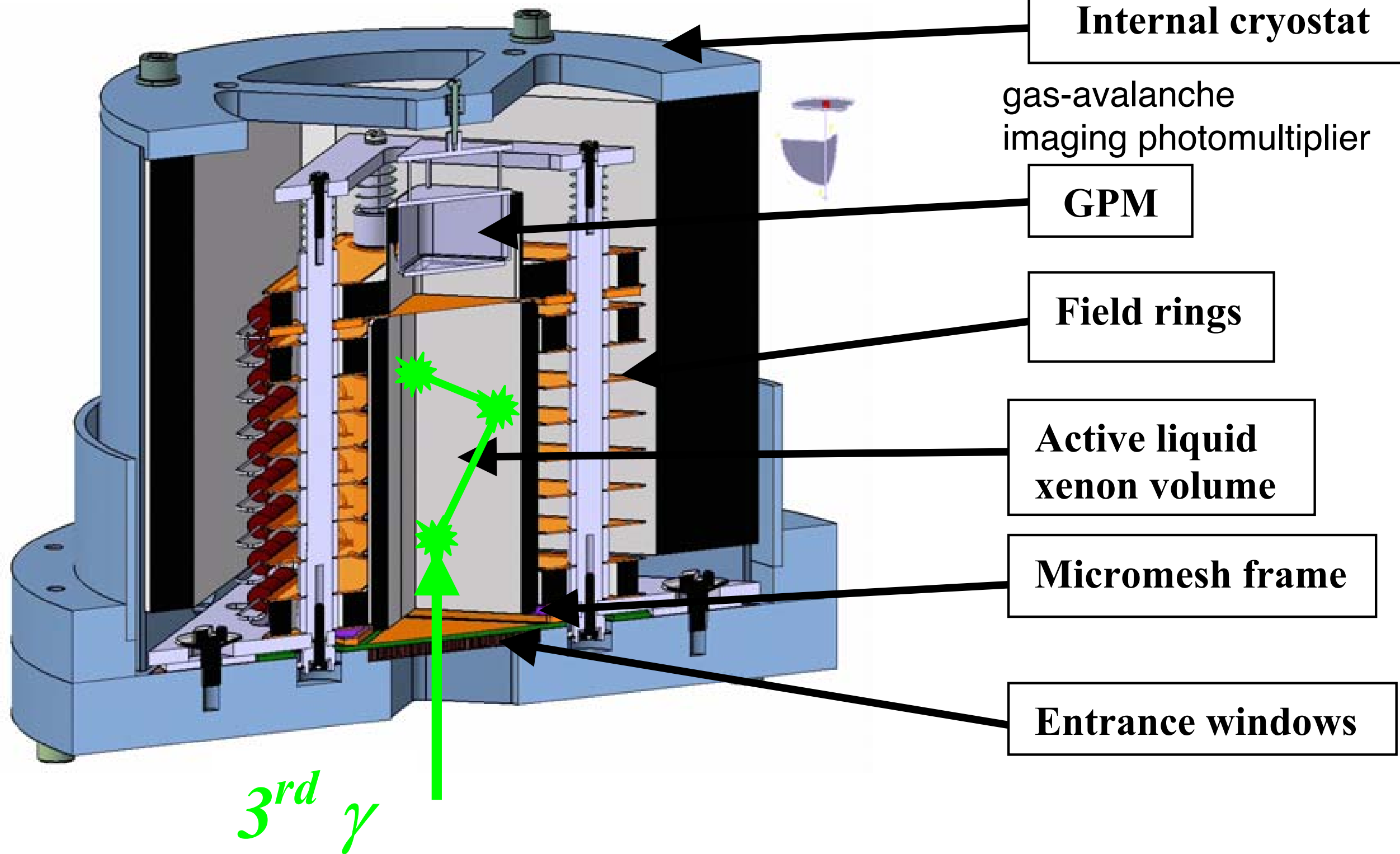
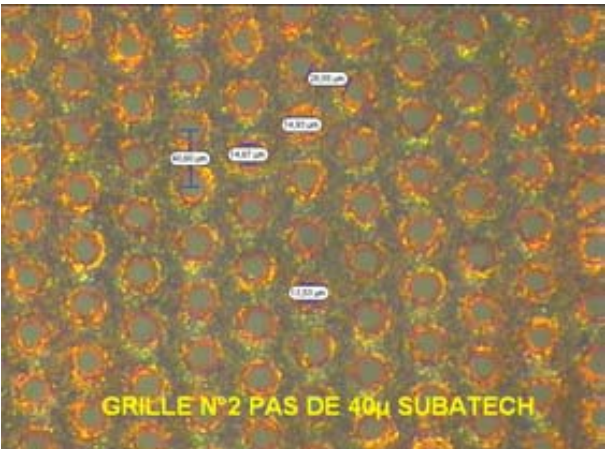


Figure 6: Active volume of the liquid xenon Compton prototype in construction

The ionization signal ($\sim 60000 \text{ e-}/\text{MeV}$) is collected by a segmented anode of $3 \times 3 \text{ cm}^2$ in the (x,y) plane, after crossing a micromesh “Frisch-Grid”. This micromesh is a copper grid of $3 \mu\text{m}$ thickness and $50 \mu\text{m}$ pitch placed $50 \mu\text{m}$ above the anode ($0.5 \times 0.5 \text{ mm}^2$ pads), readout with no-amplification,

GPM PIM (Parallel Ionization Multiplier)



Reflective photocathode



Figure 8. A microscope view of a copper micromesh produced by laser machining: holes are 14 μm diameter with a pitch of 40 μm . The concept of a PIM photon detector with a reflective photocathode.

GEM (Gas Electron Multiplier)

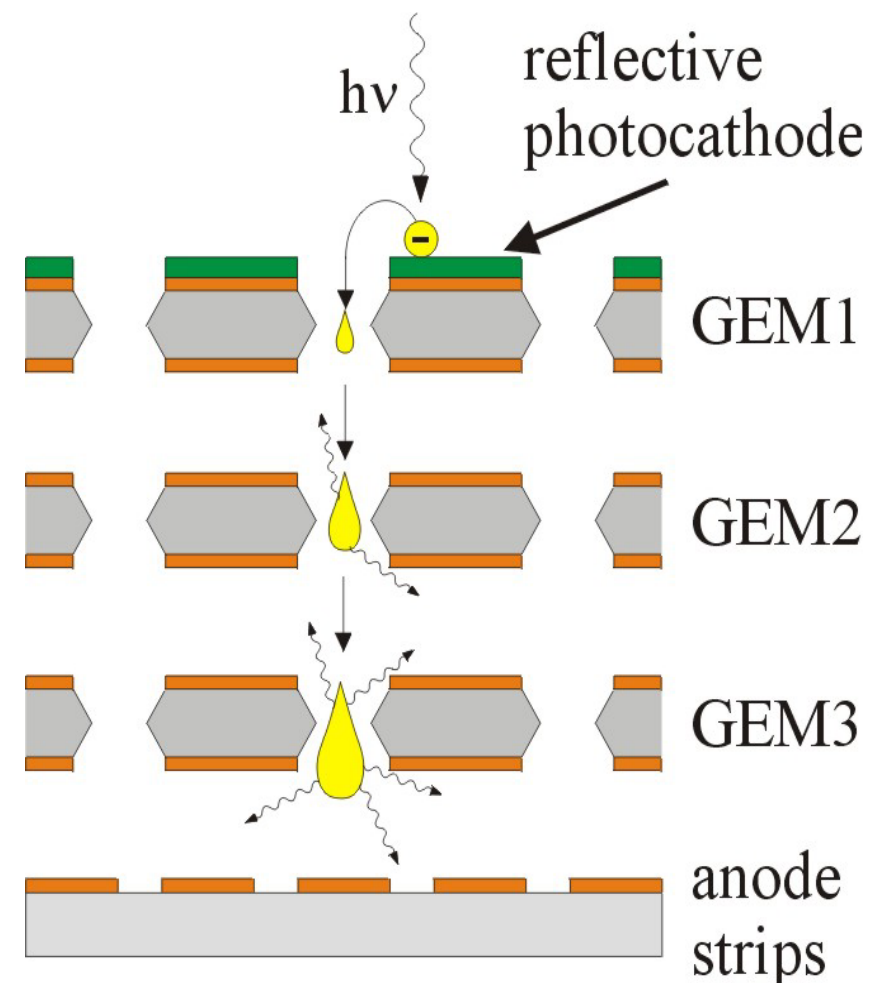
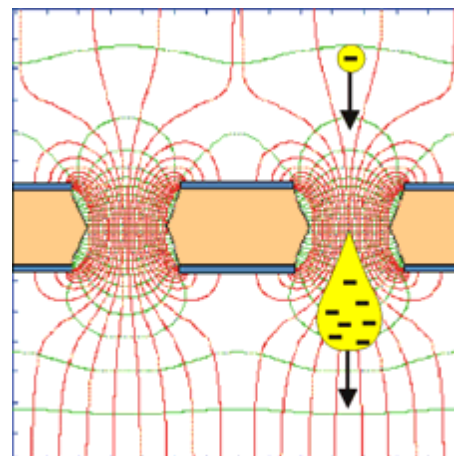
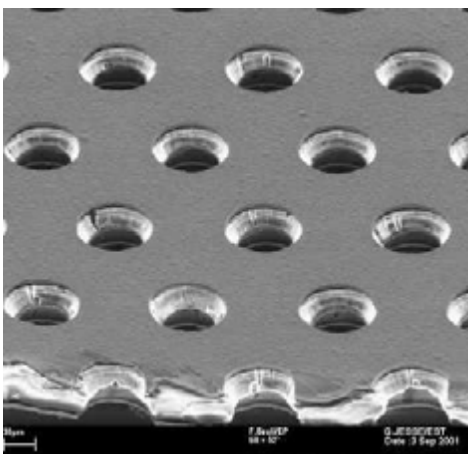


Figure 9. A microscope view of a Gas Electron Multiplier (GEM), produced of 50 micron Cu-cladded Kapton, perforated with 80 micron diameter holes; equi-potentials, electric fields and avalanche multiplication scheme occurring when the GEM is polarized by a few hundred volts; The concept of a multi-GEM photon detector, with a reflective photocathode.

Second Prototype

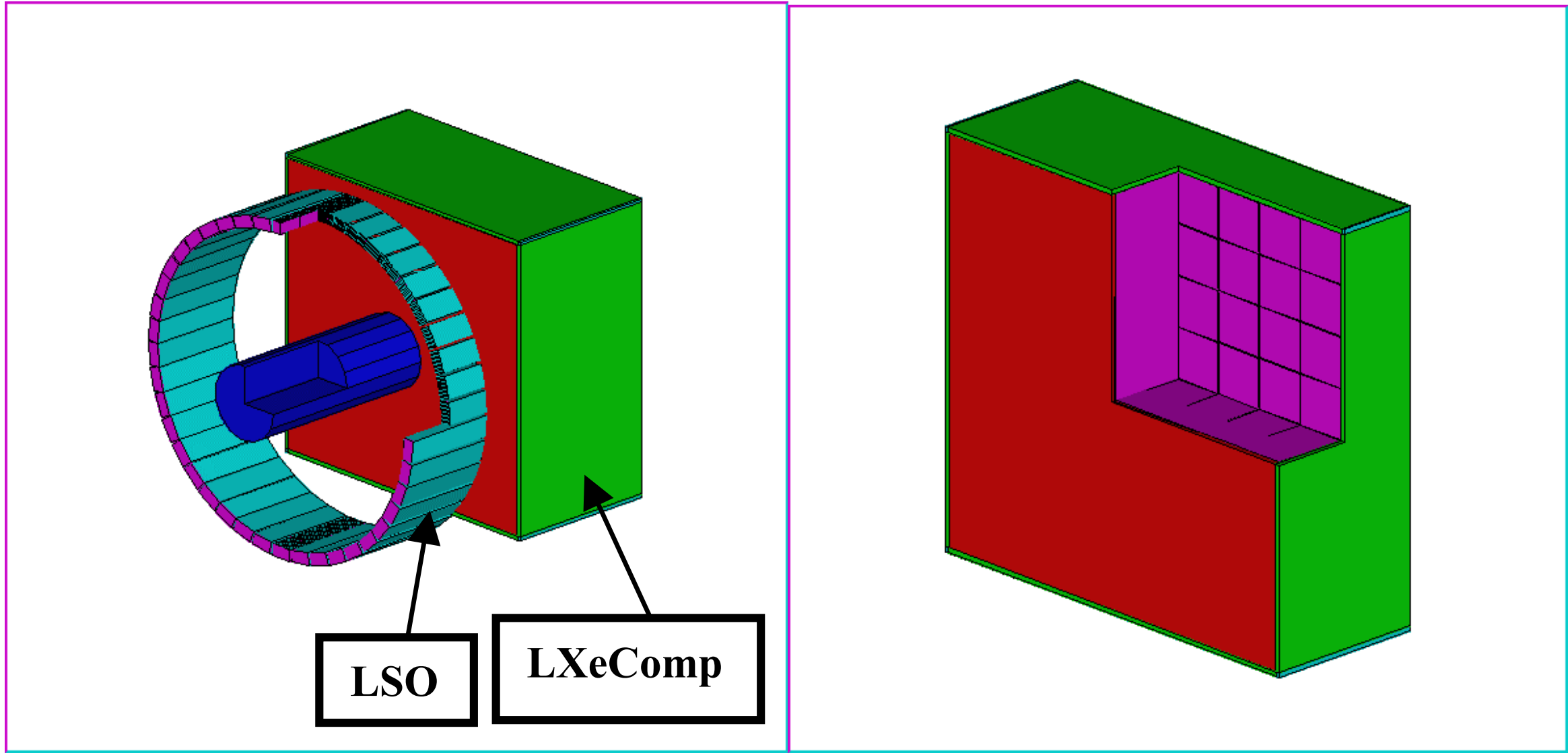
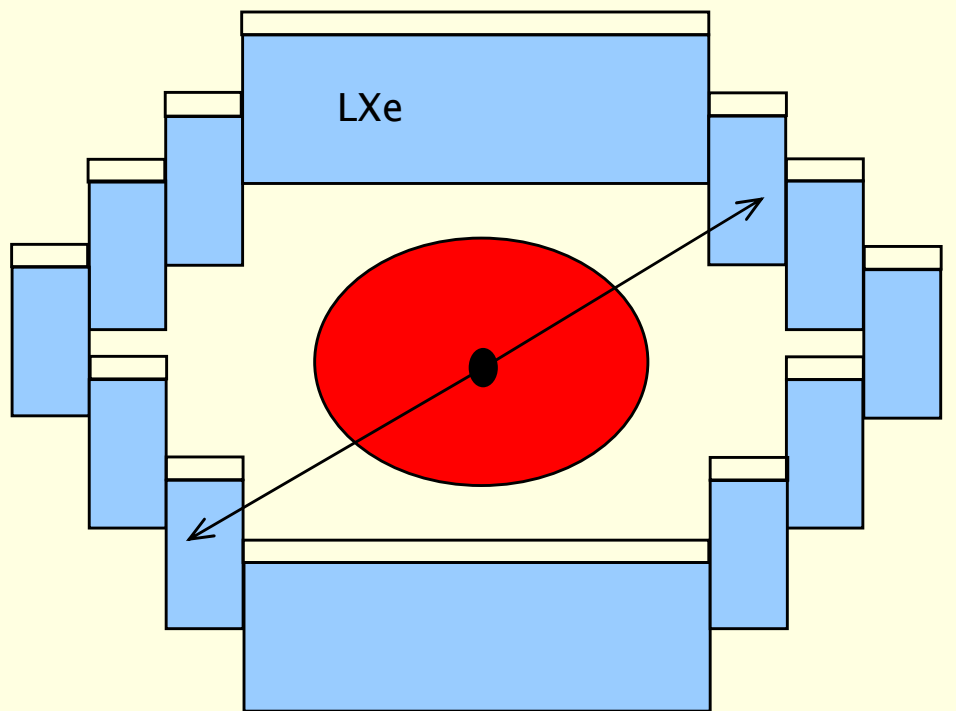


Figure 13: Liquid xenon module associated to LSO microPET camera (left). The module ($24 \times 24 \times 12 \text{ cm}^3$) is made of individual cells of $3 \times 3 \times 12 \text{ cm}^3$ separated by $500\mu\text{m}$ thick PTFE walls (right). The rat phantom is a water cylinder of 6 cm diameter and 15 cm length.

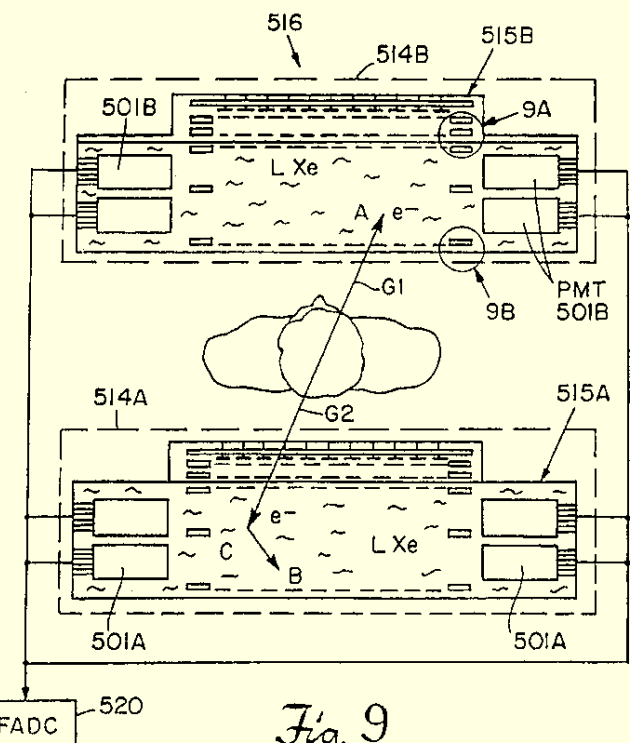
Motivation: cryogenic two-phase detectors for medical applications



GEM-based two-phase Xe or Kr avalanche detector for PET

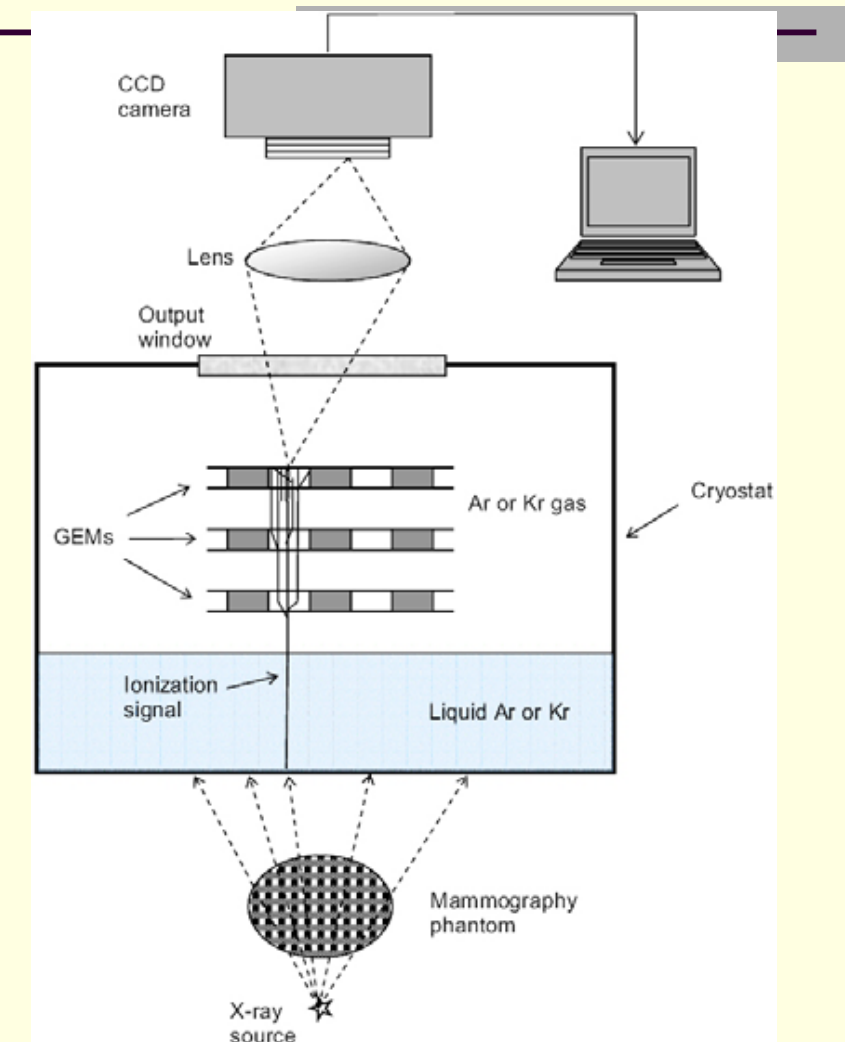
- Solving parallax problem
- Superior spatial resolution if to use GEM readout

Budker Institute: CRDF grant RP1-2550 (2003)



Two-phase Xe detector for PET
Chen & Bolozdynya,
US patent 5665971
(1997)

Fig. 9



GEM-based two-phase Ar or Kr avalanche detector for digital radiography with CCD readout

- Robust and cheap readout
- Thin (few mm) liquid layer is enough to absorb X-rays
- Primary scintillation detection is not needed

Budker Institute: INTAS grant 04-78-6744 (2005)

XENON (TPC) ; 2 phase : DM

2006

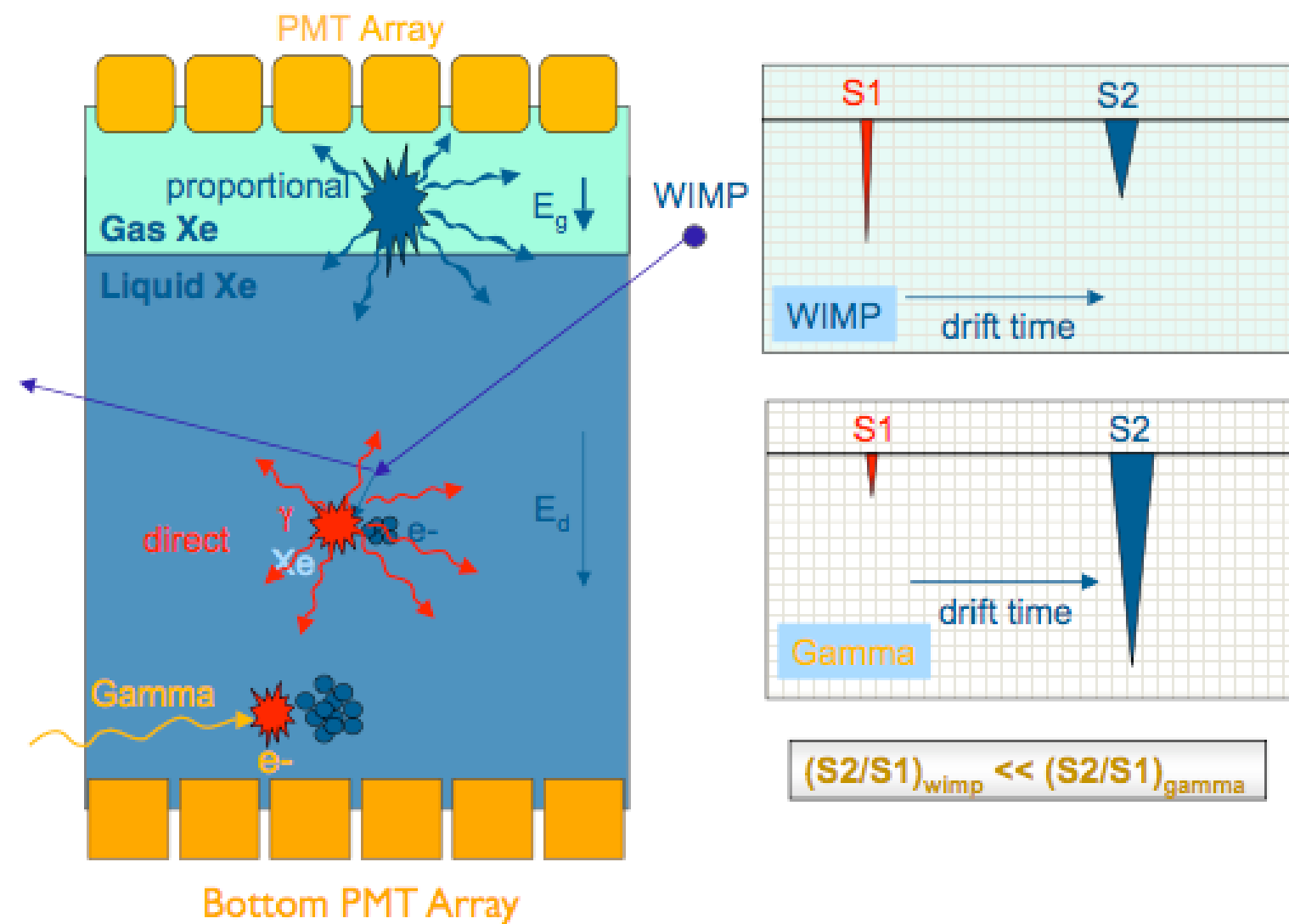
<http://www.astro.columbia.edu/~lxe/XENON/>

Gran Sasso underground lab, Italy

10kg (XENON-10) \rightarrow 1 ton with visible energy threshold of 4keV

1 ton LXeTPC consists of 10 TPCs (100kg): 38cm Φ , 30cm hight cylinder

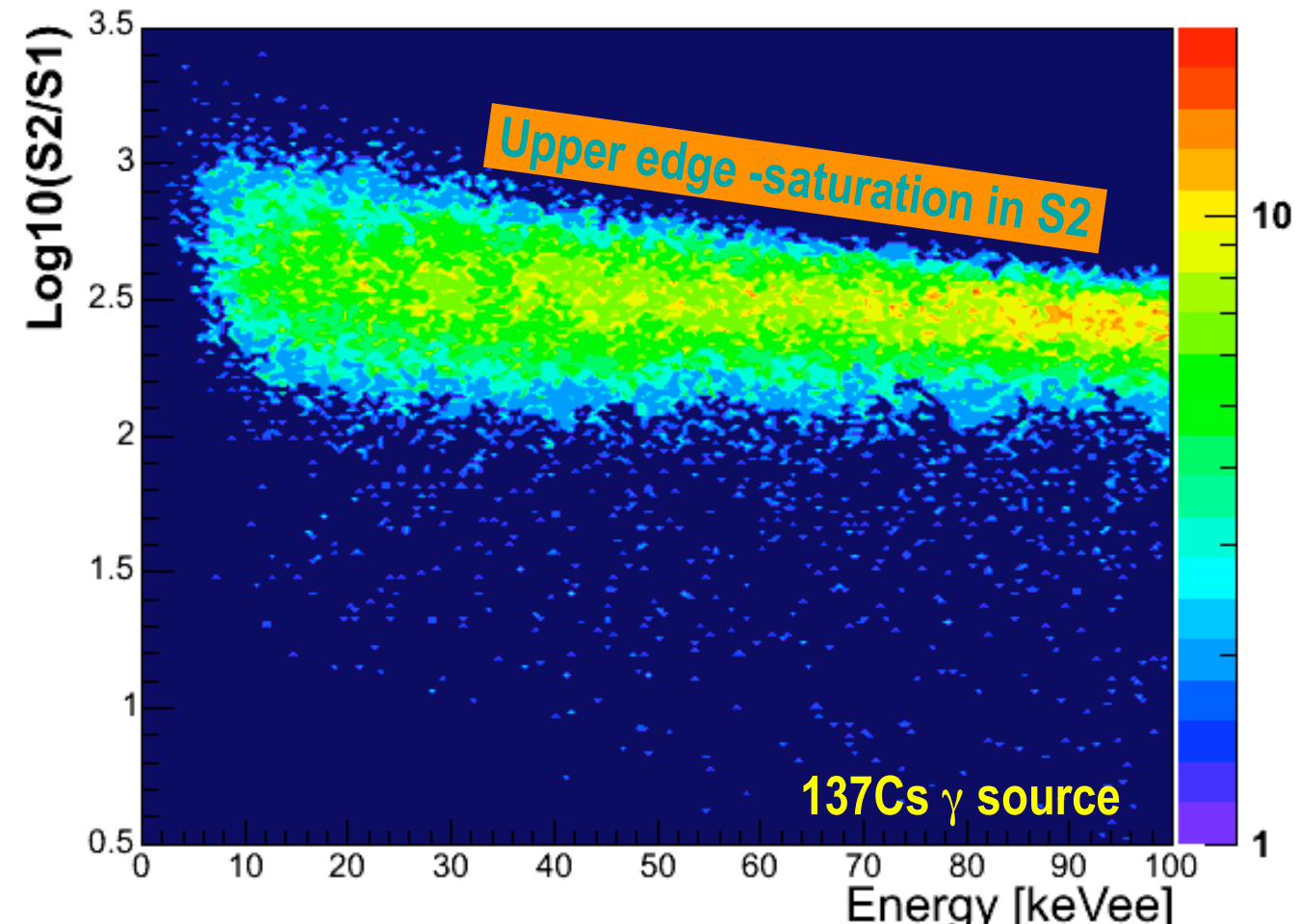
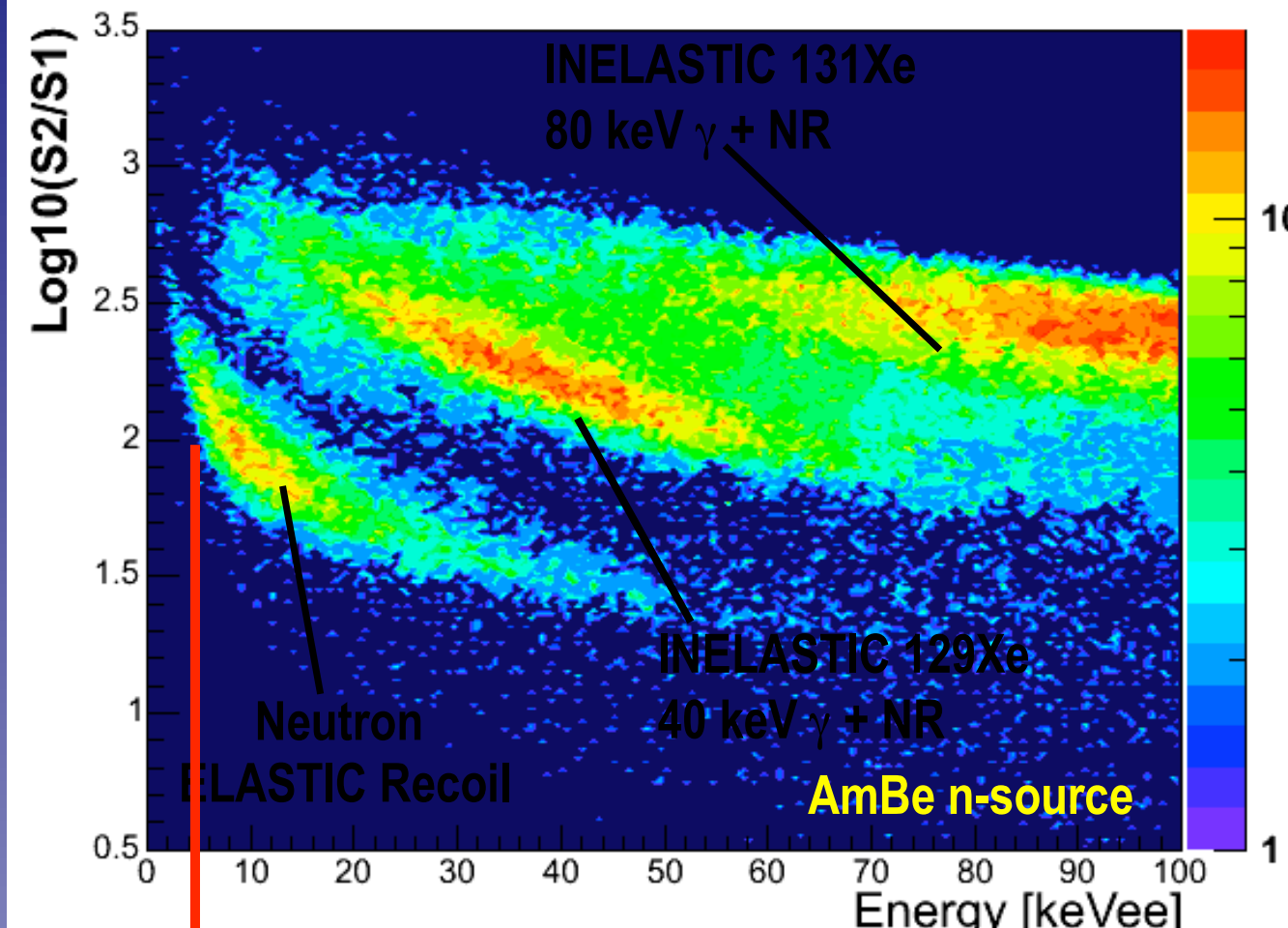
Under a high electric field, a nuclear recoil will yield a very small charge signal and a much larger light signal, compared to an electron recoil of the same energy. **The distinct charge/light ratio is the basis for nuclear recoil discrimination in a LXe (2 phase) detector.**



Roadmap:

- R&D started 2001
- XENON-3 lab. prototype 2005
- XENON-10 first DM detector now
- XENON-100 design later in 2006

Background Discrimination Capability

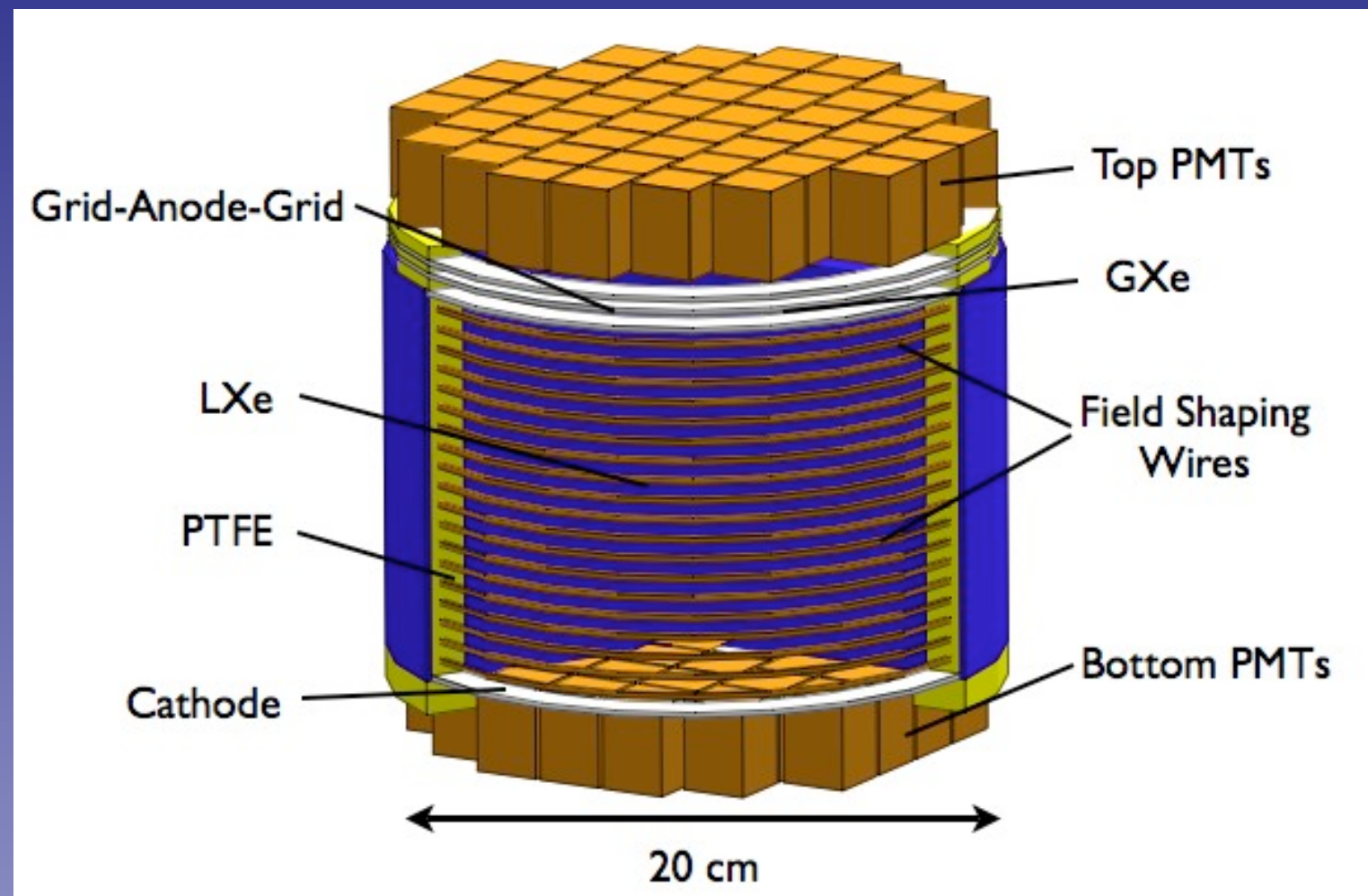
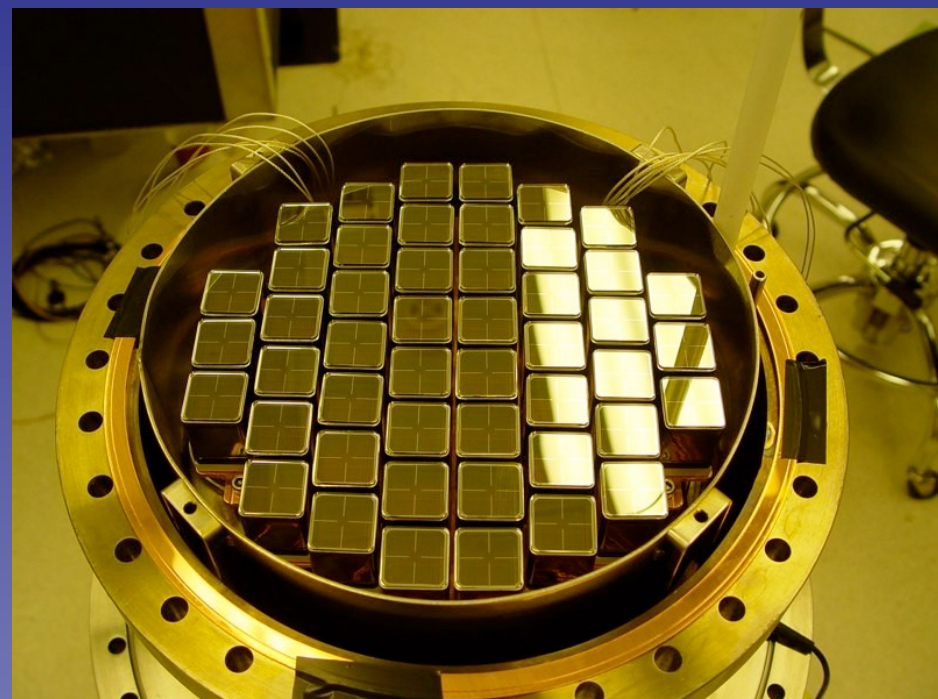


5 keVee energy threshold = 10 keV nuclear recoil

XENON-10 Detector Now at LNGS



- XENON10 now installed and being tested at LNGS (Underground laboratory Gran Sasso, Italy)
- Expect first DM search run June – August 2006



- 48 PMTs on top, 41 on bottom inside L_{Xe}
- 20 cm diameter, 15 cm drift length
- 14 kg L_{Xe}

Summary & Outlook

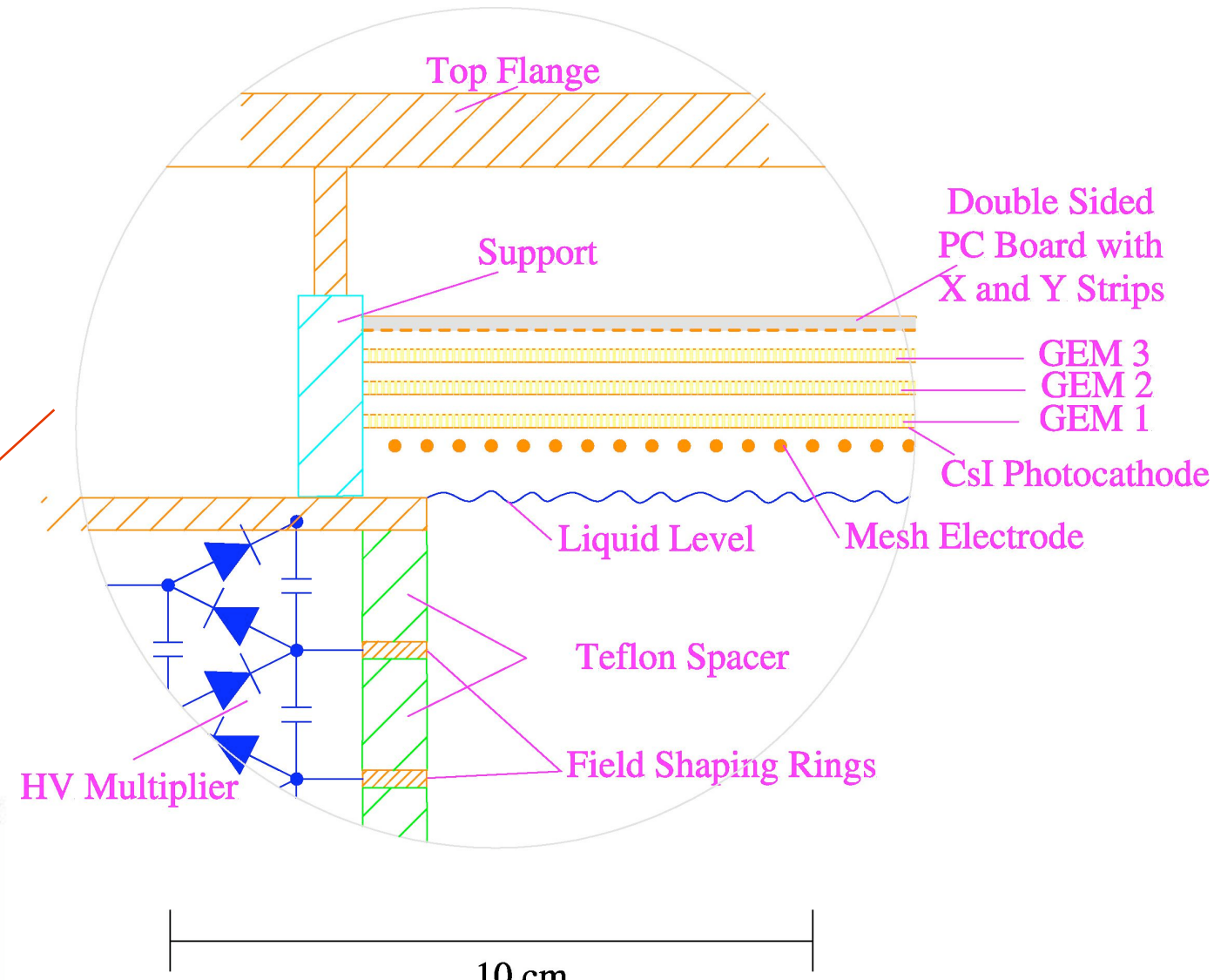
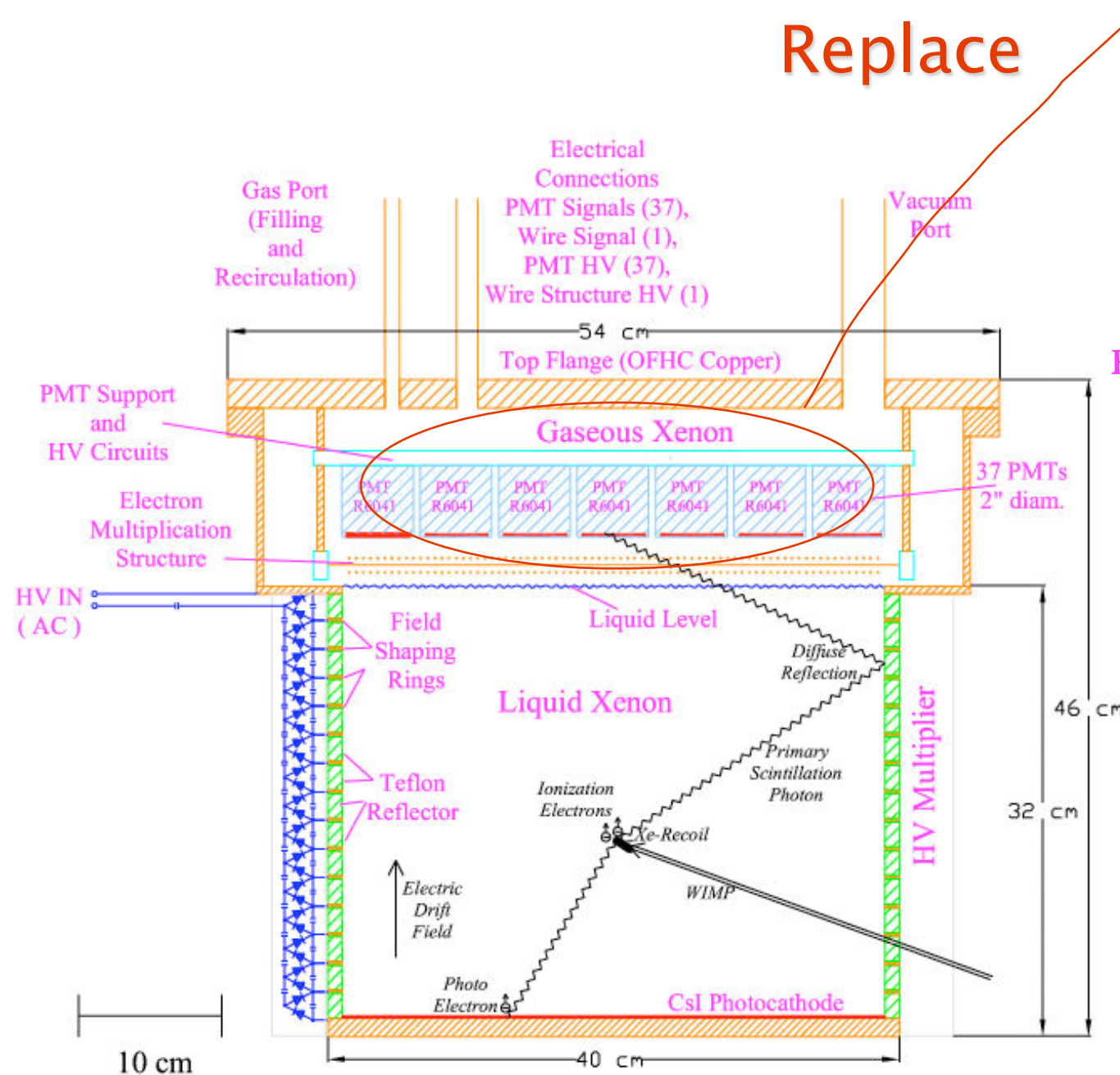
- Dual phase Xenon-TPC's have been developed and tested in the lab, and are expected to start first DM search runs soon.
- Currently, both charge and light readout are based on PMT readout of primary and secondary scintillation light.
- PMT internal radioactivity has been greatly reduced but will become a limiting factor as sensitivities continue to improve.
- Can we profit from higher X/Y spatial resolution?

Other readouts?

- Charge readout with GEM's/THGEM's/MicroMegas?
So far tested: GEM's - difficulties in Xe vapor phase.
- Light readout with sealed gaseous PMT's? Some requirements similar to RICH detectors.
- Semiconductor photosensors?

GEM Implementation in the XENON Detector

Triple-GEM structure with CsI coating.
Mesh steering electrode to tune field
for optimum charge transmission and
photoelectron extraction from the CsI.



Double-sided PC board with X/Y
strips for fine spatial resolution.

Low-noise electronics for
optimum thresholds.

ZEPLIN (TPC) ; 2 phase : DM

2001

<http://hepwww.rl.ac.uk/ukdmc/ukdmc.html>

- II UKDMC collaboration with US and Italy, 30kg
- III UKDMC collaboration with US and Russia, 6kg
- IV UKDMC collaboration with UCLA 1 ton from ZEPLIN II

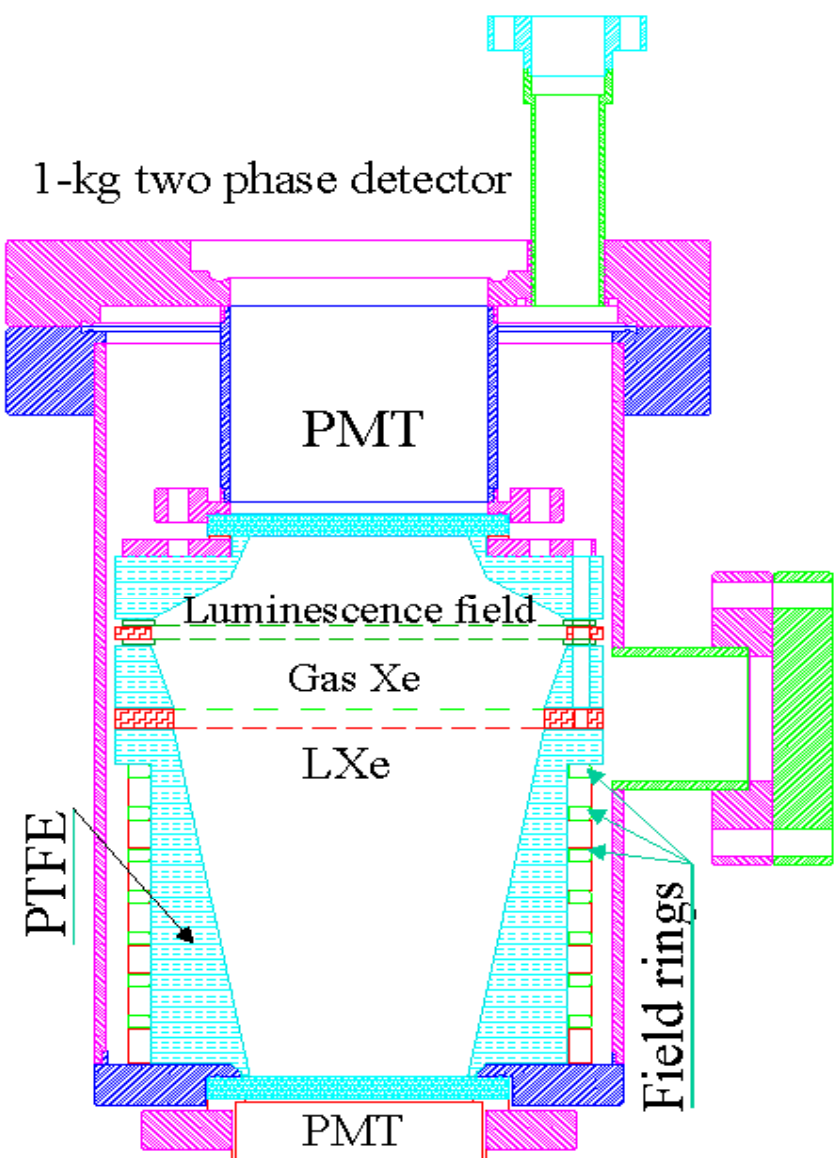


Figure 3. ZEPLIN II: Electroluminescence in gas (principle of a two-phase, 1-kg detector, developed by UCLA-CERN-Torino).

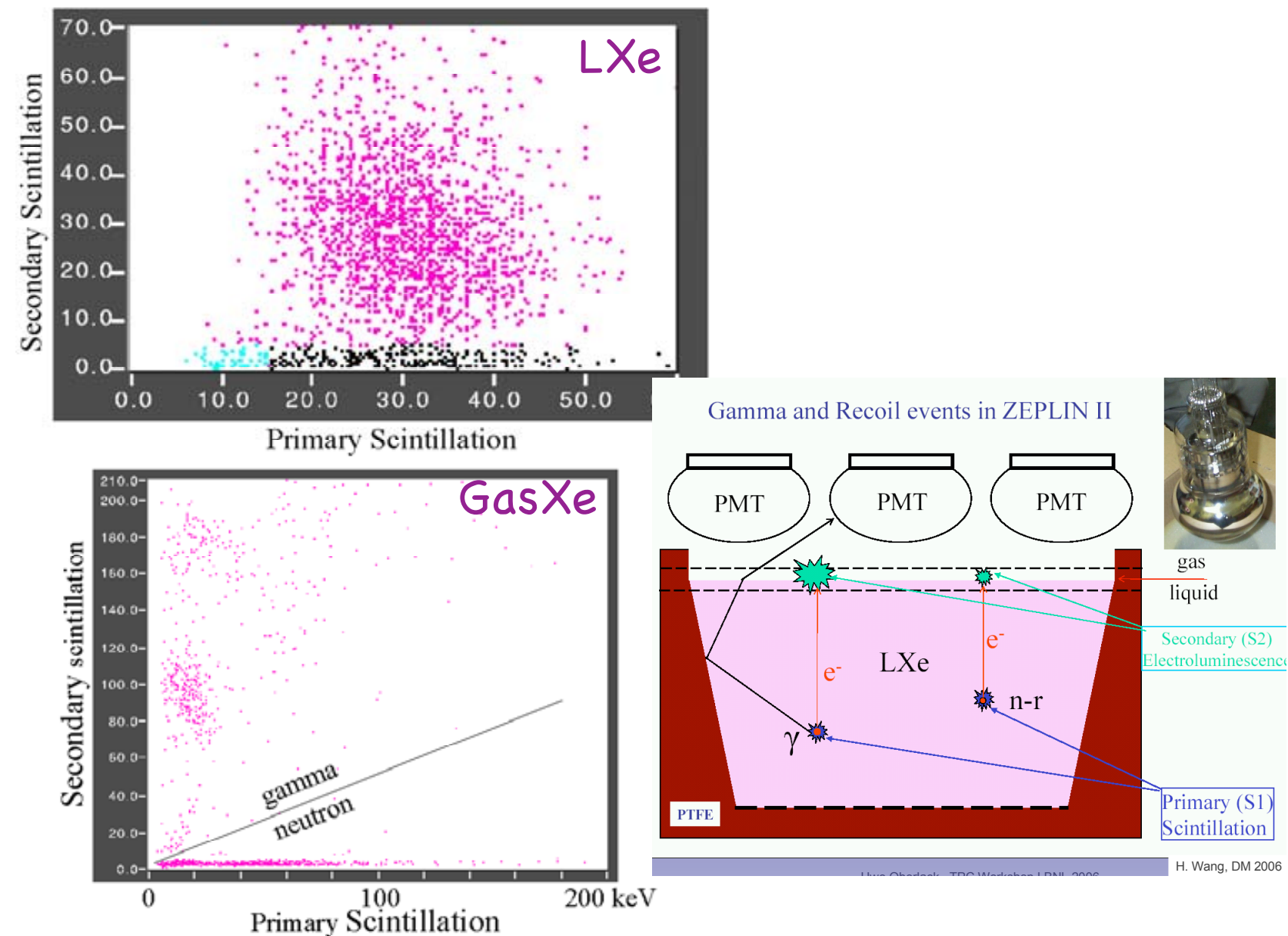
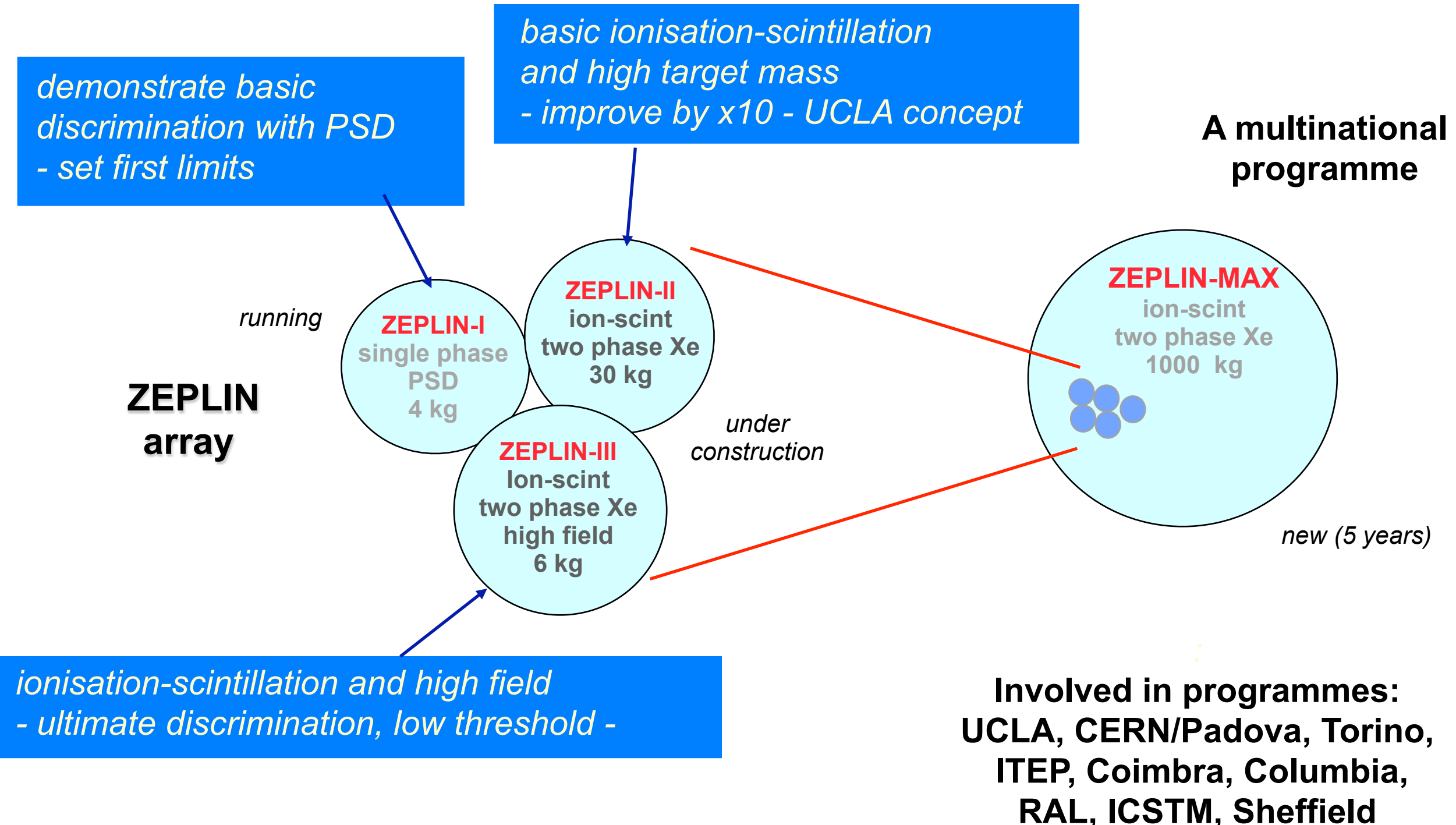


Figure 4. Secondary vs. primary scintillation plot in pure liquid Xe with mixed gamma-ray and neutron sources. The secondary scintillation are produced by proportional scintillation process in liquid Xe (top) and electroluminescent process in gaseous Xe (bottom).



Boulby Collaboration Strategy



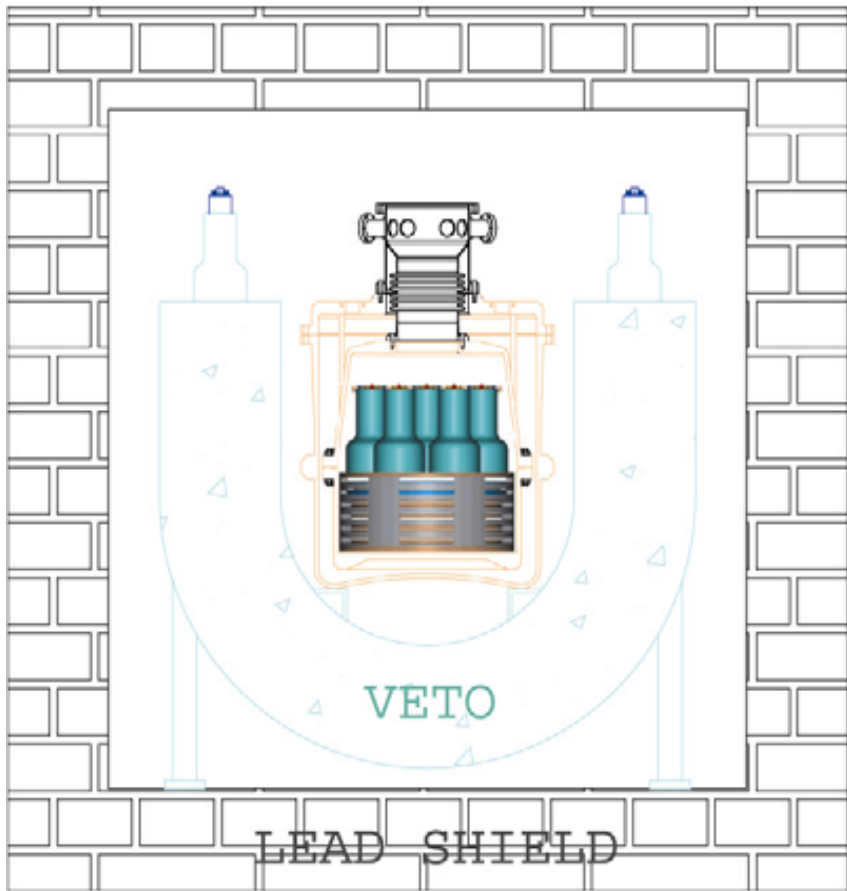


Figure 5a. System setup for Xe target (40 kg total): overall set up.

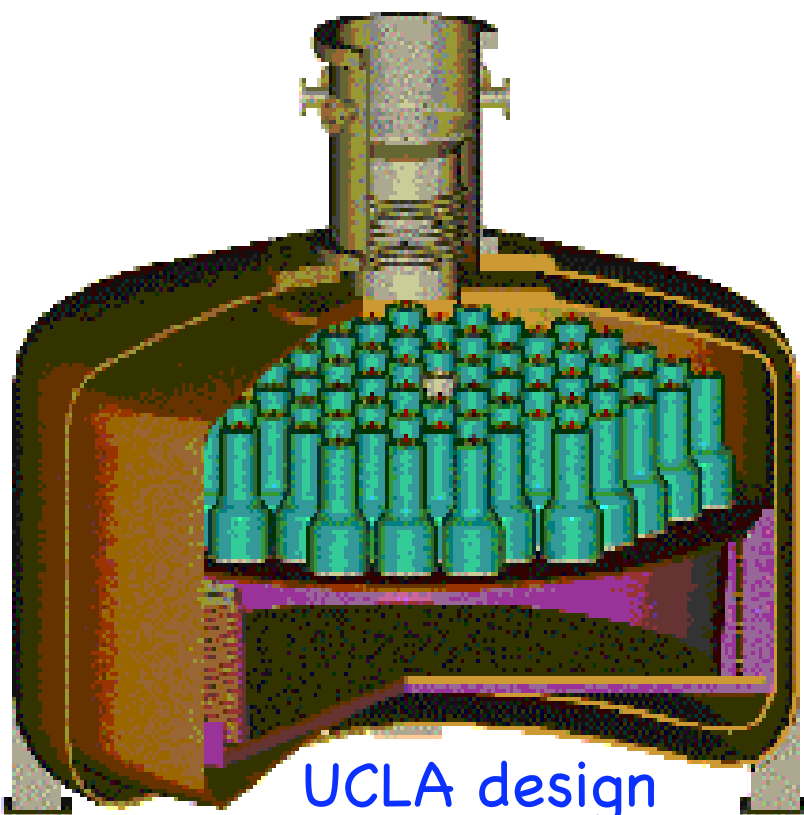


Figure 6. 1-ton scaled up (ZEPLIN IV) detector.

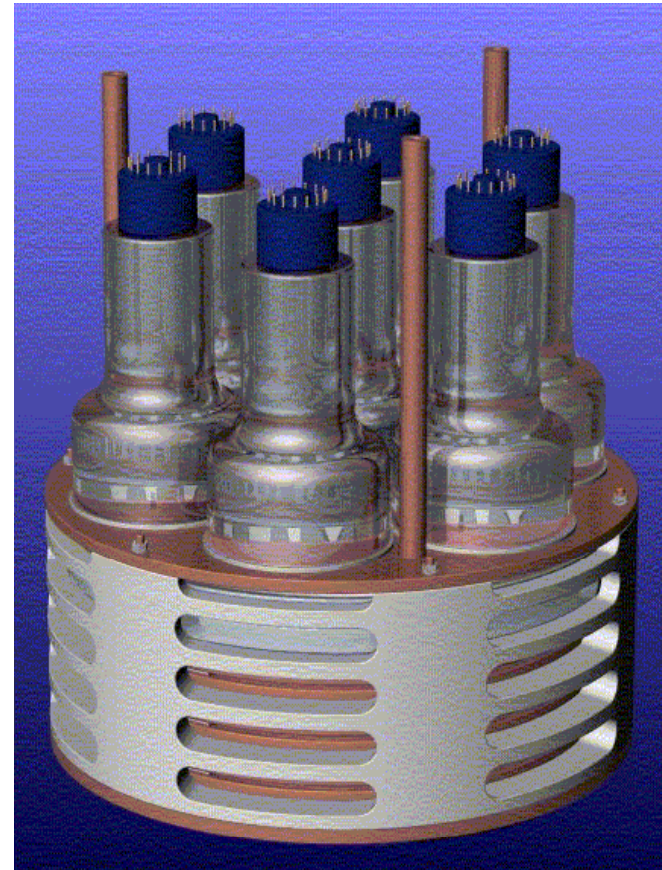


Figure 5b. ZEPLIN II central detector.

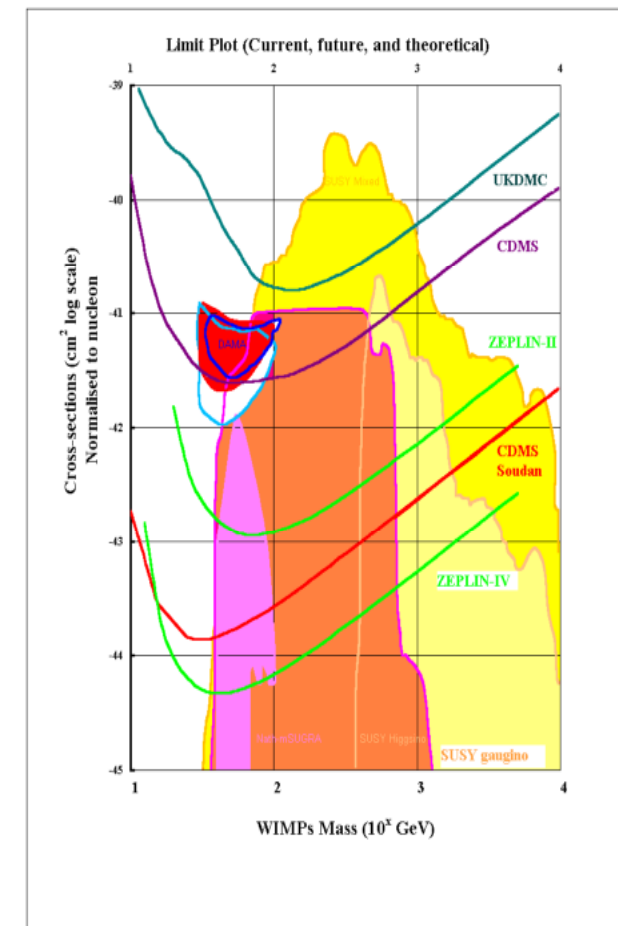
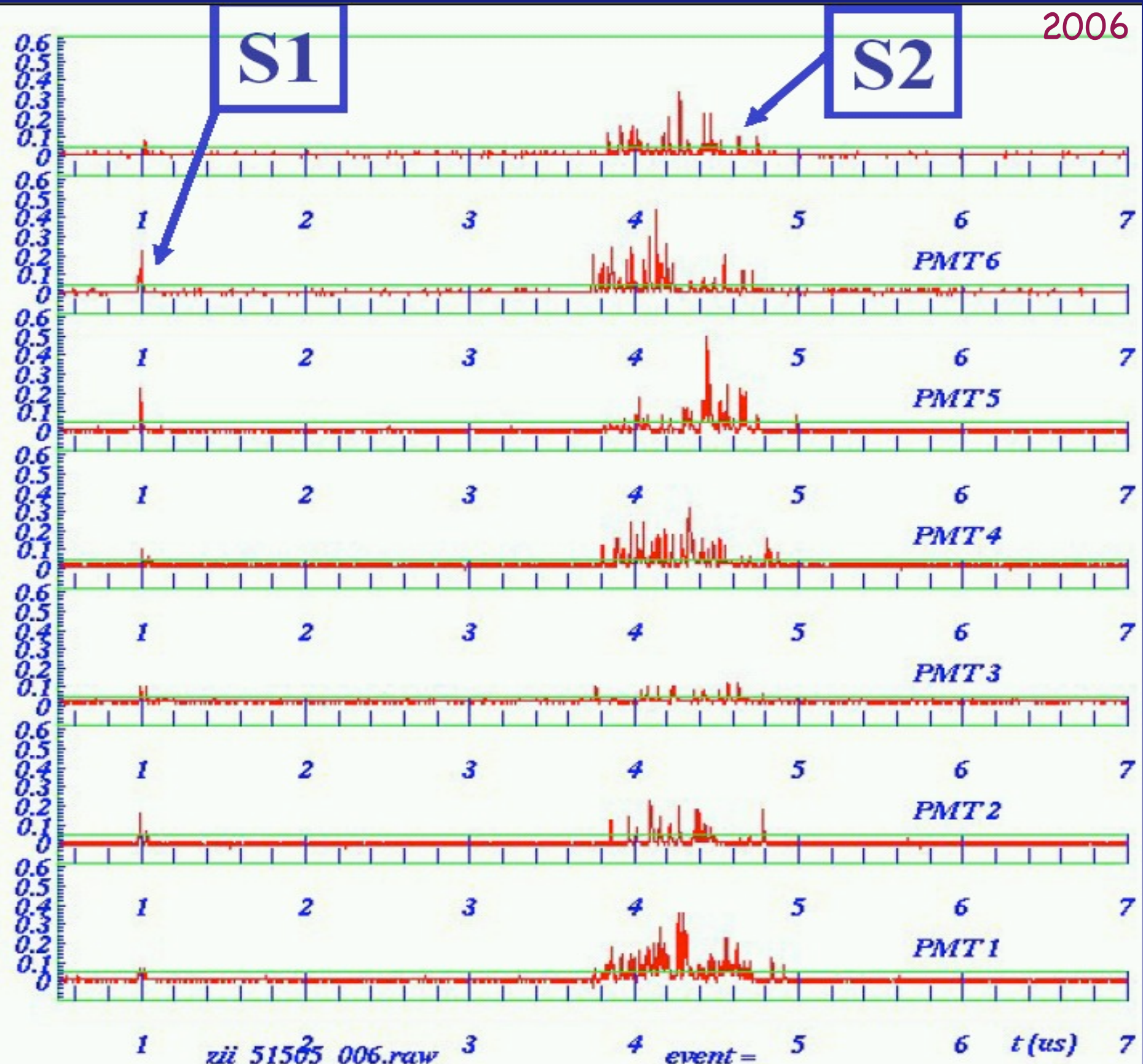


Figure 7. Limit plot (current, future and theoretical).

Recoil Event

ZEPLIN II





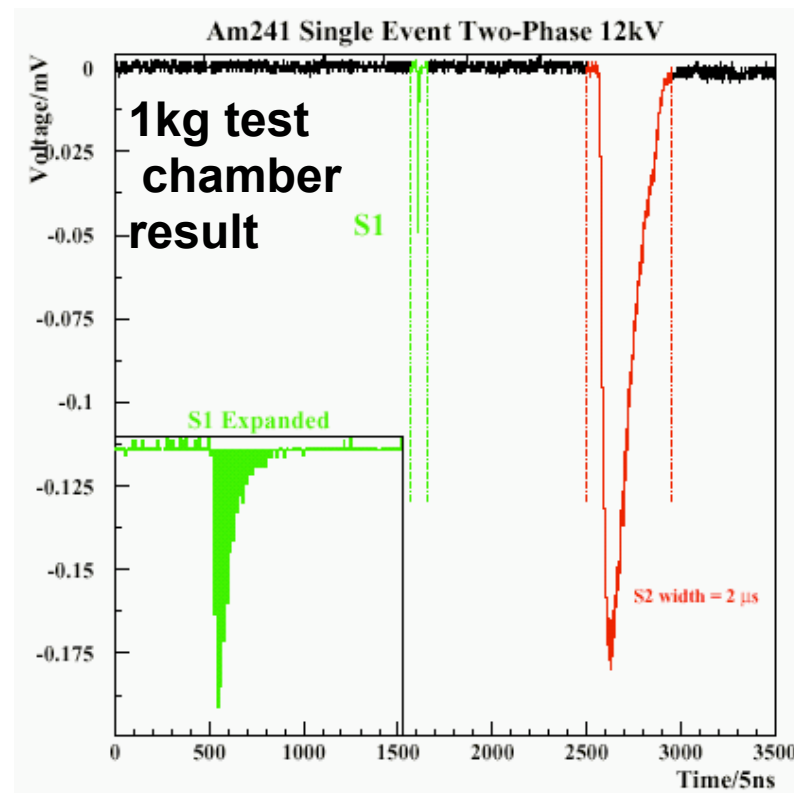
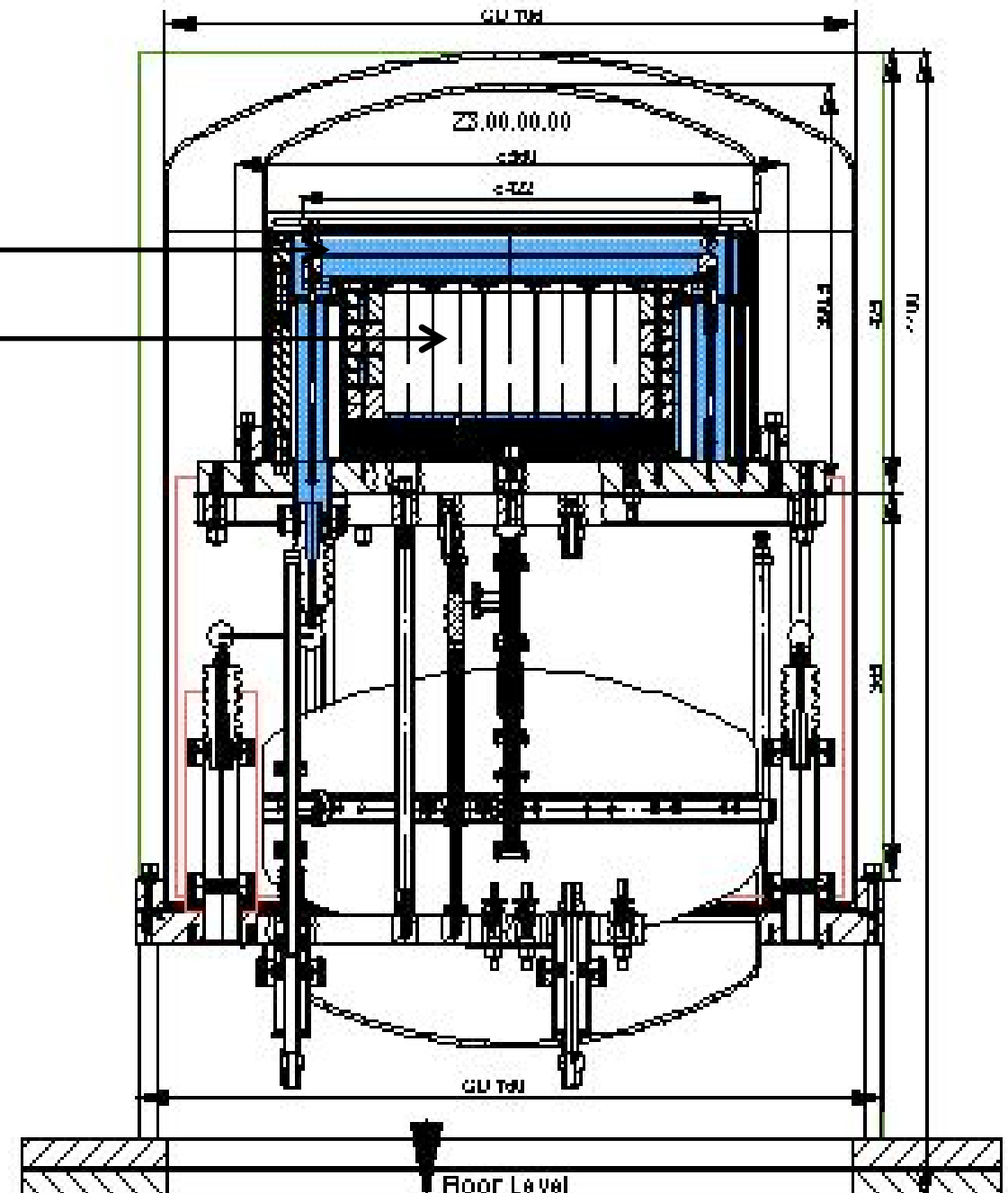
ZEPLIN III

(UKDMC collaboration
with US and Russia)

ionisation-scintillation - low threshold

- 6 kg liquid Xe
- High field (20 kV) operation for better discrimination

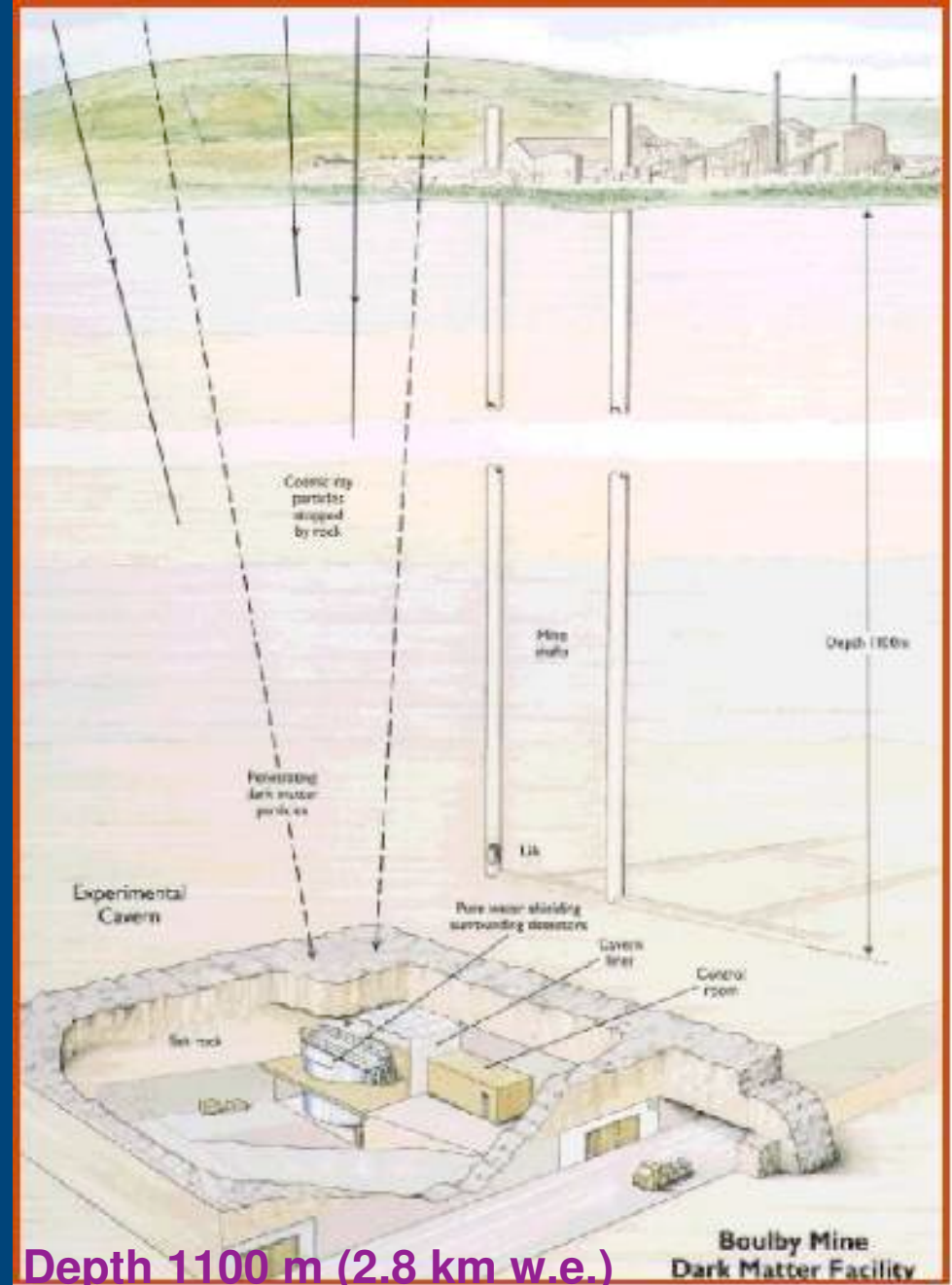
X
e
31 two-inch
photomultipliers

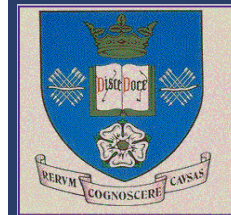


- Completion due end 2001

Zeplin III

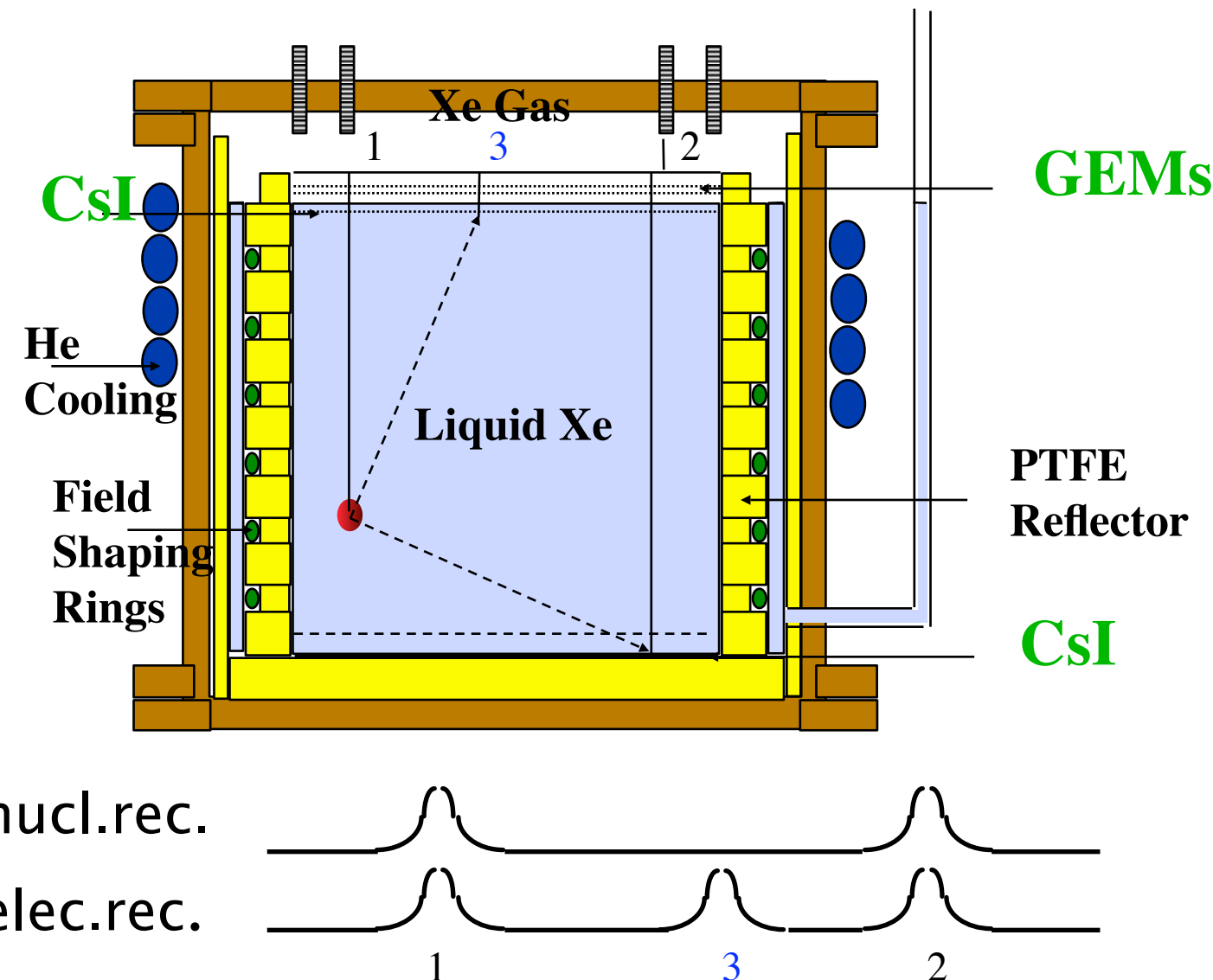
- Xenon detector for WIMP search
- Nuclear recoils from elastic scattering (WIMP – nucleus)
- Operate underground, at Boulby



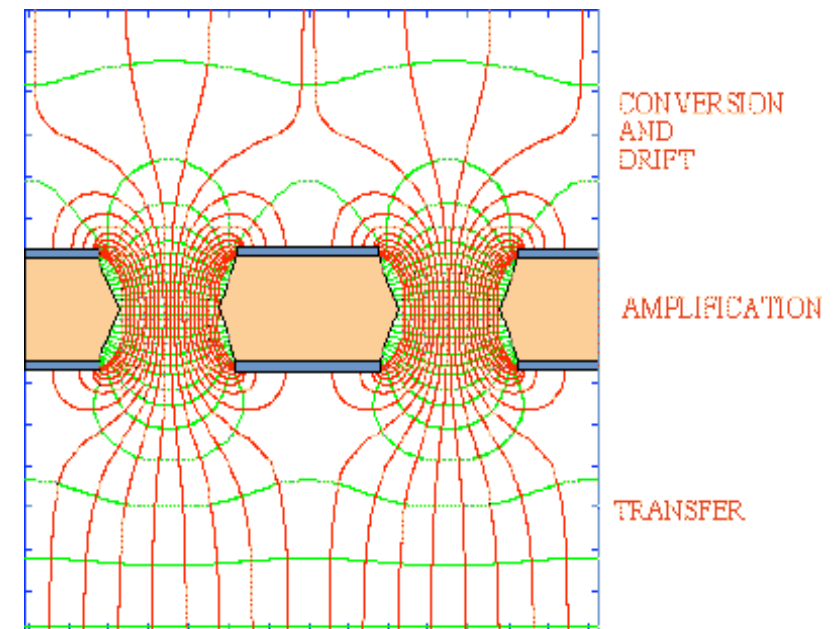


PMT Removal for Scale-Up?

- Sheffield test cell



Nuclear recoil signal events contain no (for low drift field) primary ionization between these two pulses.



CsI photocathodes in LXe: E.Aprile, NIMA 338 (1994), 328; NIMA 343 (1994), 121.

GEM phototubes in noble gases:<http://gdd.web.cern.ch/GDD/> A.Buzulutskov, NIMA, 443 (2000), 164.

Summary of 1 Phase LXe

Phase	Project	Physics	Xe weight	detector	readout	year	location	collaboration
1	EXO	double beta	10ton (3m ³)	TPC	x, y anode wires	for 10 years	WIPP, NM, USA	Enriched Xenon Observatory, US(SLAC), Canada, Swiss, Russia
			1ton		; APD for lights ,	for 5 years		
			200kg		laser - ID	Nov., 2006		
1	XMASS	DM solar ν double beta	20ton	lights	PMT		Kamioka	Japan, Korea, Russia
			1ton (800kg)					
			100kg (30 l)			2006		
1	MEG	$\mu \rightarrow e \gamma$	800 - 900 l	lights	PMT	Nov., 2006	PSI	Japan, Italy, Switzerland, Russia, USA
			70 l			2003		
1	LXe-GRIT	cosmic γ	2.4 l	TPC	x, y anode wires ; PMT for lights	1997, 1999, 2000	NSBF (National Science Balloon Facility), NM, USA	Columbia university
1	LXe-PET	PET	64.8 l	TPC	segmented pads	proposal	Nantes Cyclotron	France
1	PETYA	PET		drift chamber	anode wires or mini-strip ; PMT, APD for lights	2002 (prototype)	Univ. of Coimbra	Portugal
1	TOF-PET	PET	77.8 l	lights	PMT		Waseda univ., NIRS	Japan
			12 l			2003		

Summary of 2 Phase LXe

Phase	Project	Physics	Xe weight	detector	readout	year	location	collaboration
2	LXeComp/ ⁴⁴ Sr	PET	100 l	TPC	anode pads ; GPM for lights	simulation	Nantes Cyclotron	France, Israel, Japan
		micro-PET	13.8 l , 6.9 l			simulation		
			0.1 l			2005		
2	GEM-based	PET		TPC	GEM	2003	Budker Institute	Russia
2	US patent 5665971	PET		TPC		1997	Columbia university	USA
2	XENON	DM (WINP)	1ton:100kgx10	TPC	PMT, GEM		Gran Sasso undergroun d lab	US, Italy,Portugal
			100kg			design		
			10kg			2006		
			3kg			2005		
2	ZEPLIN	DM (WINP)	1ton (IV?)	TPC	PMT, GEM		Boulby, UK	UK, US, Italy, Russia, Portugal
			30kg (II)			2006		
			6kg (III)			2006		

Detector

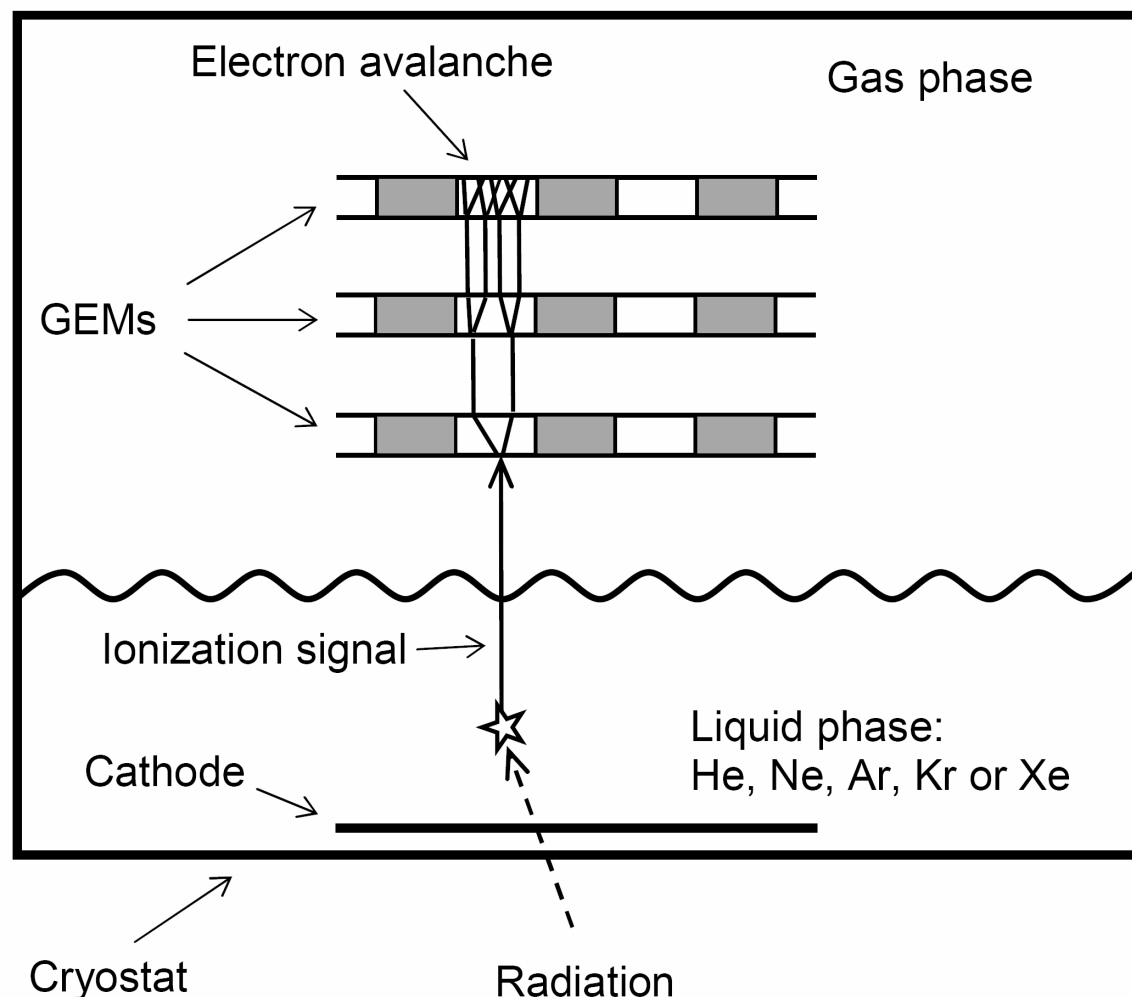
GEM: Gas Electron Multipliers

Two-phase argon and xenon avalanche detectors based on Gas Electron Multipliers

A. Bondar, A. Buzulutskov , A. Grebenuk,D. Pavlyuchenko, R. Snopkov, Y. Tikhonov

Budker Institute of Nuclear Physics, 630090 Novosibirsk, Russia.

[www.arxiv.org physics/0510266](http://www.arxiv.org/physics/0510266)



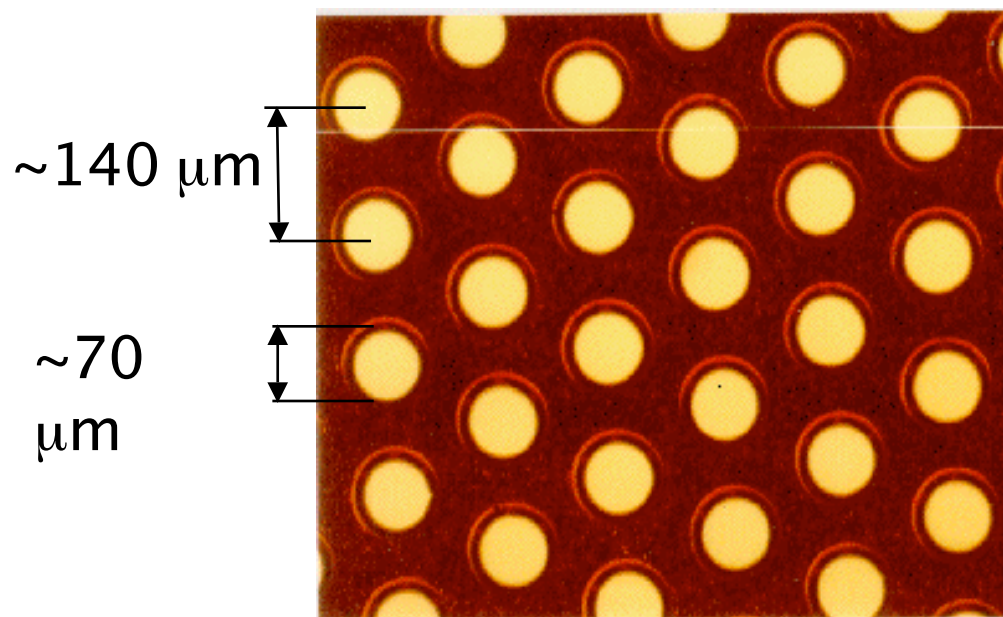
Foils : $28 \times 28 \text{ mm}^2$ each, and a cathode mesh were mounted in a cryogenic vacuum-insulated chamber of a volume of 2.5 l. The distances between the first GEM and the cathode, and between the GEMs, were 6 and 2 mm, respectively.

Fig.1 Schematic view of a two-phase avalanche detector based on GEM multipliers.

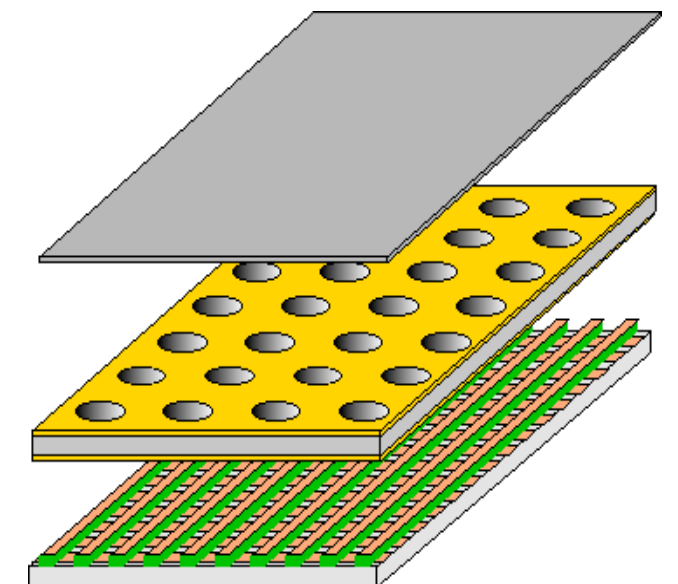
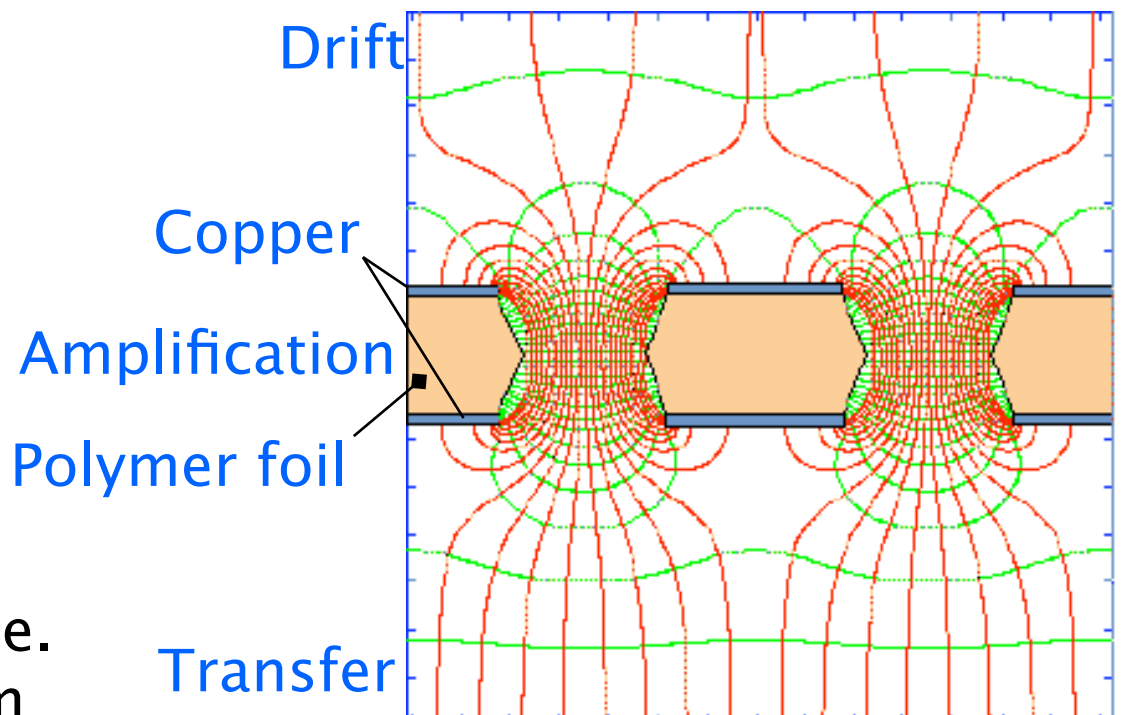
The Gas Electron Multiplier GEM

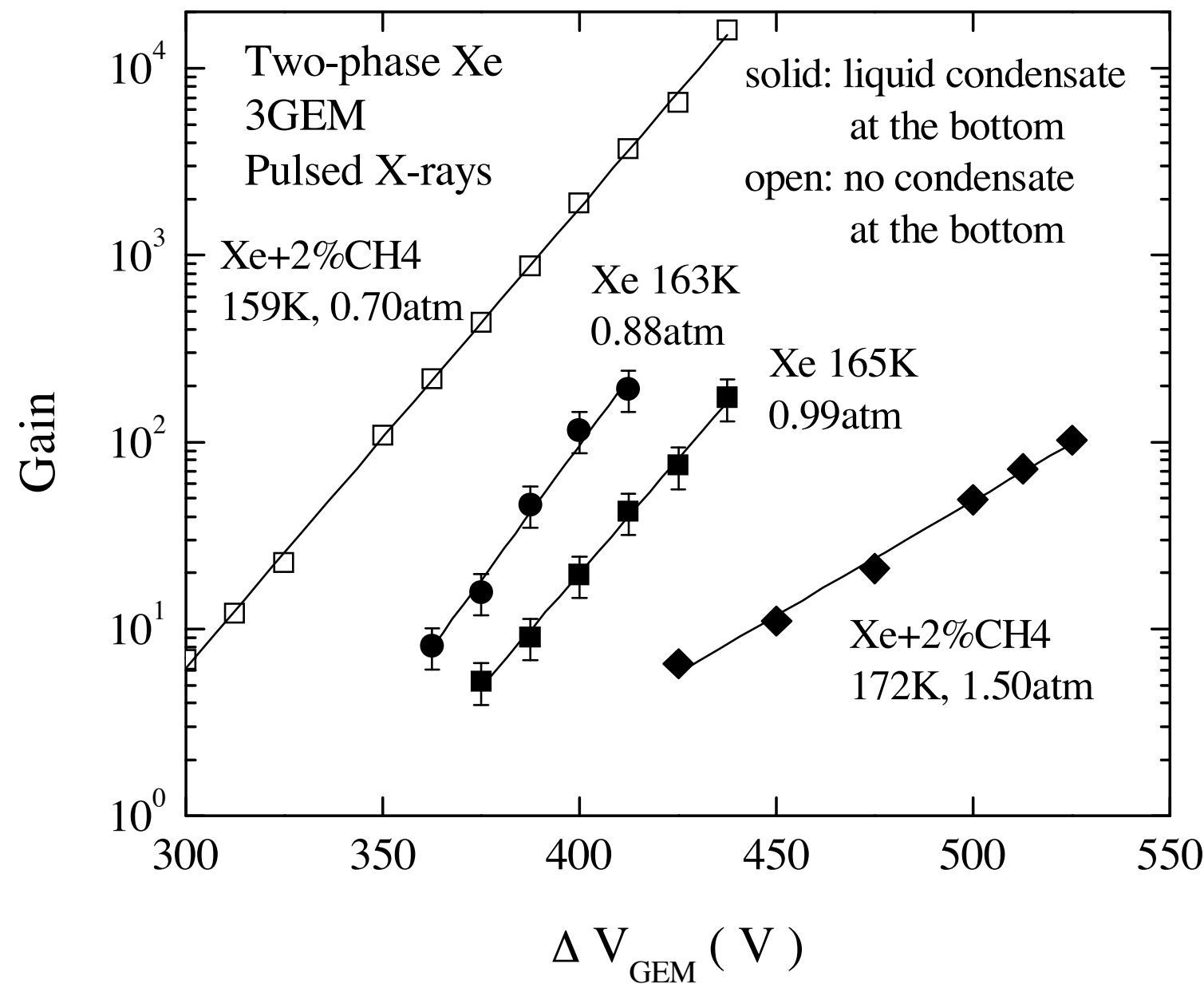
A GEM (F. Sauli, 1997) is a thin metal-insulator-metal structure, densely perforated with small holes. A voltage across the metal layers generates a sufficiently strong field within the holes to focus the electrons and multiply them.

The GEM is technically realized at CERN through copper-coating on 50 μm thick kapton (polymer) foil, with chemically etched holes of conical profile. A standard GEM has a hexagonal pattern of 70 μm diameter holes in the metal, 55 μm in the foil, with a pitch of 140 μm .



A 2D readout of strip anodes on the transfer side of the GEM can provide $\sim 1 \text{ mm}$ spatial resolution.





Preliminary results were obtained in the two-phase Xe avalanche detector: the maximum gain of the triple-GEM in two-phase Xe and Xe+2%CH₄ was about 200.

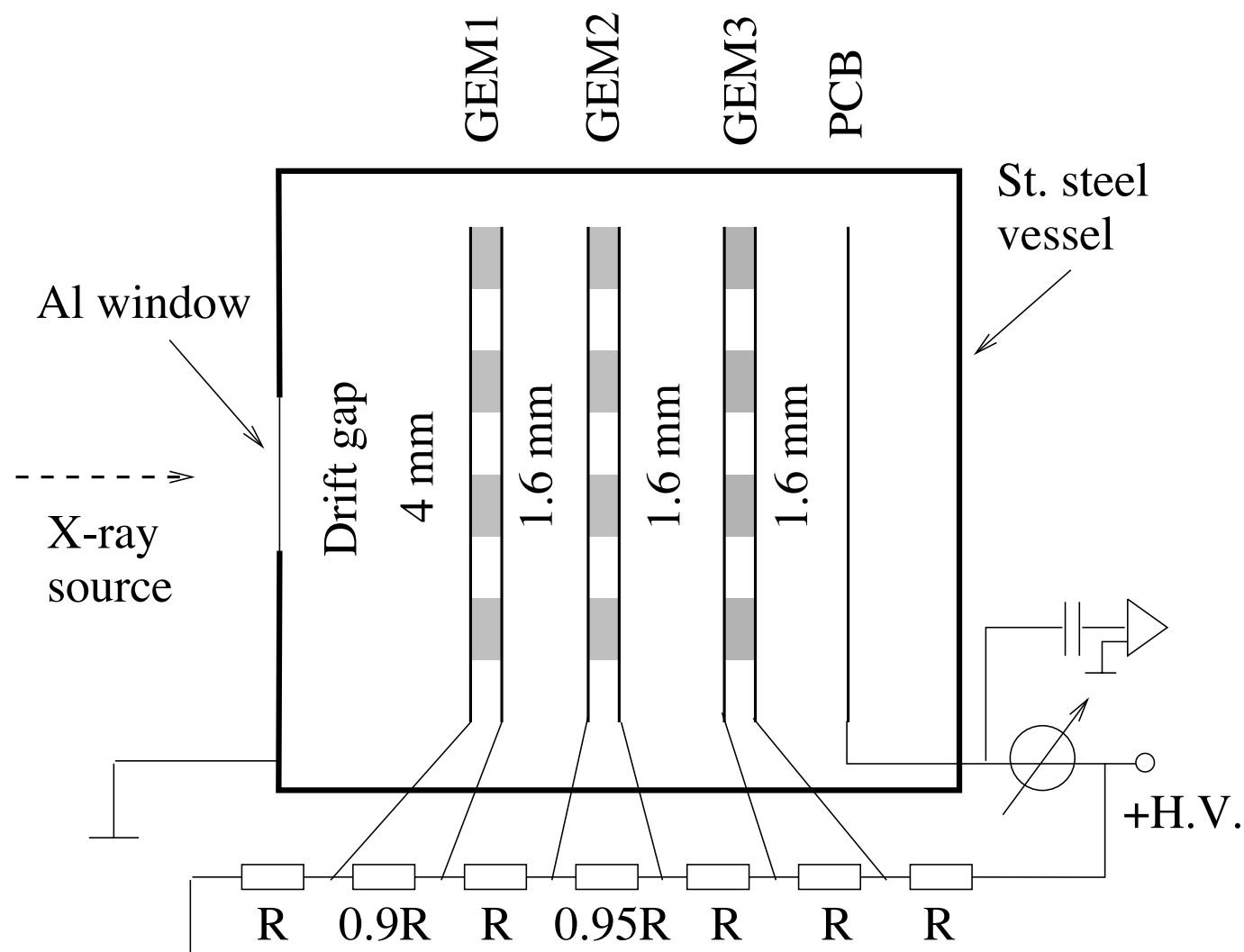
Fig.12 Gain-voltage characteristics of the triple-GEM, measured using pulsed X-rays, in two-phase Xe and two-phase Xe+CH₄, when there is a liquid condensate at the chamber bottom, and in gaseous Xe+CH₄, when there is no condensate at the bottom. The appropriate temperatures, pressures and CH₄ concentrations are indicated. In the two-phase mode, the electric field in liquid Xe is 4.0 kV/cm. The maximum gains are limited by discharges.

High pressure operation of the triple-GEMdetector in pure Ne, Ar and Xe

A. Bondar, A. Buzulutskov *, L. Shekhtman

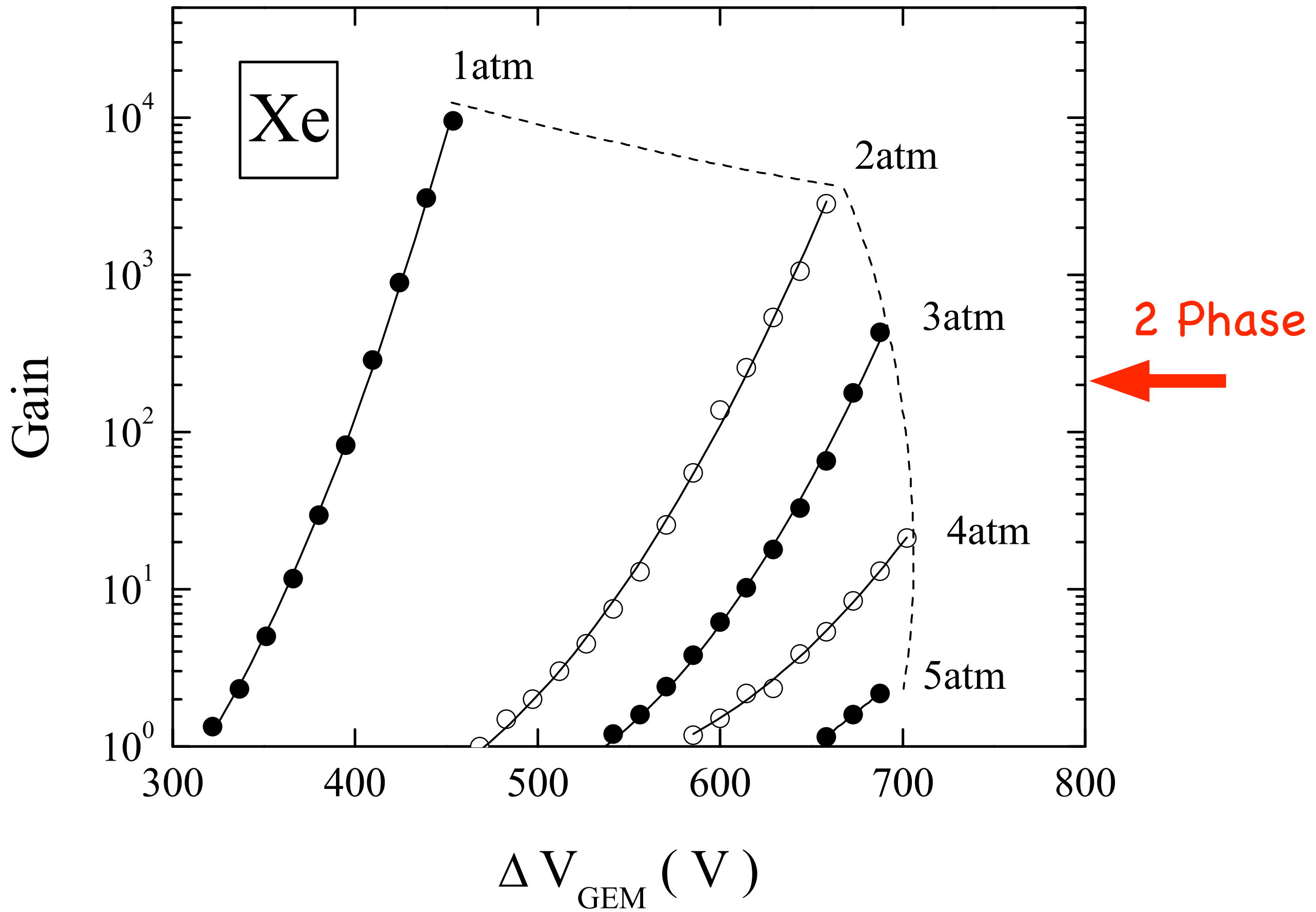
Budker Institute of Nuclear Physics, 630090 Novosibirsk, Russia

<http://xxx.sfnchc.gov.tw/abs/physics/0103082>

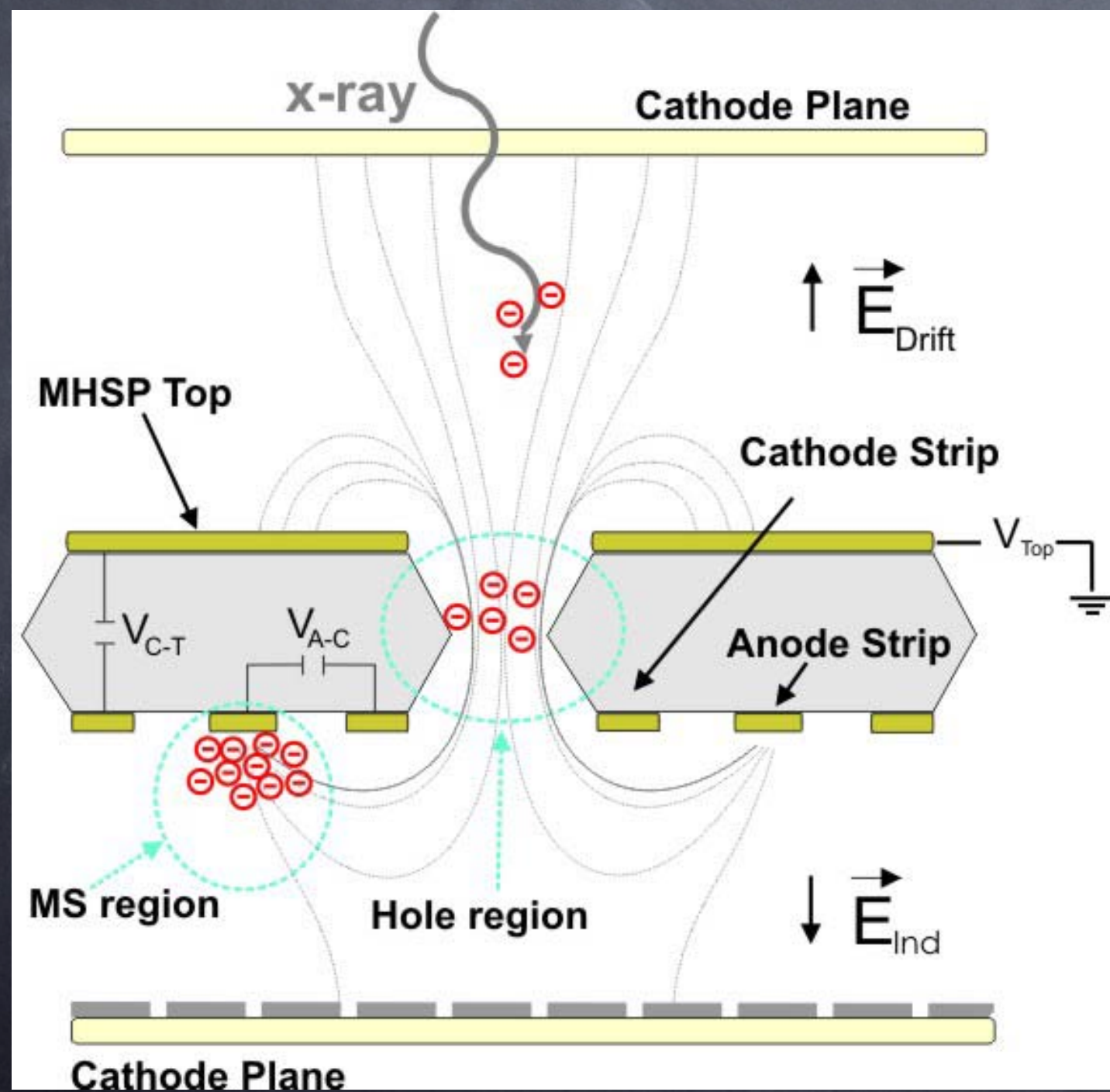


GEM foils (50 μm thick kapton, 80 μm diameter and 140 μm pitch holes, $28 \times 28 \text{ mm}^2$ active area) and a printed circuit board (PCB), mounted in cascade with 1.6 mm gaps

the density of noble gases near the boiling point, at normal pressure, is higher compared to that at room temperature.
Xe : higher density by 1.6 times

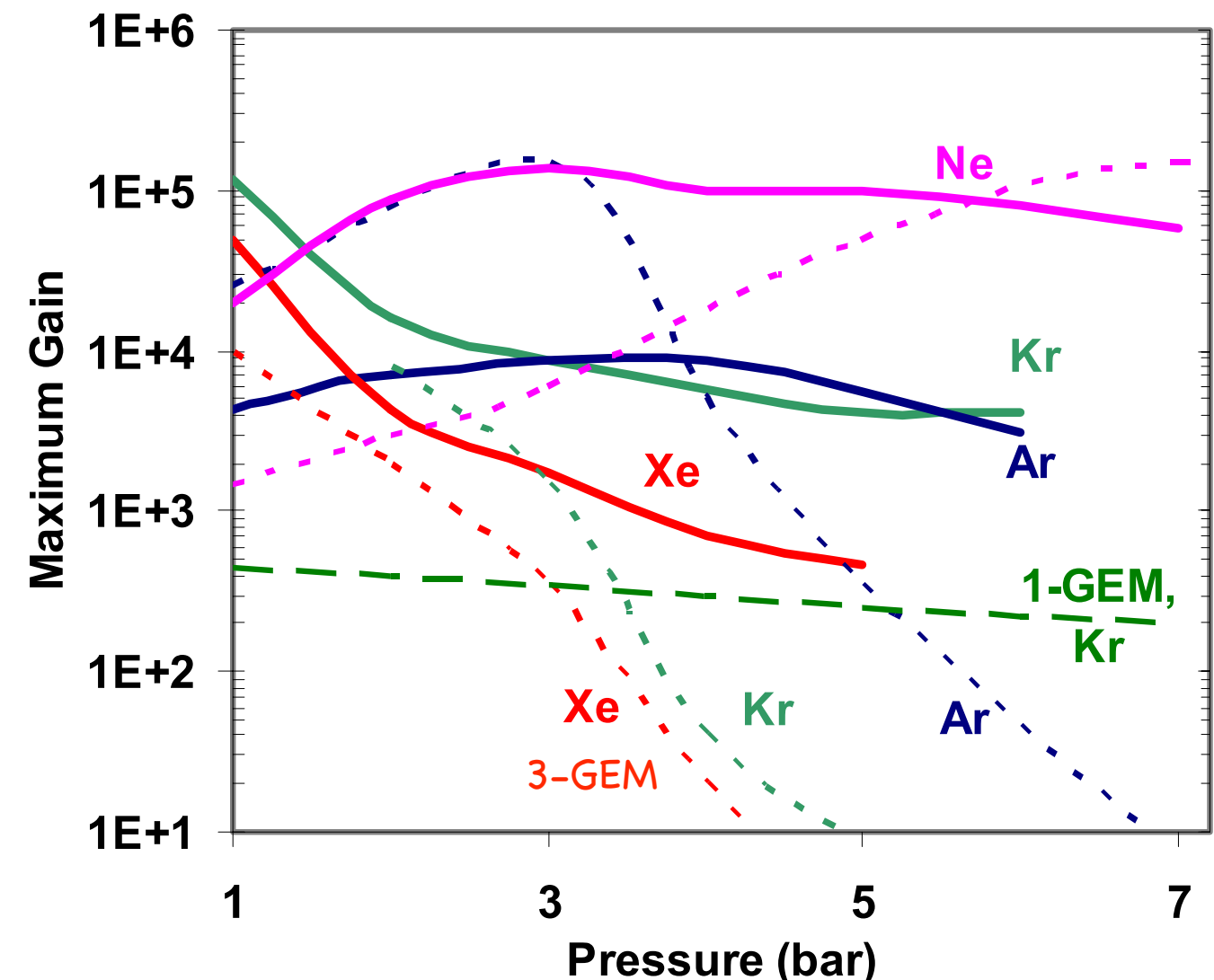
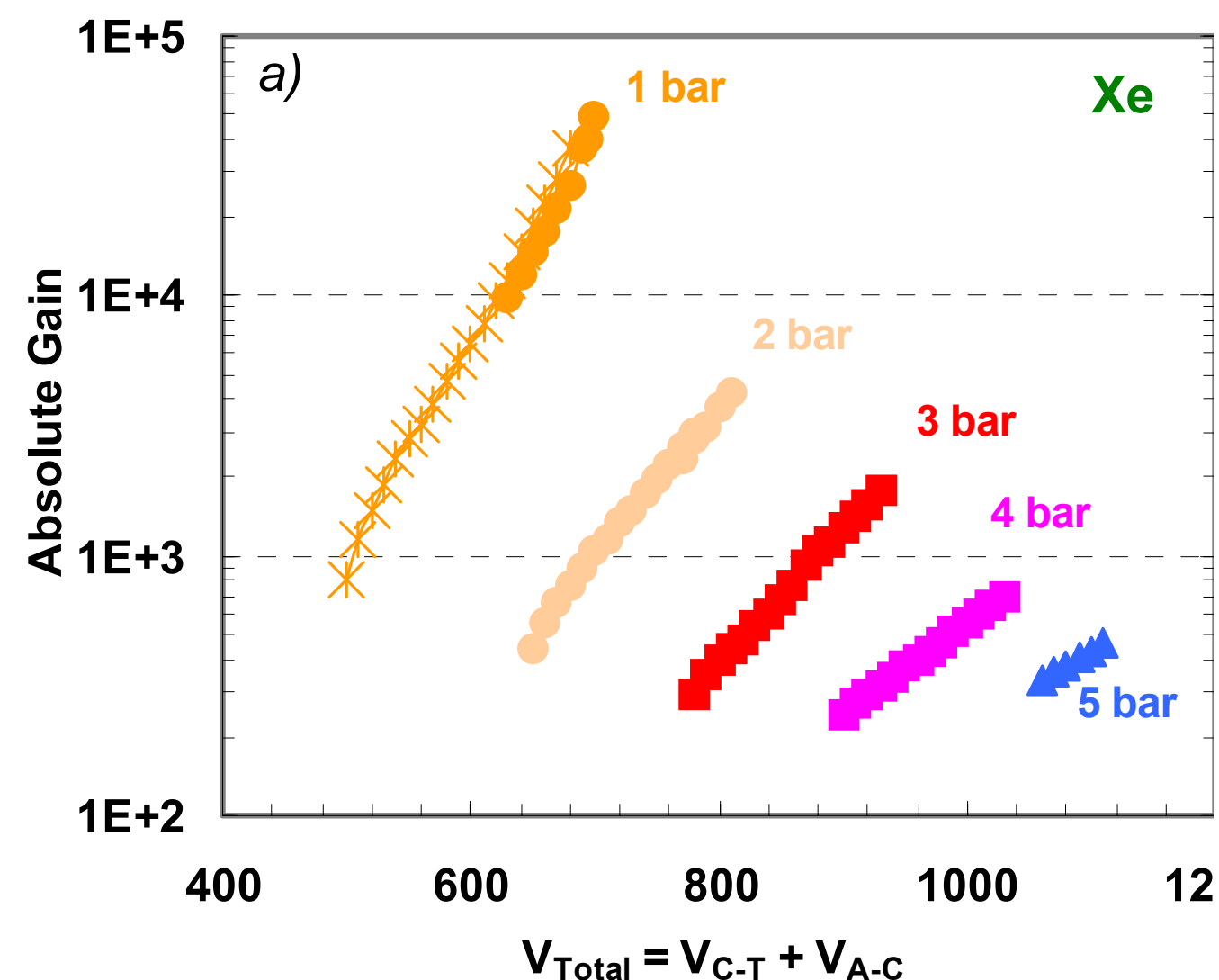


MHSP : Micro-Hole & Strip Plate electron multiplier



28 x 28 mm², 50 µm thick Kapton with a
5 µm copper clad coating on both sides.

bi-conical holes of about 40/70 μm in diameter, arranged in an asymmetric hexagonal lattice of 140- and 200- μm pitch in the direction parallel and perpendicular to the strips pattern in the bottom side, with the holes centered within the cathode strips, \sim 100 μm wide, while the anodes, \sim 35 μm wide, run between them, in a 200 μm pitch



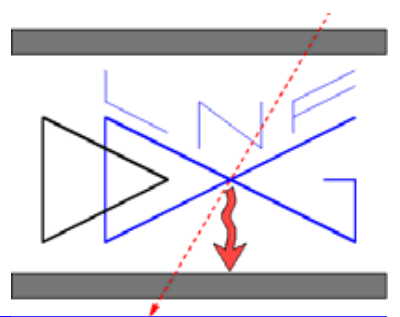
[arxiv.org/pdf/physics/0601120](https://arxiv.org/pdf/physics/0601120.pdf)

Operation of MHSP multipliers in high pressure pure noble-gas F. D.
Amaroa, J. F. C. A. Velosoa,b, A. Breskinc, R. Chechikc, J. M. F. dos Santosa,*

aPhysics Dept., University of Coimbra, 3004-516 Coimbra, Portugal bPhysics Dept.,
University of Aveiro, 3810-193 Aveiro, Portugal cDept. of Particle Physics, The Weizmann
Institute of Science, 76100 Rehovot, Israel

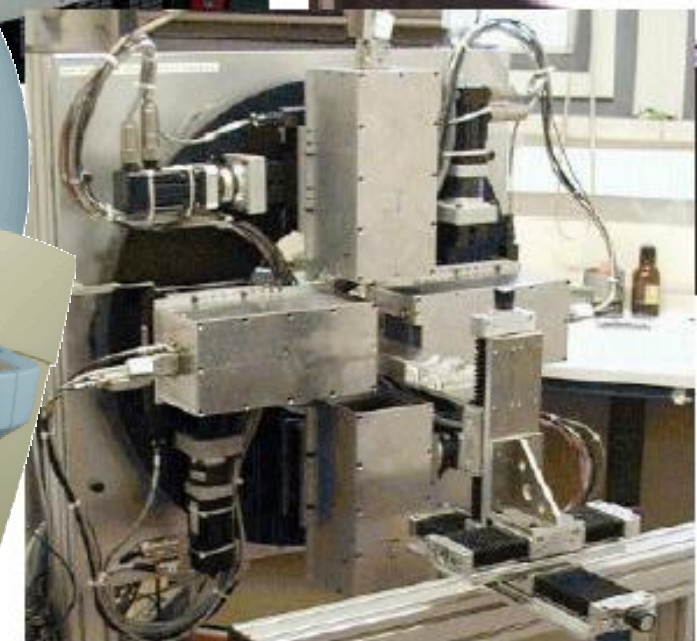
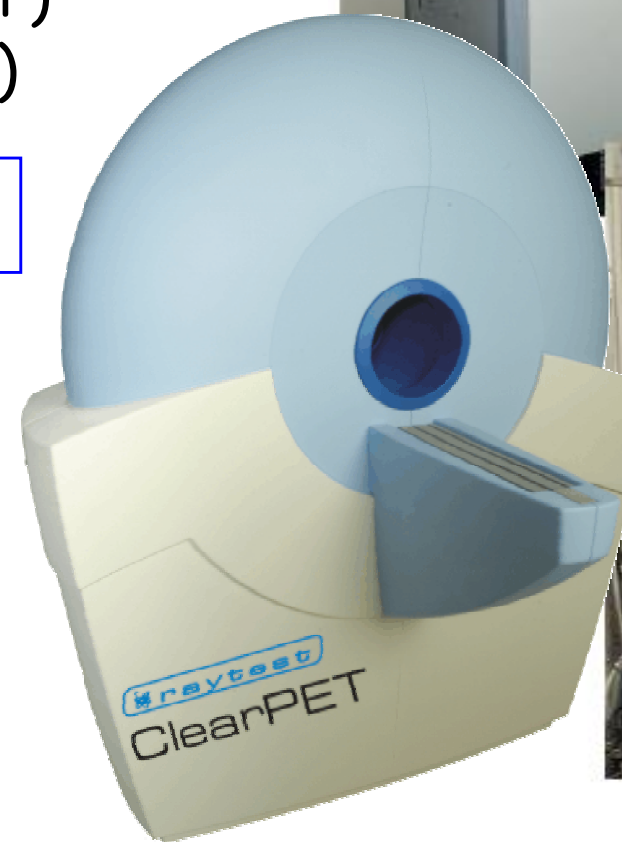
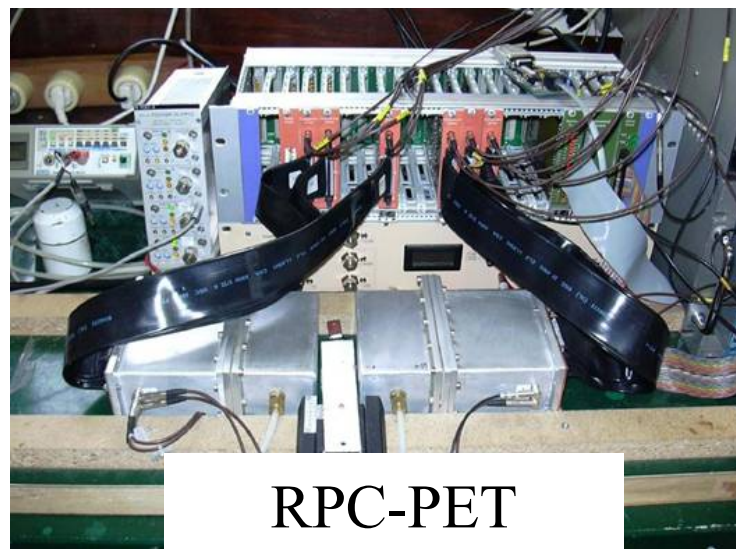
Small
Animal
PET

Small Animal PET

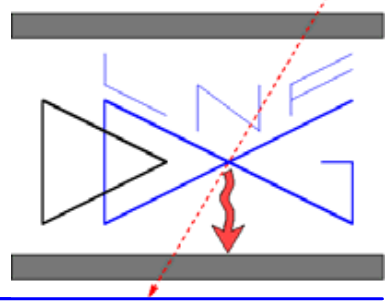


- Medicine experimentation on mice
- Very high image resolution required
- Low efficiency tolerated
(increase the dose)
- Mostly based on exotic crystals
YAP, LSO, LYSO, LuYAP
[microPET](#), [ClearPET](#)
- 2 gaseous detectors:
[HIDAC](#) (MWPC with Pb converter)
[RPC-PET](#) (RPC with Cu converter)

Spatial resolution: 2mm FWHM

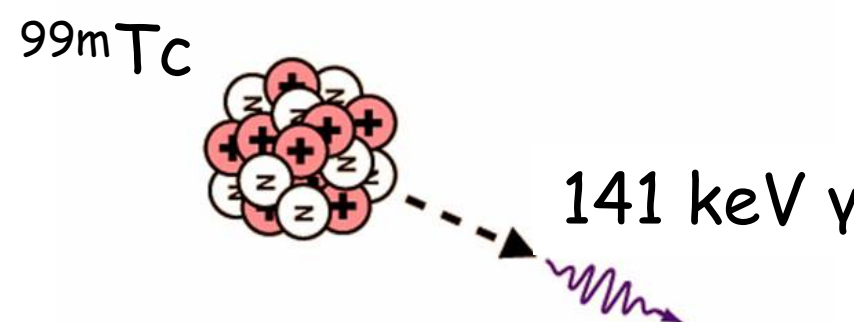


SPECT and PET

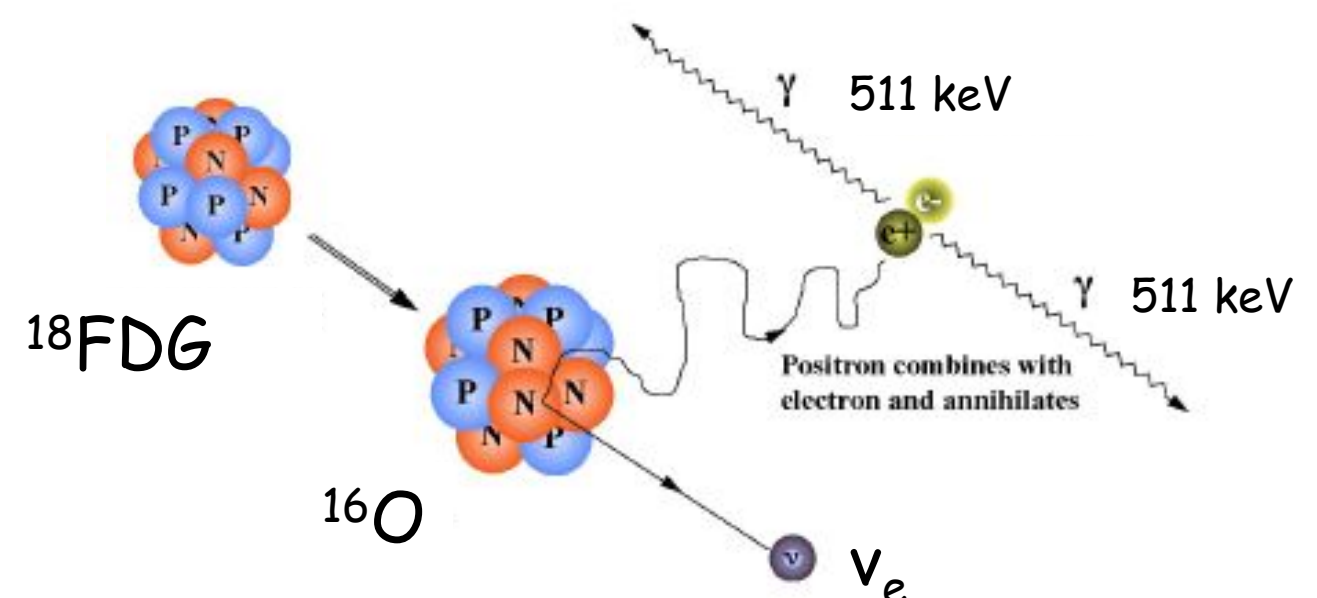


- SPECT (Single Photon Emission Computed Tomography) and PET (Positron Emission Tomography) are medical imaging techniques in which a radiotracer is injected into the subject to study.
- The concentration of tracer is measured by detecting the products of nuclear reactions.
- Differently from transmission imaging techniques (e.g. X-Rays) the information is both **morphologic** and **physiologic**

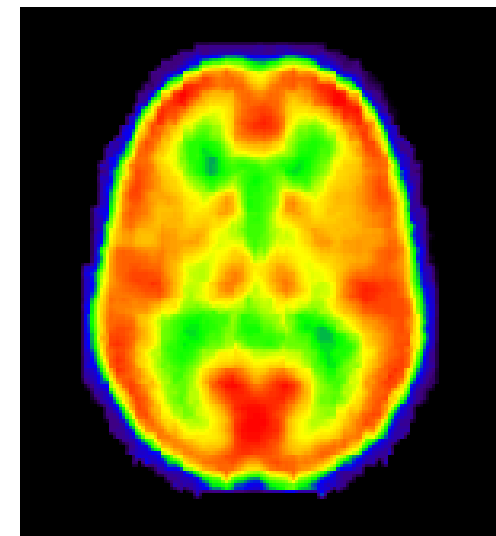
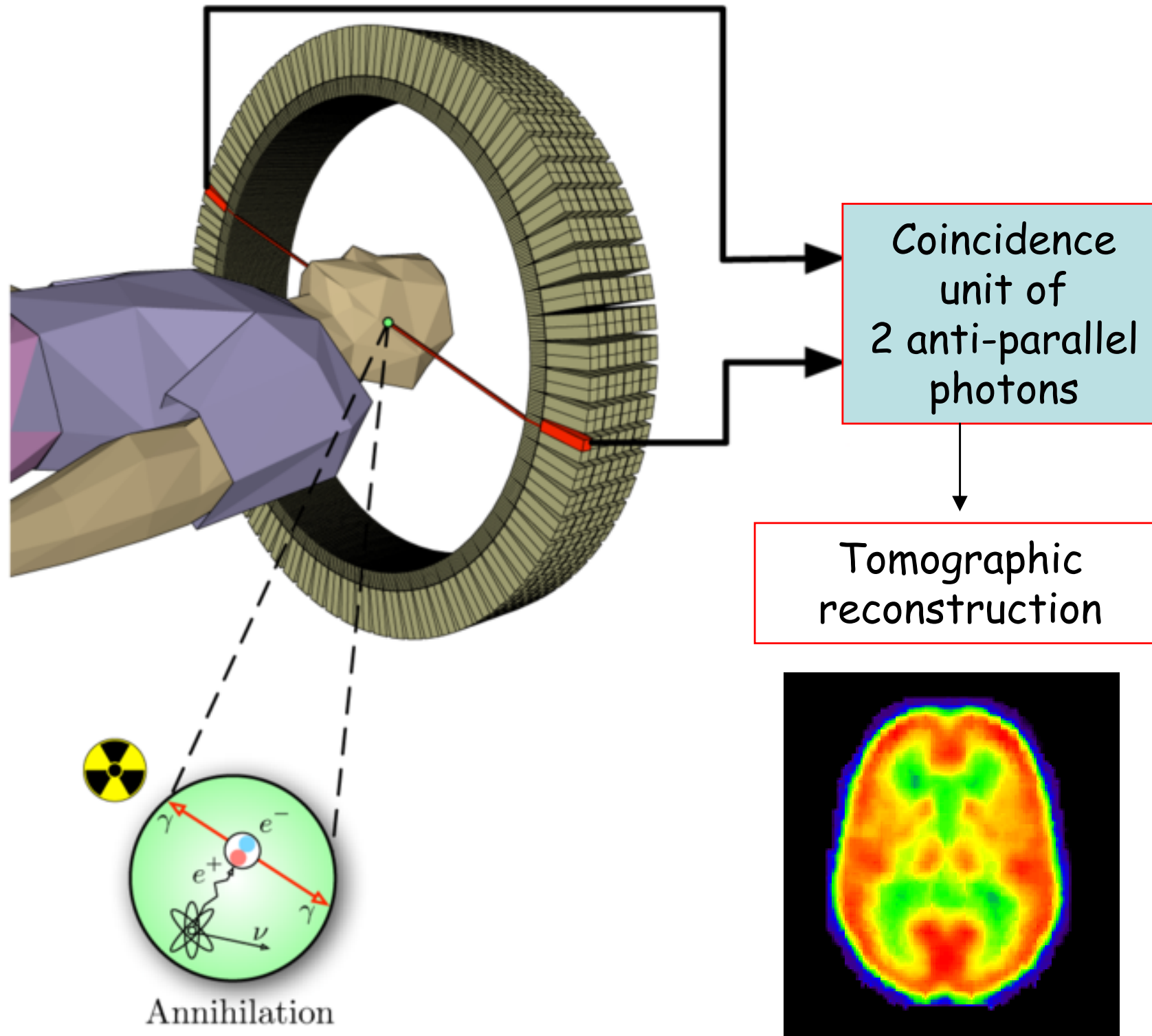
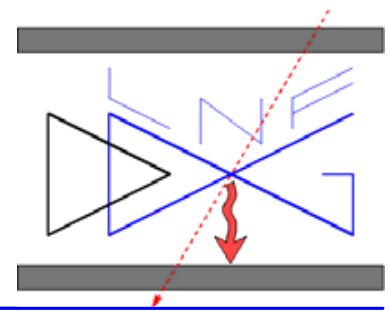
SPECT



PET

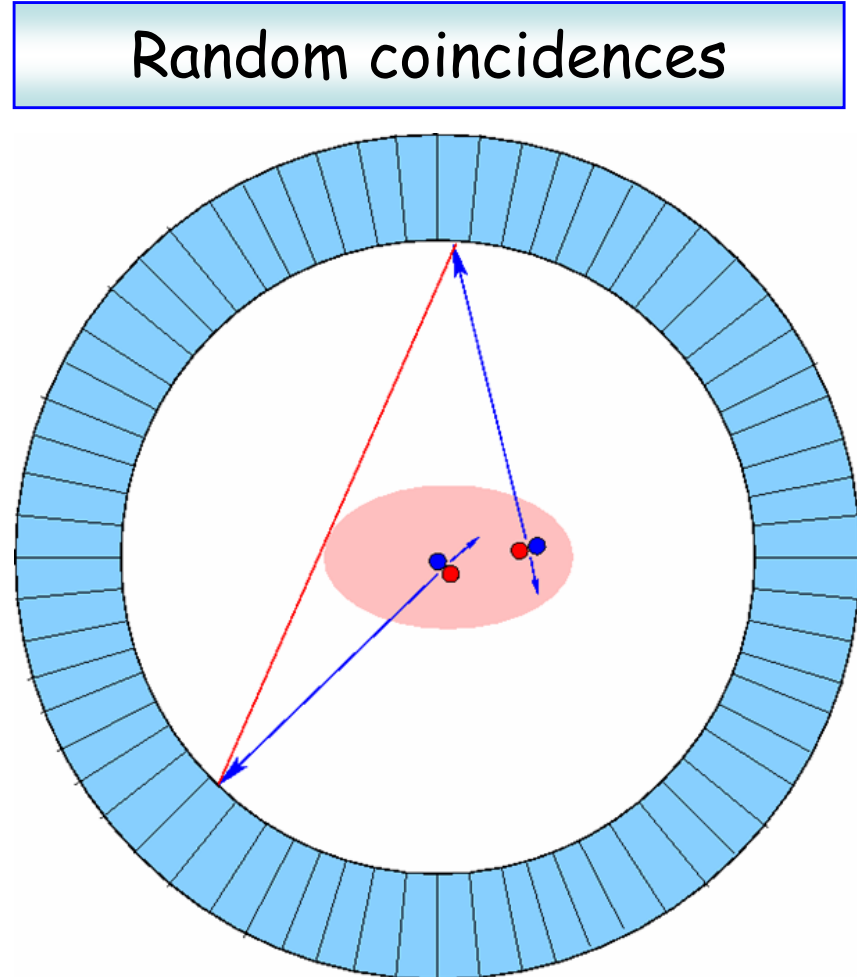
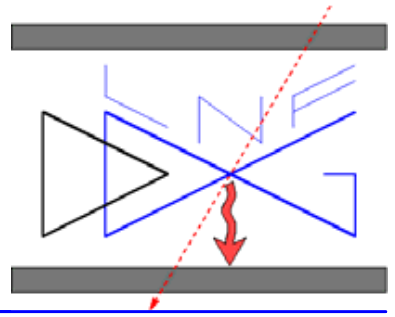


Positron Emission Tomography



Typical image resolution
 $5 \div 10 \text{ mm}$

PET Image Degradation Sources



Random coincidences



Scattered events



Off-center emission
Parallax error

Anti-Compton with peak
determination
Energy resolution

Random events $\propto 2t_w$
Time resolution

TOF + DOI \rightarrow constraint on
Z reconstruction

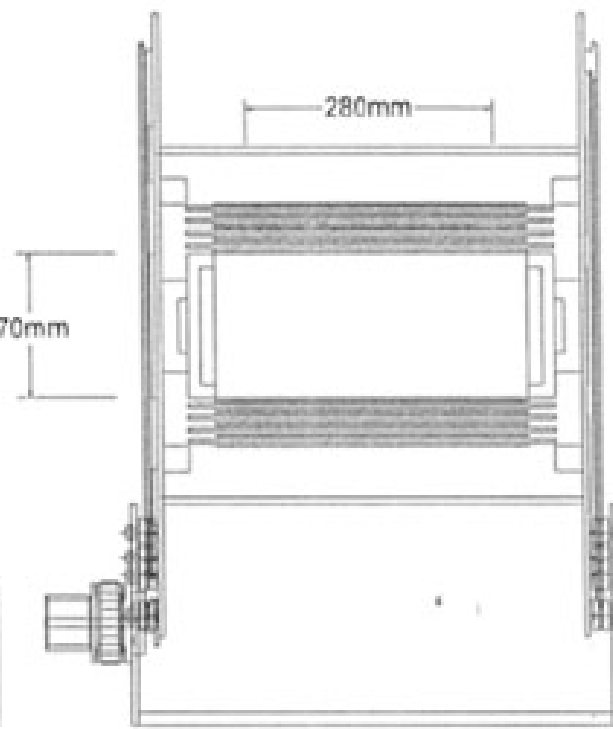
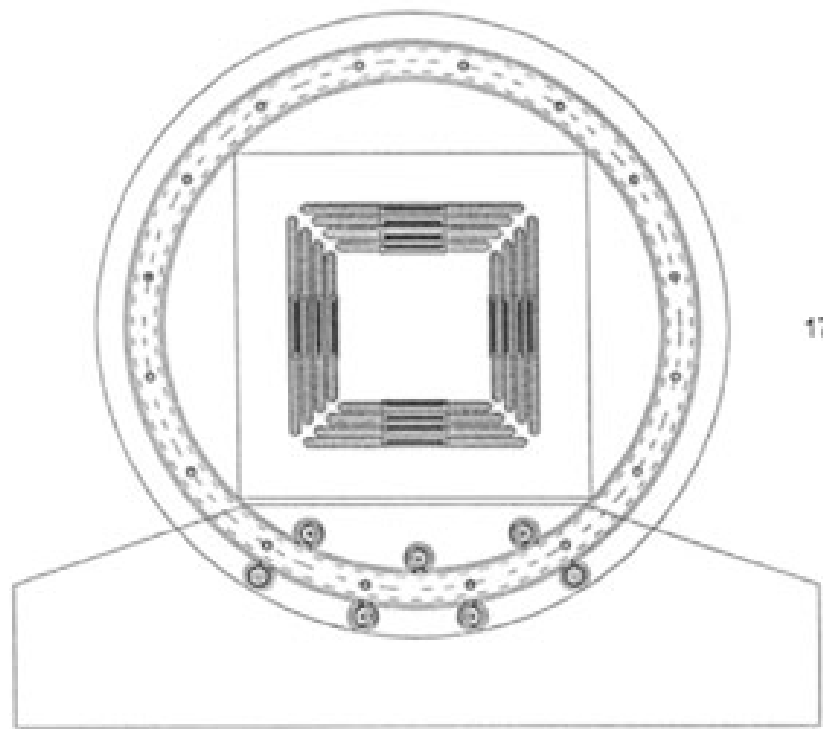
Depth Of Interaction
determination

HIDAC

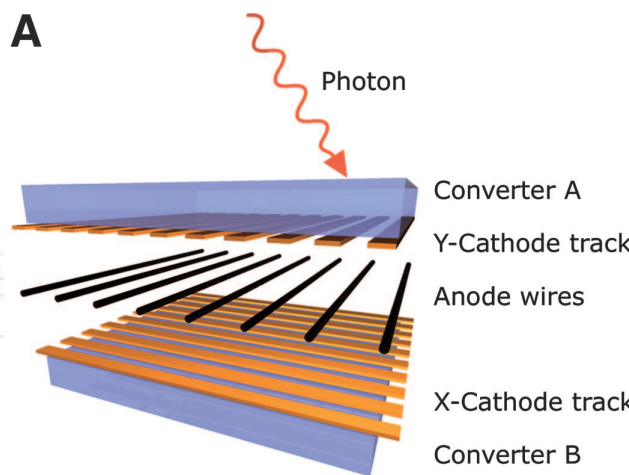
High Density Avalanche Chamber

QUAD-HIDAC-16

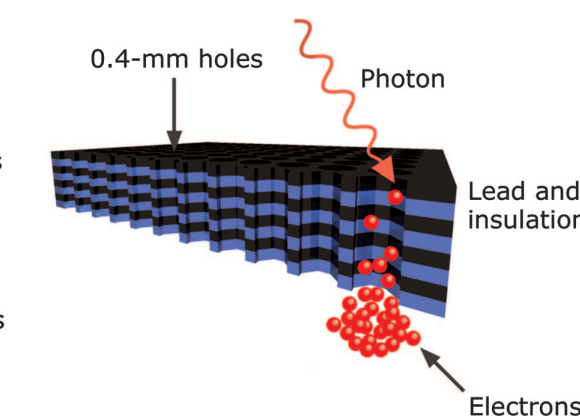
Oxford Positron System, UK



A



B



16-Module : 4 layers/QUAD

32-Module : 8 layers/QUAD

Figure 1. Schematic design of quad-HIDAC tomograph detector configuration. The 16 modules are clearly visible.

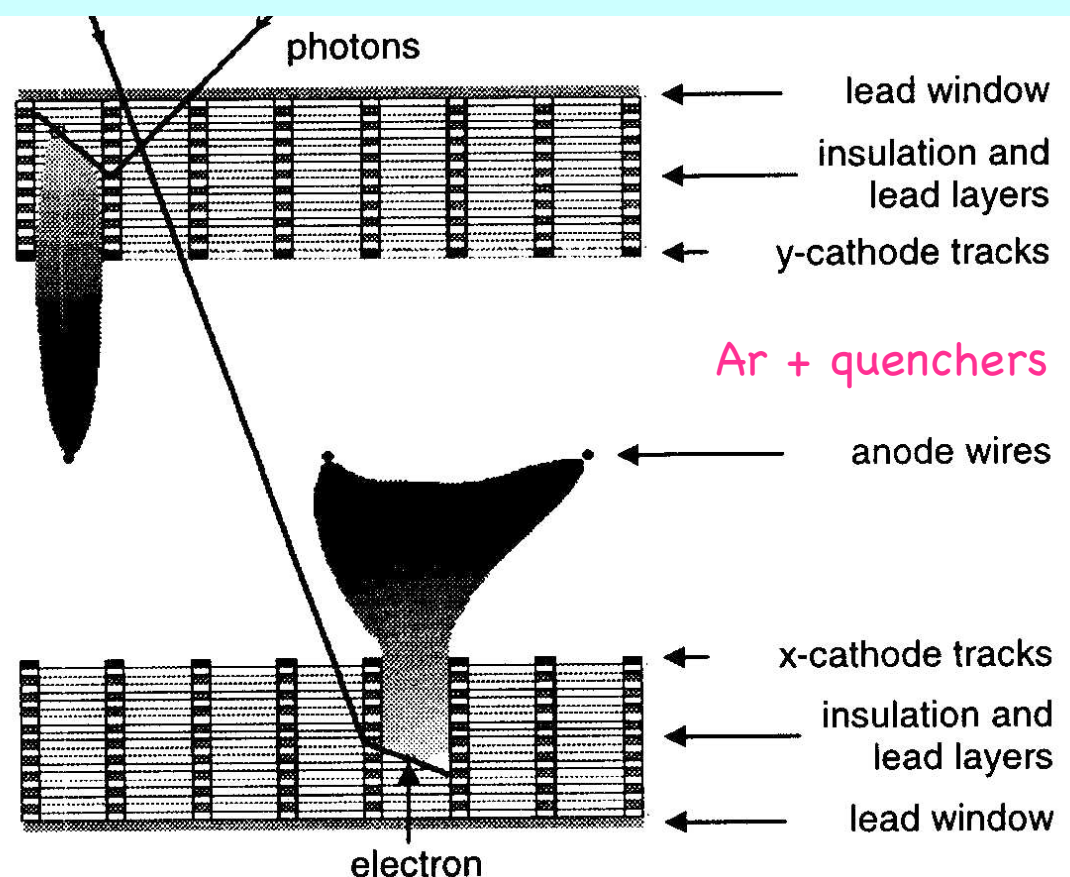
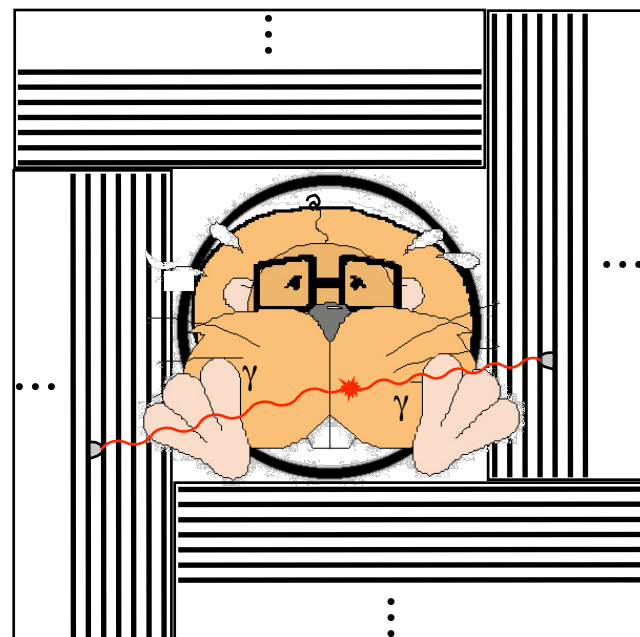


Table 1. Selected system parameters of 16-module quad-HIDAC small animal PET tomograph. The reconstructed image size is specified in terms of diameter and length of the field-of-view.

	Detector	
Hole diameter	0.4 mm	
Separation between hole centres	0.5 mm	
Cathode track separation	1 mm	
Anode wire separation	1.5 mm	
Lead thickness/module	12 × 50 μ m	
Coincidence window	40 ns	
	Dimensions	
Detector length	280 mm	
Inner detector separation	170 mm	
	Data sets	
List mode file size	~100 MB/10 ⁷ counts	
Typical binning percentage	90%	
Reconstructed image size: 60 mm × 100 mm at 0.3 mm	52 MB	
Sampling distance	0.1 mm–1 mm variable	

RPC-PET

Portugal, Spain



Spatial resolution
~ 580 μm FWHM

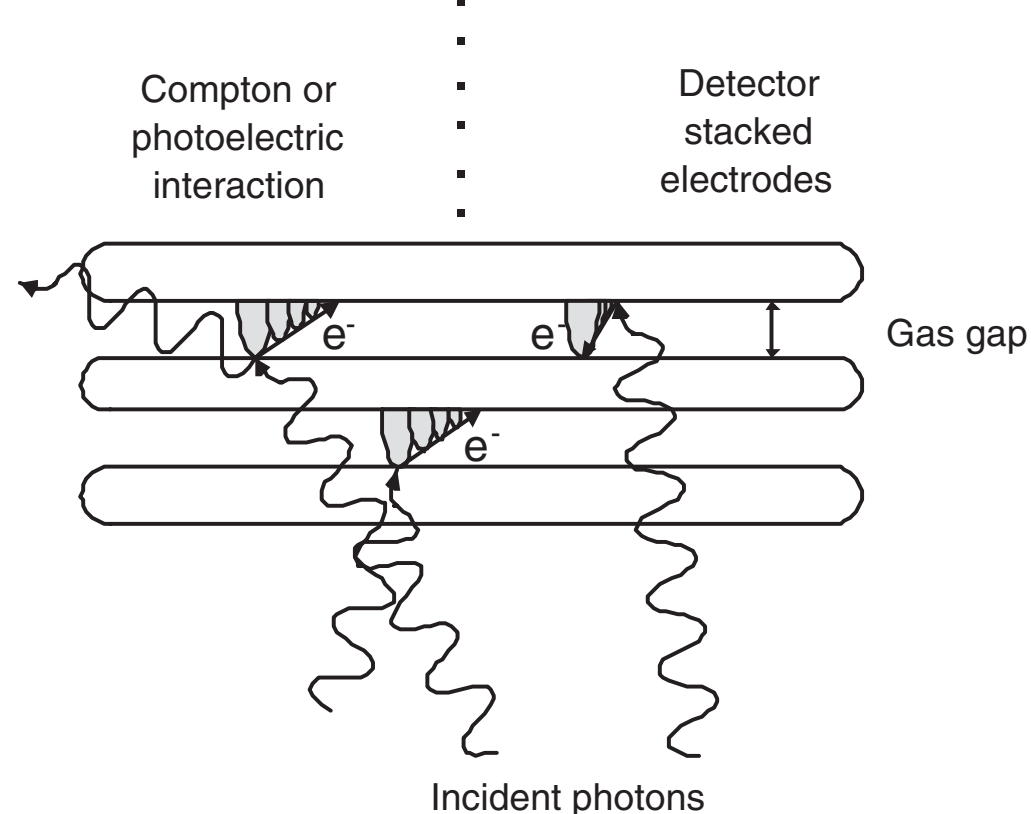
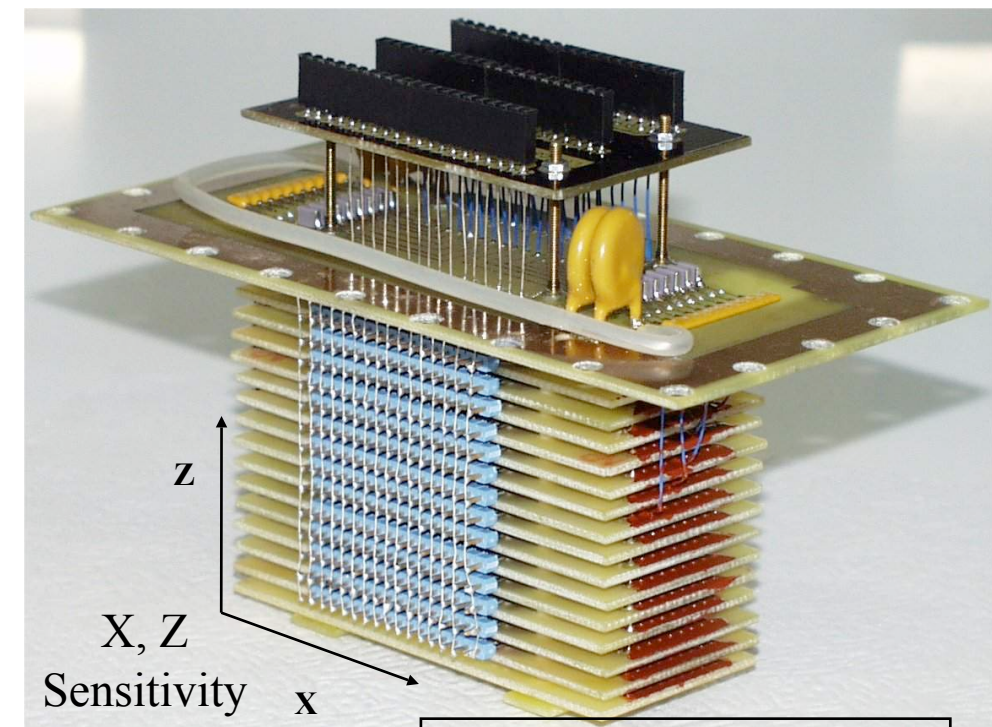


Fig. 1. Schematic view of the detecting element, showing the detection process of the incident gamma photons, which take profit of the stacked construction of the RPCs.

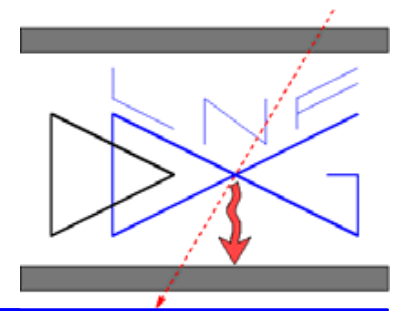
the metallic cathode of one RPC on one side and on the opposite side the resistive anode of the next RPC in $\text{C}_2\text{H}_2\text{F}_4$ 85 %, SF_6 10%, C_4H_{10} 5%



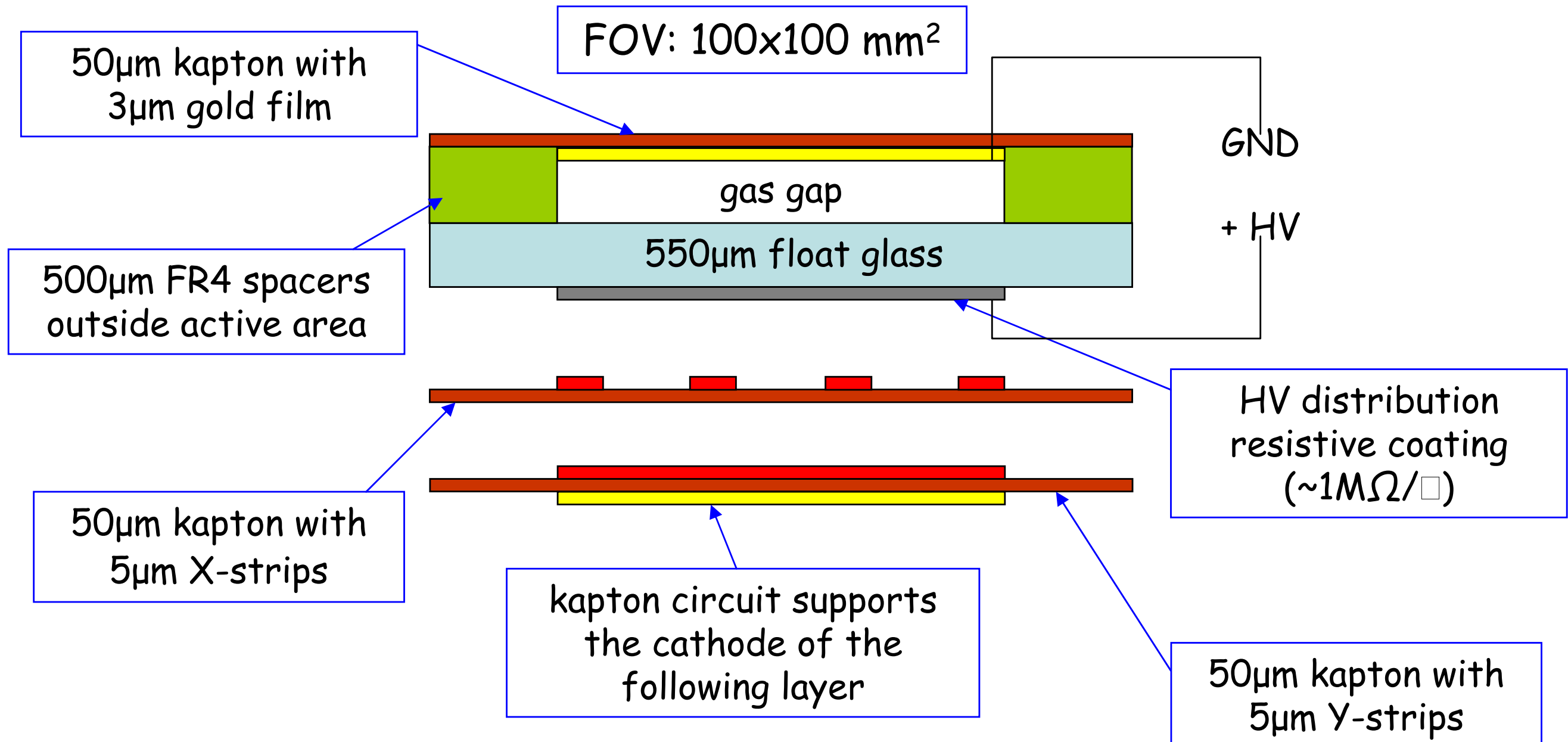
Active area 32 x 10 mm^2

- Copper (on a PCB) and glass electrodes.
- 0.3 mm Gap.
- 32 1-mm wide X pickup strips.
- Not optimized for high efficiency.

Hybrid Parallel Plate Counter

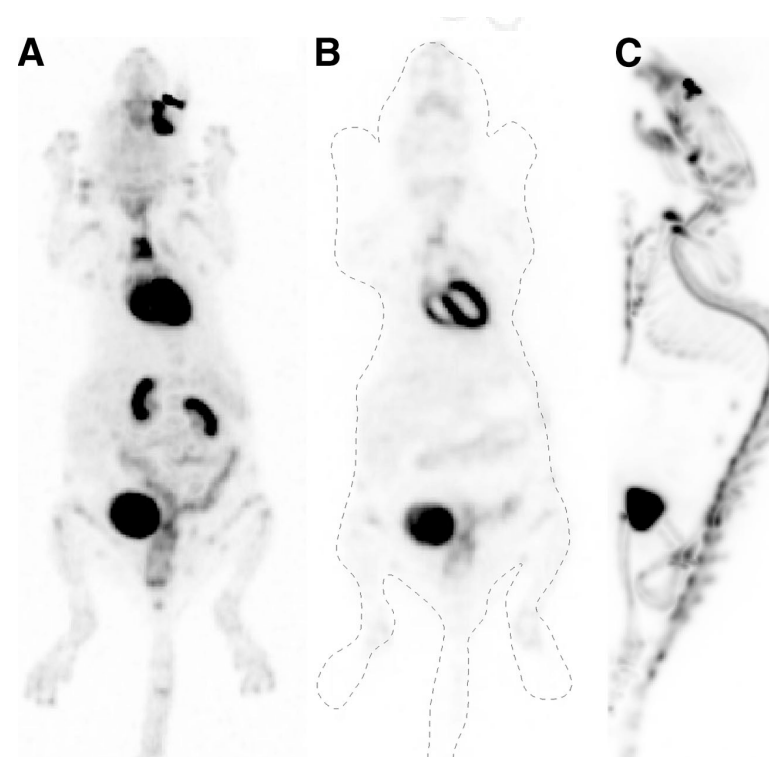
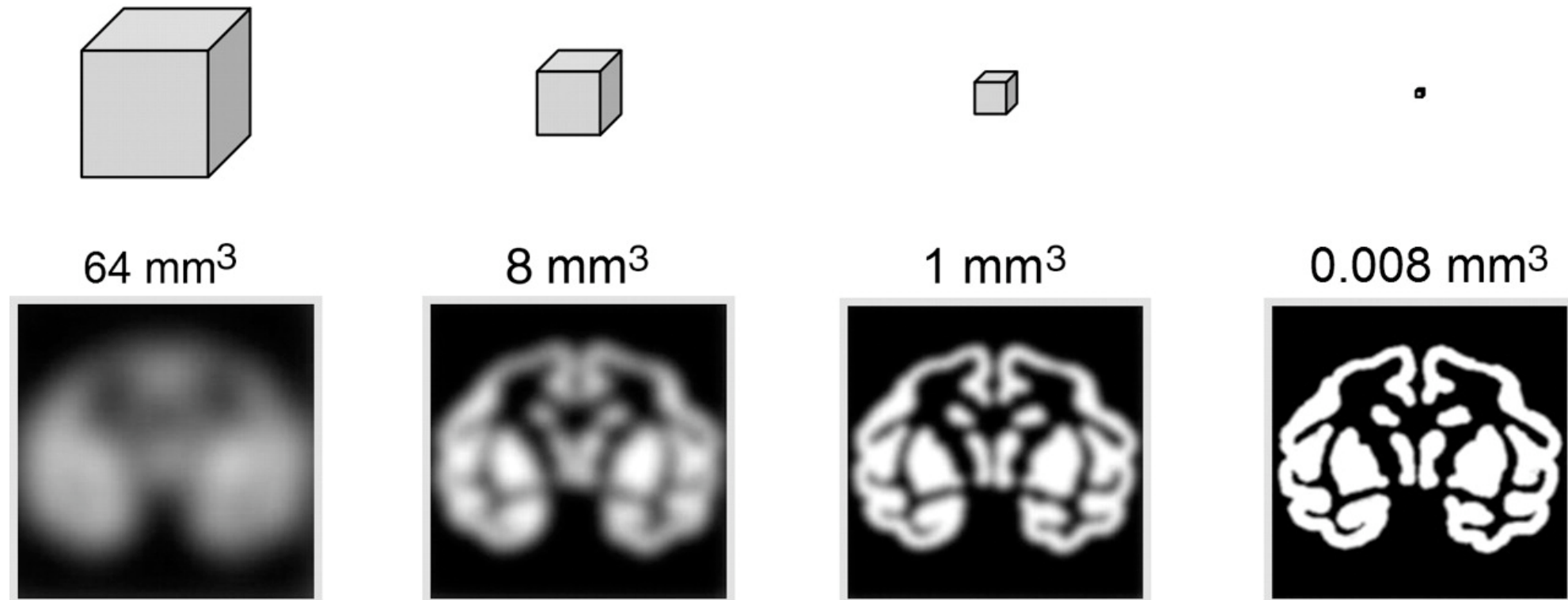


Hybrid: the anode is resistive (glass), the cathode is conductive (gold)



Many single layers are stacked to realize one detector

HR+ (1995) microPET I (1997) microPET II (2003) Autoradiography



HIDAC, 32-module

FIGURE 6. (A and B) Images (OPL-EM) of 22-g mouse, acquired in 15 min, 1 h after injection of ^{18}F -FDG show maximum intensity projection (A) and a single central slice (B). (C) Maximum intensity projection of 27-g mouse, 1 h after injection of ^{18}F fluoride.

Summary of small animal PETs

TABLE II. COMPARISON BETWEEN DIFFERENT SMALL ANIMAL PET PARAMETERS AND THE EXPECTED PARAMETERS OF THE RPC-PET.

Scanner	Image Spatial resolution, FBP (mm)	Time resolution (ns FWHM)	FOV (mm $\varnothing \times$ mm)	Central point absolute sensitivity (cps/kBq)	Source (mm $\varnothing \times$ mm)	Peak NEC (kcps)
microPET II® [1],[15]	1.1	3	160 x 49	23 - 33	25 x 70 mouse size 60 x 150 rat size	235 at ~2.35 MBq/cm³ 24.6 at ~0.19 MBq/cm³
YAP-PET [2],[16]	1.6	2	40 x 40	18 at ($\varnothing = 150$ mm)	-	90 (not peak) at ~16.6 MBq
Quad HIDAC (32 modules) [7],[17]	0.95	-	170 x 280	18	-	100 at ~0.2MBq/cm³
RPC-PET	0.5*	0.3	60 x 100	21**	25 x 70 mouse size	318** at ~ 2.63 MBq/cm³

* Measured, ** Simulated

ClearPET 1.25-2 5.7 (135-225)x110 (125-200)x110

Imaging 2006

INTERNATIONAL CONFERENCE ON IMAGING TECHNIQUES IN SUBATOMIC PHYSICS,
ASTROPHYSICS, MEDICINE, BIOLOGY AND INDUSTRY

Stockholm, Sweden 27-30 June 2006

<http://lepton.particle.kth.se/imaging2006/index.php>

MEG-TPC

LXe-PET : no segmentation with PMT, TPC

333 l, 80cm Φ , 12cm depth, 24cm axial length

(1)

2"PM^T : $4 \times 54 = 216$

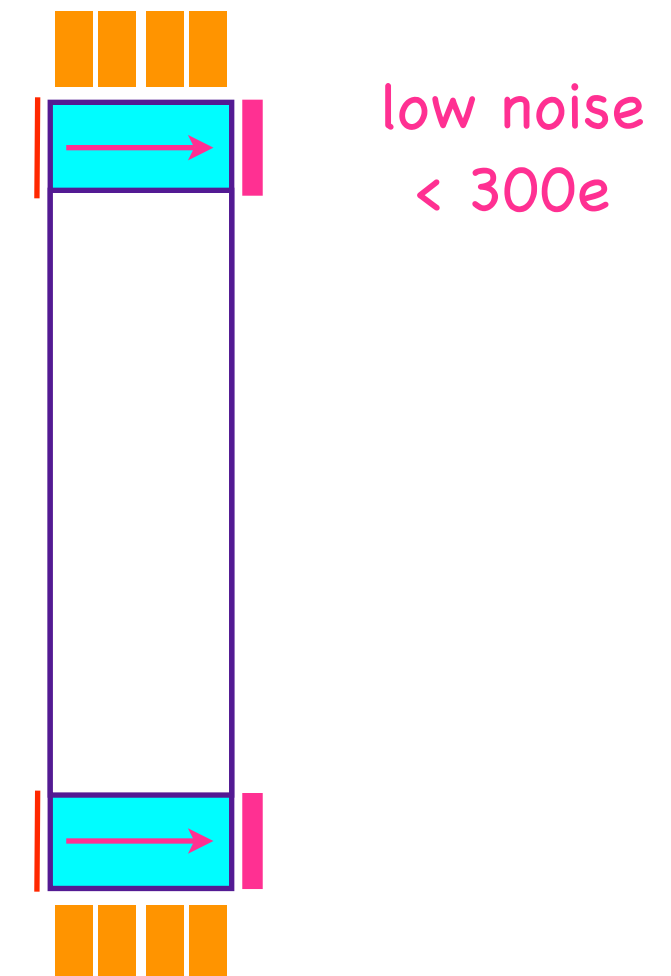
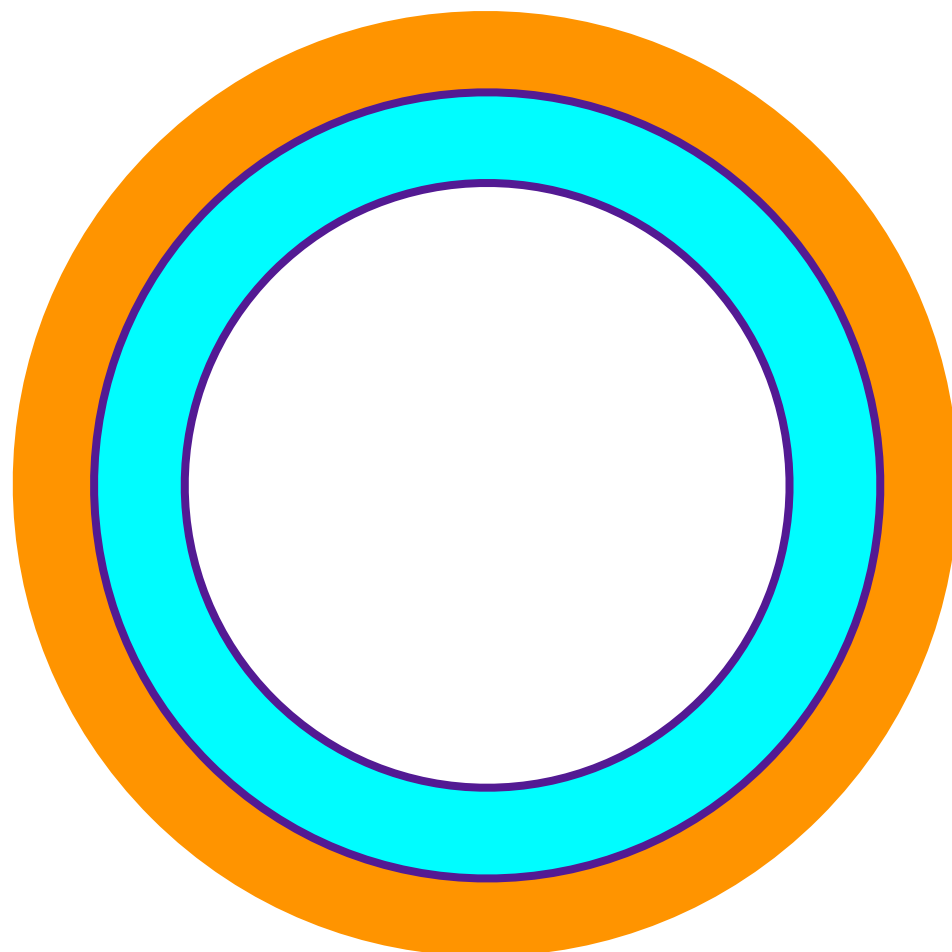
Spatial resolution = 2 mm

Time resolution = 1 nsec
timing for the TPC

TPC : 48kV

52.2 μ sec/24cm
(2.3mm/ μ sec)

continuous readout
with time stamp by PMT



LXe-PET : no segmentation with PMT, TPC

333 l, 80cm Φ , 12cm depth, 24cm axial length

(2) 2"PM T : $4 \times 54 = 216$

Spatial resolution = 2 mm

Time resolution = 1 nsec

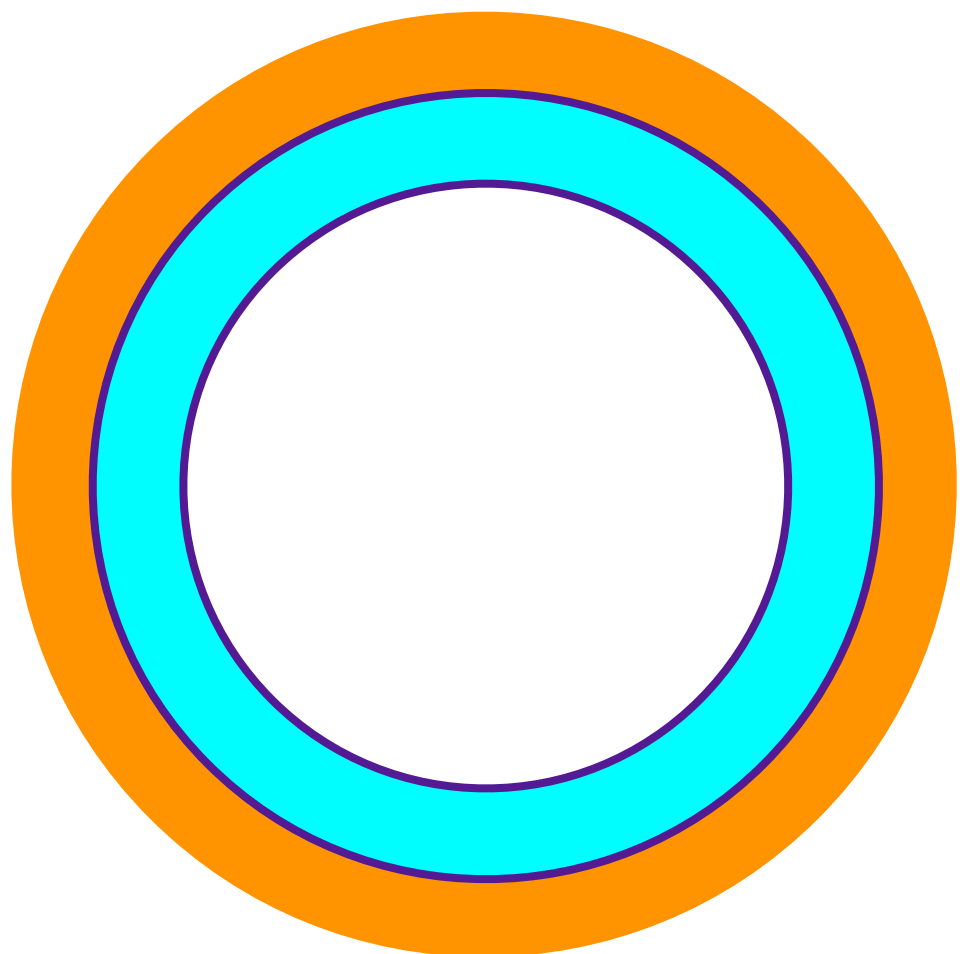
timing for the TPC

TPC : 48kV

52.2 μ sec/24cm

(2.3mm/ μ sec)

continuous readout
with time stamp by PMT



detection in 2 phase
GEM, MHSP

